Analysis of Heparan Sulfate role in bone development and Multiple Osteochondromas syndrome.

Inaugural-Dissertation
zur
Erlangung des Doktorgrades
Dr. rer. nat.

der Fakultät für
Biologie und Geografie
an der

Universität Duisburg-Essen

vorgelegt von

Virginia Piombo

aus Savona

August 2010

Die der vorliegenden Arbeit zugrunde liegenden Experimente wurden am Zentrum für Medizinische Biotechnologie in der Abteilung für Entwicklungsbiologie der Universität Duisburg-Essen durchgeführt.

1. Gutachter: Prof´in Dr. Andrea Vortkamp

2. Gutachter: Prof´in Dr. Perihan Nalbant

3. Gutachter: Prof. Dr. Jens Fischer

Vorsitzender des Prüfungsausschusses: Prof´in Dr. Verena Jendrossek

Tag der mündlichen Prüfung: 09. November 2010

Table of Content

1. Introduction

1.1 The vertebrate skeleton

The vertebrate skeleton is a complex organ responsible for several functions during vertebrate life. It serves as a scaffold to protect the internal organs such as brain, lungs and heart. It is also the site of haematopoiesis that takes place in thered bone marrow. Furthermore in the skeleton the bone matrix which contains high level of calcium hydroxylapatite serve as regulator for calcium homeostasis. The skeleton consists of more than 200 individual elements which are supported by ligaments, tendons, muscles and cartilage to ensure the flexibility of movements. Skeletal elements are organized along the longitudinal axis form the axial skeleton. This consists of the vertebral column, the thoracic cage and the skull. The appendicular skeleton, to which the upper and lower limbs belong, is attached by the pectoral and pelvic girdles to the axial skeleton (Cormack, 1987).

The major types of vertebrate skeletal bones are divided in four categories: 1. long (e.g. the arm and leg bones), 2. short (e.g. the small bones in the wrists and ankles), 3. flat (e.g. the bones of the skull) and 4. irregular (e.g. vertebrae). Long, short, and irregular bones develop by endochondral ossification process and cartilage is replaced by bone. Flat bones develop by intramembranous ossification, in which bone is formed within sheets of connective tissue.

1.2 Ossification

1.2.1 Intramembraneous ossification

During intramembraneous ossification skeletal elements develop directly from a soft connective tissue into mineralized bone. First, mesenchymal cells migrate and aggregate into a mesenchymal condensation. These cells differentiate directly into osteoblasts, depositing a bone matrix rich in Collagen type 1 (Col1). Membranous bones constitute a small percentage of the skeletal elements, including the flat bones of the skull, calvaria and mandibles, and parts of the clavicles (Hall, 1988; Huang et al., 1997).

1.2.2 Endochondral ossification

Most bones of the vertebrate skeleton develop by endochondral ossification. The first phase of endochondral ossification starts around embryonic day 10.5 (E10.5) when the mesenchymal condensations are formed, generating the templates of the future bones (Hall and Miyake, 2000; Mariani and Martin, 2003). At the time that cartilage forms, blood vessels which had occupied the mesenchyme regress at the sites of the condensations (Feinberg et al., 1986; Yin and Pacifici, 2001). Cells of the early template produce an extracellular matrix (ECM), which is consists mainly of Col1. Cells in the center of the skeletal anlagen differentiate into chondrocytes, producing an extracellular matrix, rich in Collagen type 2 (Col2) and the proteoglycan aggrecan (Agc1) (Horton et al., 1993). Cells in the periphery of the anlagen aquire a more elongated shape, continue to produce Col1 and differentiate into fibroblast like perichondrial cells (Caplan and Pechak, 1987). From about E13.5 on, different chondrocyte subpopulations can morphologically be distinguished. At the distal ends of the cartilage anlagen the low proliferating chondrocytes have a small and round shape, while towards the center chondrocytes increase their proliferation rate, flatten and align into columns along the longitudinal axis of the skeletal elements. In the center of the anlagen, chondrocytes exit the cell cycle, stop proliferating and differentiate into pre-hypertrophic and hypertrophic chondrocytes, producing a type X Collagen (ColX) rich matrix, typical for this chondrocytes subpopulation (Linsenmayer et al., 1991; Poole 1991).

At this stage, cells in the perichondrium surrounding the hypertrophic chondrocytes differentiate into osteoblasts, which mineralize the Col1 rich matrix and form the bone collar (Caplan and Pechak 1987). Vascular invasion of the hypertrophic cartilage starts from the bone collar (Vu et al., 1998). Hypertrophic chondrocytes differentiate into terminal hypertrophic cells, which express matrix metalloprotease 13 (Mmp13) and eventually undergo apoptosis. Mmp13 is a collagenase that degrades the hypertrophic cartilage, thereby facilitating the invasion of the blood vessels (Ortega et al., 2004). Invading osteoclasts further degrade the ColX rich matrix, thereby allowing deposition of a new mineralized bone matrix by osteoblasts. The zone of the skeletal anlagen which starts to mineralize during chondrocyte differentiation is called “primary ossification center” or diaphysis. Ossification progress and erosion of diaphyseal cartilage restricts

chondrocytes to the distal end of the elements, called epiphyses. At postnatal day 7 (P7) the chondrocytes from the center of the epiphysis start to become hypertrophic, while at the same time so called “cartilage canals” are generated (Blumer et al., 2007; Burkus et al., 1993; Doschak et al., 2003; Ganey et al.,1995; Rivas and Shapiro., 2002). Formation of the secondary ossification center is regulated by mechanisms similar to those that regulate the formation of the primary ossification center. Around P14 hypertrophic chondrocytes undergo apoptosis, the ColX matrix is resorbed and blood vessels allow the invasion of osteoblasts, which deposit a mineralized matrix, generating the secondary ossification center. Between the primary and the secondary ossification center a cartilaginous zone persists, called epiphyseal plate or growth plate (Fig.1). The proliferation and hypertrophic differentiation of the epiphyseal plate is necessary for the continuous longitudinal growth of the bones (reviewed in Blumer et al., 2008). In humans, growth continues until the end of the puberty when the growth plate closes and disappears. In mine most growth plates are maintained postnatally, but chondrocytes cease to proliferate.

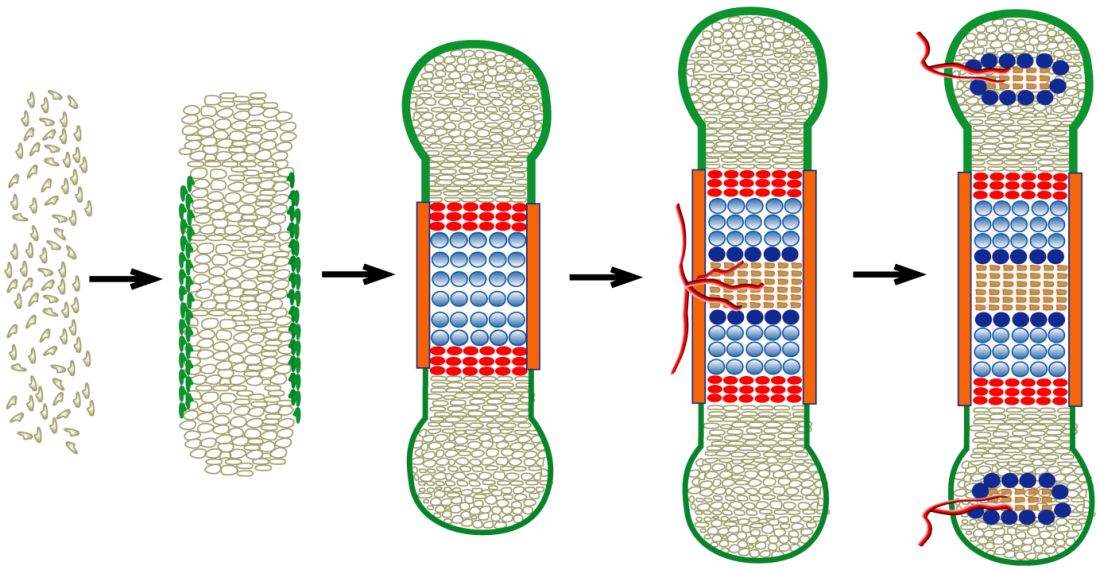

Figure 1. Schematic model of the endochondral ossification process. First mesenchymal cells condense and differentiate into chondrocytes (grey) forming the cartilage anlagen. Perichondral cells (green) surround the cartilage anlagen. In the center of the skeletal element the chondrocytes undergo hypertrophy (prehypertrophic chondrocytes, red; hypertrophic chondrocytes, blue) and secrete a ColX rich ECM. Perichondrial cells adjacent to the hypertrophic zone differentiate into osteoblasts and form the bone collar (orange). Terminal hypertrophic chondrocytes (dark blue) at the diaphyses undergo apoptosis, which allows the invasion of blood vessels and osteogenic cells. Osteoblasts and osteoclasts replace the cartilaginous structure by bone and bone matrix (beige). Postnatally secondary ossification centers develop at the epiphyses. Chondrocytes turn hypertrophic and cartilage canals are formed by invagination of the perichondrium. Blood vessels invade the epiphyses, bringing osteoblasts and osteoclasts, and mineralization starts.

1.2.3 Groove of Ranvier

Bone growth in length is detrimental to bone stability, but this effect is counteracted by concomitant bone growth in width. This is accomplished by the perichondrial groove of Ranvier, a morphological structure surrounding the periphery of the epiphyseal cartilage. Three different groups of cells can be distinguished within the groove. Surrounding the epiphyseal growth-plate region and adjacent to the metaphysis, a group of densely packed cells deep in the groove can be found the osteoblasts progenitors that will form the bone cortex. Towards the center more widely dispersed and relatively undifferentiated mesenchymal cells and fibroblasts, some of which are presumably chondroblast

precursors, can be found. These probably contribute to appositional chondrogenesis and growth in width of the epiphyseal cartilage. Fibroblasts and fibrocytes among sheets of highly oriented and organized collagen fibers form a fibrous layer that is continuous with the outer fibrous layer of the periosteum and perichondrium (Gigante et al., 1996; Karlsson et al., 2009; Shapiro et al, 1977).

1.2.4 Articular cartilage

To allow movement of the body, the skeletal elements articulate in a structure called “joint”. Joints are subdivided into different types based on their anatomical structure, mobility and shape. They are classified in three major groups:

1. **Fibrous** (synarthrodial) - immobile joints.

2**. Cartilagenous** (synchondroses and sympheses) - partially moveable joints.

3. **Synovial** (diarthrosis) - freely moveable joints that are the most common in the skeleton.

Fibrous joints are connected by dense connective tissue, consisting mainly of collagen and are further subdivided into three types: sutures, between bones of the skull; syndesmosis found between long bones, such as radius and ulna, tibia and fibula; gomphosis between the root of a tooth and the sockets. Cartilagineous joints are connected entirely by cartilage, fibrocartilage or hyaline, which consists of a mixture of white fibrous tissue and cartilagineous tissue, and contains Col1 in addition to Col2. They allow more movement between bones than a fibrous joint. The synovial joint is a complex structure consisting of several different tissues and can be subdivided in three major structures.

1. The articular capsule is continuous with the periosteum of bone, is highly innervated but avascular.
2. The articular cartilage lines the epiphyses of joint end of bone and provides the loading and unloading mechanism to resist load and shock.
3. The synovial membrane can be found in the inner layer of the fibrous articular capsule and covers the lining of the synovial cavity where articular cartilage is absent.

Ligaments and tendons support and control movement with the aid of muscles. These are separated from the bones by a bursa, a small fluid-filled sac lined by

synovial membrane. The synovial membrane secretes synovial fluid, which smoothes the friction between the two bone ends. In the knee joint the meniscus, an additional curved part of cartilage, acts as a cushion and distributes the weight. Synovial fluid can be also found in the bursae, providing a cushion between bones, tendons and muscles (Cormack, 1987; Dorland´s medical dictionary 31st ed.; Gray´s anatomy, 2005; Seibel and Woitge, 1999).

During embryogenesis the position of future joints is defined at early stages of development. In the mouse this happens around E10.5, soon after the cartilaginous templates are formed. At first, a yet unidentified inductive signal delimits thin areas of higher cell density called interzones, which consists of elongated cells (Edwards et al., 1994). Several data support the hypothesis that this cell population is prespecified. Removal of the developing skeletal element does not disturb the formation of an interzone, and removal of the presumptive joint before its morphological appearance leads to the fusion of adjacent elements (Holder 1977). Furthermore retroviral overexpression of the signaling factor *Wnt9a*, one of the earliest markers of the interzone, in developing chicken limb bud, results in the formation of a non-cartilaginous skeletal structure, which resembles the interzone (Hartmann and Tabin, 2001). This early joint is maintained by the expression of several genes, especially *Wnt9a* and *Gdf5* (Storm and Kingsley 1999), a growth factor belonging to the bone morphogenetic protein (BMP) family. Perturbance of any of these growth factors involved in joint sustenance results in joint fusion, as joint-forming cell fate is specified but not fixed during development (Khan et al., 2007). Joint cavity development (cavitation) occurs along planes of the future articular surfaces of synovial joints. A number of different markers have been described to be expressed at the time of cavitation. One example is hyaluronan (HA) a glycosaminoglycan found in joint fluid, which has a key role in resisting compressive forces (Edwards et al., 1994). HA and its receptor CD44 are differentially expressed in the interzone and on the articular surface (Archer et al., 1994; Craig et al., 1990; Dowthwaite et al., 1998; Edwards et al., 1994; Pitsillides et al., 1995) and the interaction between HA and CD44 can induce both cell adhesion and cell separation. This mechanism is depending on receptor saturation and HA concentration, with increasing HA amounts leading to cell separation (Toole 1991).

In contrast to growth plate cartilage, articular cartilage remains unmineralized and forms a resilient, low friction surface capable of absorbing shocks due to mechanical loading. It consists of an avascular matrix rich in Col2 and Agc1 and maintained by few chondrocytes. Articular cartilage can be subdivided into three distinct zones based on different characteristics that include cell shape, cell morphology and orientation, and pericellular matrix (PM) deposition (Fig. 2) (Youn et al., 2006). In the superficial zone (SZ) cells are small and elongated in shape. These are oriented parallel relative to the surface, and lack an extensive PM. The middle zone (MZ) is characterized by rounded cells that do not exhibit an organized orientation relative to the surface. Deep zone (DZ) cells are identified by an extensive PM deposition with chondrons in groups of three or more cells arranged in columns oriented perpendicular to the surface (Grogan et al., 2009; Tyyni and Karlsson 2000; Youn et al., 2006).

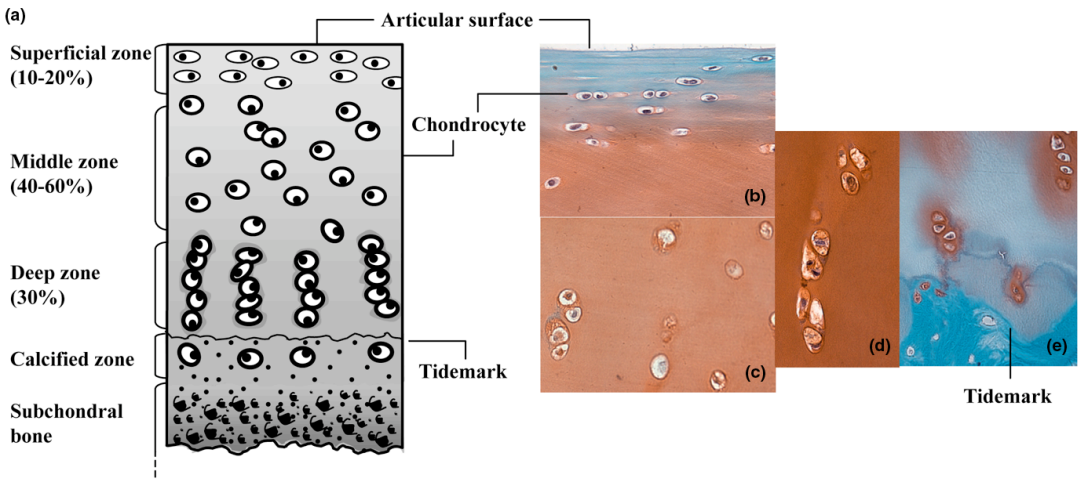

Figure 2. Overview of the structure and zonal architecture of articular cartilage. (a) Schematic representation of the articular surface**.** Each zone can be identified on the base of several characteristics like cell shape, morphology, orientation, and pericellular matrix (PM) deposition. Adapted from Tyyni and Karlsson (2000). Small, flattened cells in the superficial zone (SZ) are arranged parallel to the surface (b), and lack an extensive PM. The middle zone (MZ) is populated by rounded cells which show no orientation relative to the surface (c) They are rich in proteoglycans and show highly-developed PM. Deep zone (DZ) cells are organized in clusters of three or more cells arranged in columns that are oriented perpendicular to the surface (d). They show an extensive PM deposition and are in contact with the calcified zone (e). (Grogan et al., 2009)

1.3 Molecular mechanisms underlying endochondral bone formation

The molecular mechanisms which regulate endochondral ossification comprise a large number of signaling pathways. Different human genetic disorders characterized by abnormalities of the ossification process are linked to functional defects in many of these pathways.

1.3.1 Indian Hedgehog signaling during chondrocyte differentiation

The secreted growth factor Indian hedgehog (Ihh), one of the key regulators of endochondral ossification, is expressed in prehypertrophic and early hypertrophic chondrocytes. Ihh regulates the onset of hypertrophic differentiation interacting with a second secreted growth factor, Parathyroid hormone (PTH) related protein (PTHrP), also known as Pthlh. Ihh signals through its receptor Patched-1 (Ptch1) to the distal periarticular chondrocytes to upregulate the expression of PTHrP. PTHrP in turn signals back to its receptor, the PTH/PTHrP receptor (PPR), expressed in proliferating and prehypertrophic chondrocytes, thereby inhibiting the differentiation of proliferating cells into the *Ihh* expressing prehypertrophic cell type (Lanske et al., 1996; Long et al., 2001; St-Jacques et al., 1999). This negative feedback loop is responsible for slowing down chondrocyte differentiation and maintaining cells in a proliferative state (Fig.3A) (Vortkamp et al., 1996). In addition, Ihh has been shown to play a role in chondrocyte proliferation. $Ihh^{-/-}$ mice show normal mesenchymal condensation but the cartilage elements remain small. In $Ihh^{-/-}$ chondrocytes chondrocyte proliferation is severely decreased (St-Jacques et al., 1999). The regulation of chondrocyte proliferation seems to be independent of PTHrP regulation. Correspondingly, overexpression of a constitutive active PPR in *Ihh* deficient mice can rescue the onset of hypertrophic differentiation but does not increase the proliferation rate (Karp et al., 2000). Therefore *Ihh* signaling seems to have a direct function on the regulation of chondrocyte proliferation. Furthermore targeted deletion of Smoothened ($Smo^{n/n}$), which results in ablation of all Hh signals results in a strong decrease of chondrocyte proliferation, whereas overexpression of *Ihh* or a constitutive activation of *Smo* in chondrocytes leads to an increased proliferation rate (Long et al., 2001; Minina et al., 2001).

Moreover, *Ihh* deficient mice lack osteoblasts in endochondral bones. Although chondrocytes undergo premature differentiation into hypertrophic cells, these are not surrounded by a bone collar. As the ossification of intramembranous bones occurs normally, Ihh seem to be necessary to provide an inductive signal specifically in endochondral bones. Analysis of mice carrying a targeted deletion of *Smo* in the perichondrium supported this idea as $Smo^{n/n}$ perichondrial cells did not differentiate into osteoblasts, whereas mesenchymal cells outside the deletion area formed an abnormal bone collar (Long et al., 2004).

1.3.2 Fibroblast growth factor signaling during chondrocyte differentiation

Several syndromes affecting the normal development of the skeleton have been linked to mutations of the fibroblast growth factor (FGF) signaling. For example Achondroplasia (ACH), which is the most common genetic cause of dwarfism in human, and Thanatophoric dysplasia (TD), which is less frequent than the first but shows a more severe phenotype. Both syndromes arise from mutations, which lead to the constitutional activation of FGFR3, one of four transmembrane receptors of the FGF family (Adviezer et al., 2003; Bonaventure et al., 2007; Dakouane Giudicelli et al., 2007; Lievens and Liboi et al., 2003; Richette et al., 2007; Zoltan et al., 2000; Vajo et al., 2000). A mouse model for ACH, the human mutation of *FgfR*3 ($FGFR3^{ach}$), has been generated, which develops a similar phenotype as the human patients. Analyses of these mice showed that dwarfism is most likely due to a direct effect of FGF signaling on chondrocyte proliferation and differentiation (Naski et al., 1996, 1998; Minina et al., 2002). FGF genes are highly conserved in the evolutionary scale from nematode to human. They all share a core of 120 aminoacids which confer them a common tridimensional structure, associated with the ability to bind heparin, heparin sulfate (HS) and glycosaminoglycan (GAG). FGFs are secreted in the ECM and bind to HS with high affinity, allowing the binding to their tyrosine kinase receptors which in turn dimerize on the cell surface (Courmoul and Deng, 2003; Koga et al., 1999; Olsen et al., 2003; Ornitz and Itoh, 2001). It has been shown that activation of FGF signaling can rescue the phenotype induced by the reduced synthesis of HS. For example, fusion of forelimb synovial joint could be rescued by the constitutional activation of FGFR3 (Koziel et al., 2004). The role of the FGF signaling pathway is

not limited to early ossification stages. Mesenchymal skeletal progenitor cells in the groove of Ranvier have been shown to express *FgfR3* (Robinson et al., 1999). Moreover, analyses of human fetuses affected by ACH or TD confirmed a strong influence of the activated signaling pathway downstream of FGFR3 on the development of the groove of Ranvier (Cormier et al., 2002).

1.3.3 Vascularization of the cartilage anlagen

1.3.3.1 Vascular endothelial growth factor role during ossification

Vascular endothelial growth factor A (VEGF-A) plays a key role during vascularization, being expressed in both cartilage and perichondrium during early development. During the early stages of endochondral ossification the cartilage template is an avascular structure. By interaction of different signaling pathways it develops into a highly vascularized element, the marrow cavity (Karsenty and Wagner, 2002). When chondrocytes turn hypertrophic, they start to produce angiogenic factors, inducing the first capillary invasion of the cartilage template (Colnot and Helms, 2001; Zelzer et al., 2001). The vasculature supplies the template with cells belonging to the osteoblast and osteoclast lineage (Zelzer et al., 2002; Colnot et al., 2004). *Vegf-A* inactivation impairs vascular invasion, thereby disturbing subsequent steps of endochondral ossification (Colnot et al., 2004; Fenwick et al., 1997; Gerber et al., 1999; Maes et al., 2002; Zelzer et al., 2001, 2002). VEGF-A belongs to the family of VEGF related molecules, which in mammals consists of VEGF-A to F and placenta growth factor. Human *VEGF-A* can be alternatively spliced into 5 different isoforms of 121, 145, 165, 189 and 206 amino acids. The respective isoforms are each one amino acid longer than the murine counterparts (Houck et al., 1991; Tischer et al., 1991). They have a biological role in endothelial cell (EC) proliferation, migration and osteoclastogenesis (Cramer, 2004; Houck 1992; Poltorak, 1997; Wise and Yao, 2003). VEGF-A^{165} is the most abundant isoform of VEGF-A and transgenic mice expressing only the correspondent isoform (VEGF-$A^{164/164}$) display normal vascular development, whereas mice expressing only the VEGF-A^{120} isoform are characterized by a delayed recruitment of EC into the perichondrium and delayed blood vessel invasion into the primary ossification center (Maes et al., 2002, 2004; Zelzer et al., 2002, 2004). *In vitro* experiments have shown that chondrocytes

cultured under hypoxic conditions are stimulated to produce VEGF-A^{165} (Pfander et al., 2003). Although VEGF-A^{189} stimulates EC proliferation and migration *in vitro* (Herve et al., 2005), VEGF-$A^{188/188}$ mice show dwarfism, impaired development of endochondral bones and knee joint dysplasia, leading to the conclusion that this isoform might not play a key role during embryonic development, especially with regard to chondrocytes differentiation (Maes et al., 2004).

1.3.3.2 VEGF Receptors

The biological response to VEGF signaling is mediated by at least three receptors (VEGFR1/Flt1, VEGFR2/Flk1 and VEGFR3/Flt4). These synergistically interact with HS and 2 co-receptors neuropilin (Nrp1 and Nrp2). VEGFR1-3 belong to the Platelet derived growth factor receptor subfamily of receptor tyrosine kinases (RTKs) (Fig. 4) (Ferrara et al., 2003). VEGFR1 (or fms-like tyrosine kinase receptor1 (Flt-1)) is a 180 kDa transmembrane protein. Evidences suggest that it might regulate angiogenesis in two ways. It might act as a negative mediator, via its ligand binding domain interacting with VEGFR2 (or kinase insert domain-containing receptor (KDR)/fetal liver kinase 1 (Flk-1)), and as a positive mediator, via its tyrosine kinase domain (Gille et al., 2001). Supporting data comes from *in vitro* studies of *VEGFR1*$^{-/-}$ embryonic stem cells, in which the differentiation into EC is increased, but increased VEGFR2 phosphorylation causes these cells to assemble into abnormal vascular channels (Fong et al., 1995; Roberts et al., 2004). Moreover, VEGFR2-induced EC proliferation can be inhibited by VEGFR1 (Zeng et al., 2001). VEGFR2, is a 230 kDa glycoprotein which has been proposed to play a major role in the biological response of ECs to VEGF signaling (Neufeld et al., 1999). VEGFR2 is mainly located on the surface of ECs and its phosphorylation on several intracellular sites can initiate signaling, leading to EC proliferation, migration and angiogenesis *in vivo* (Hutchings et al., 2003). Deletion of VEGFR2 leads to embryonic lethality, due to impaired vasculogenesis and hematopoiesis (Shalaby et al., 1995). VEGFR3 (or fms-related tyrosine kinase 4(flt4)) is mainly expressed by veins and lymphatic vessels (Adams and Alitalo, 2007) and the expression of soluble VEGFR3 in the skin inhibits fetal lymphangiogenesis (Makinen et al., 2001a). Nrp1 and 2 have been identified as VEGF co-receptors and belong to the non-tyrosine kinase transmembrane receptors, with a small cytoplasmatic domain and multiple extracellular domains

(Soker, 1998). Although they lack an intracellular signal transduction domain, Nrp1 and 2 have an active role as mediator in immune response, neuronal development and angiogenesis (Klagsbrun et al., 2002). Nrp1 is involved in angiogenesis and in bone formation. It has a high affinity for VEGFR2 (Shraga-Heled et al., 2007) and induces the formation of extra-digits when overexpressed (Kitsukawa et al., 1997). NRP2 acts mainly on lymphangiogenesis (Yuan et al., 2002).

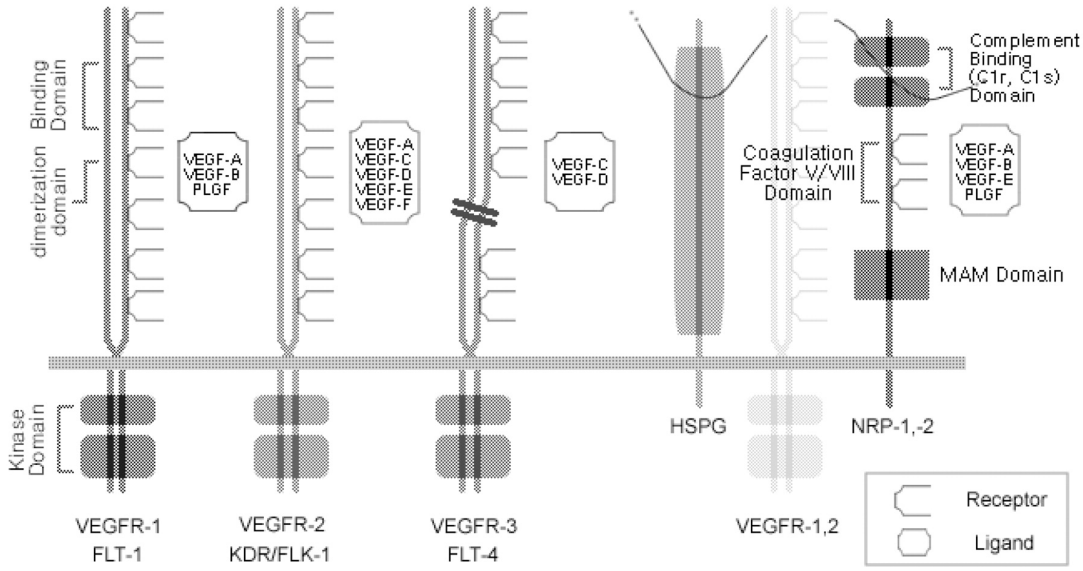

Figure 4. Schematic representation of the VEGF receptors and their ligands. The tyrosine kinase receptors (VEGFR-1/Flt-1, VEGFR-2/KDR/Flk-1, VEGFR-3/Flt-4) have 7 extracellular immunoglobulin (Ig)-like domains. The second and third Ig-like domains bind to VEGF. The fourth Ig-like domains interact directly with each other in a ligand-induced receptor dimerization. The extracellular domain is followed by a single transmembrane region and an intracellular tyrosine-kinase domain. Interactions of VEGFRs with either Nrps or HS (HSPG) facilitate the binding of VEGF to its receptor. Preferential ligand-receptor bindings are indicated (Dai and Rabie, 2007).

1.4 Heparan sulfate role during endochondral ossification

1.4.1 Heparan sulfate biosynthesis

Heparan sulfate proteoglycans (HSPGs) are a major component of the extracellular matrices. HSPGs are large macromolecules composed of heparan sulfate glycosaminoglycan (HS-GAG) chains. These are linear polysaccharides composed of alternating sugar residues of D-glucuronic acid (GlcA) and N-acetyl-D-glucosamine (GlcNAc), linked to a protein core (Zhang and Esko, 1994). Core proteins are subdivided into extracellular matrix core proteins like Agc1 and

perlecan (Hspg2), and membrane-associated core proteins such as syndecans (Sdc1–4), glypicans (Gpc1–6), and CD44. HS biosynthesis is a complex process involving, among others, multiple glycosyltransferases, sulfotransferases and an epimerase. Together, they are responsible for the elongation and modifications of the GAG chains (Fig. 5). The first step of HS biosynthesis is the transfer of xylose from UDP-xylose by xylosyltransferase to specific serine residues within the PG core polypeptide. Galactosyltransferases I and II attach two galactose (Gal) residues and glucuronosyltransferase I completes the formation of a core protein linker tetrasaccharide by adding a GlcA residue. This linker sequence is common to chondroitin sulfates (CS) and HS. In the next step, exostosin like 2 (EXTL2) defines the polymerization of HS rather than CS by adding a single GlcNAc residue (Kitagawa et al., 1999). Upon this the glycosyltransferases complex consisting of Exostosin1/2 (EXT1/2) catalyzes the addition of alternating units of GlcA and GlcNAc residues (Lind et al., 1998; McCormick et al., 1998). Subsequent to the polymerization of the GAG chains, the individual sugar residues undergo further modification, that include GlcNAc *N*-deacetylation and *N*-sulfation (*Ndst1–4*), C5 epimerization of GlcA to iduronic acid (*Glce*), *O*-sulfation at C2 of iduronic acid and GlcA (*Hs2st*), and *O*-sulfation at C6 of GlcNAc and GlcNS (*Hs6st1–3*). These modifications generate tissue specific patterns of differentially sulfated motives, resulting in the formation of specific growth factor binding sites. (Bernfield et al., 1999; Esko and Lindahl, 2001; Lander and Selleck, 2000; Lindahl et al., 1998).

HS binds to a variety of protein ligands, as growth factors, extracellular enzymes and cytokines and regulates a wide range of biological activities, including development, angiogenesis, blood coagulation and tumor metastasis (Esko and Selleck, 2002). HS also binds with high affinity to FGF and is required for the diffusion of several morphogens, including Ihh, Bone morphogenetic proteins (BMPs) and Wnt.

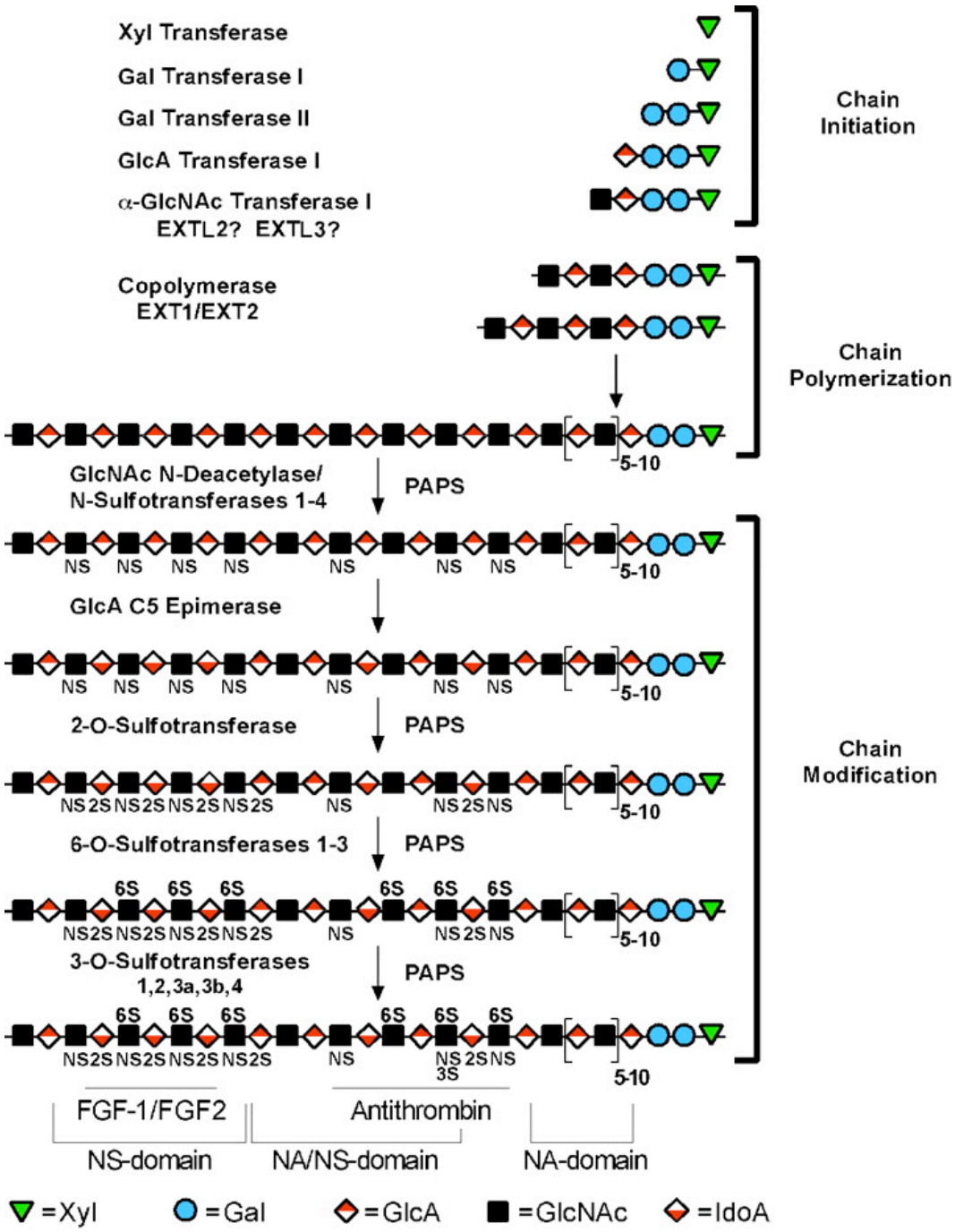

Figure. 5. Schematic representation of heparan sulfate synthesis and modification. GAG side chains are attached to specific serine residues of core proteins. GAG synthesis is initiated by the addition of a common tetrasaccharide linker (-Xyl-Gal-Gal-IdoA-). HS synthesis starts by adding *N*-acetyl-D-glucosamine (GlcNAc) to the linker by *Extl2*. The HS chain is elongated by alternate addition of glucuronic acid (GlcA) and GlcNAc by the EXT1/2 complex. The nascent HS chains undergo modifications including N-deacetylation/N-sulfation, epimerization, and O-sulfation (6-O; 3-O and 2-O sulfation), generating tissue specific patterns of differentially sulfated motives. (NS, C2-*N*-sulfation; 2S, C2-*O*-sulfation; 6S, C6-*O*-sulfation). (Esko and Selleck, 2002)

1.4.2 Multiple Osteochondromas syndrome

Multiple osteochondromas (MO) syndrome is an autosomal dominant disease characterized by the formation of benign bone tumors at the distal ends of long bones, which are also known as exostoses (Ahn et al., 1995; Stickens et al., 1996). Osteochondromas develop and increase in size during childhood and cease to grow when the growth plate closes at puberty. Morphologically, they consist of a bony stalk which is in contact with the cortical bone and the bone marrow and is flanked by a cartilage cap at the distal end (Fig. 6B). Histological analyses revealed that chondrocytes from the cartilage cap show a similar cellular organization as the growth plate. Most osteochondromas develop predominantly around the knee and vary widely in size. Osteochondromas can be peduncolate or sessile, with a broad base (Hennekam, 1991). Complications of the syndrome include osseous deformities, bursa formation and arthritis. Furthermore, impingements on adjacent tendons, nerves, vessels or the spinal cord have been observed (Vanhoenacker, 2001; Wicklung et al., 1995). In up to 5% of human patients osteochondromas can transform into malignant osteochondrosarcomas (Gordon et al., 1981; Legeai-Mallet et al., 1997; Peterson, 1989; Schmale et al., 1994; Wicklund et al., 1995;). Furthermore MO syndrome has been linked to mutations in two main loci, *EXT1* on chromosome 8q24.1 (Ahn et al., 1995; Lüdecke et al., 1997) and *EXT2* on chromosome 11p11-p12 (Bovée et al., 1999; Wuyts et al., 1998, Wuyts and Van Hul, 2000).

The severity of the MO phenotype is defined by the degree of stature shortening, the number of tumors and the severity of skeletal deformities. A genetic screen revealed that mutation in either *EXT1* or *EXT2* could be identified equally and occurred in 83% of the human patients. Interestingly, the more severe phenotypes have been correlated to mutation in *EXT1* rather than *EXT2* (Fig.6A) (Porter et al., 2004). Human EXT1 and EXT2 are ubiquitously expressed proteins of 746 and 718 amino acids, respectively. They are highly conserved displaying a 70% homology on protein level (Ahn et al., 1995; Wuyts et al., 1996). Both proteins are glycosyltransferases with a predicted type II transmembrane glycoprotein structure (Lind et al., 1998; McCormick et al., 1998). *In vitro* studies have shown that EXT1 and EXT2 co-localize at the Golgi membrane, forming a heterodimeric complex, which promotes the elongation of HS chains (McCormick et al., 2000). Mutations in both genes are occurring mainly in evolutionarily highly conserved residues that

are crucial for the activity of the protein. Approximately 80% of the mutations are either nonsense, frameshift, or splice site mutations leading to premature termination of EXT proteins (Francannet et al., 2001; Park et al., 1999; Raskind et al., 1998; Seki et al., 2001; Wuyts et al., 1998; Xu et al., 1999;). The majority of missense mutations also lead to defective EXT function (Cheung et al., 2001) (Fig.6C).

Osteochondromas have for a long time been considered the consequence of skeletal dysplasia. It is now generally accepted that exostoses are neoplastic, as somatic mutations have been found within the cartilage cap. As mutations are autosomally dominant inherited, the *EXT* genes has been considered as a tumor suppressor gene. Correspondely loss of heterozigosity has been demonstrated in the cartilage cap of osteochondromas from MO patients (Bovée et al, 1999, Hameetman et al., 2007). However, this second mutation could not be detected in all MO patients, raising the question for the initial event in the development of the disease.

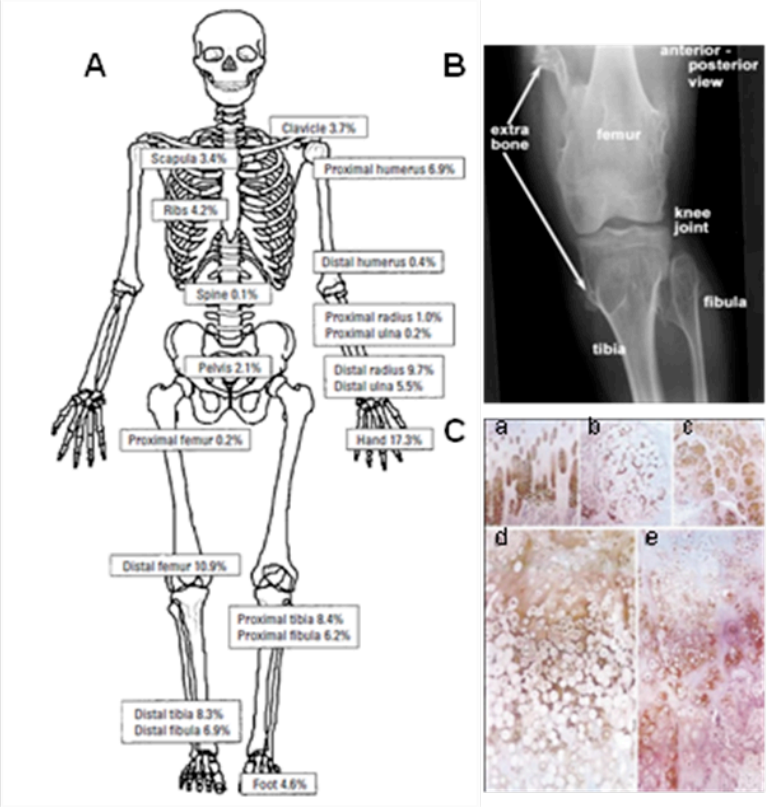

Figure 6. Human phenotype of osteochondromas syndrome. (A) Percentage and distribution of palpable osteochondromas found in a study conducted by Porter and colleagues on 172 individuals affected from MO (Porter et al., 2004). (B) X-ray analysis of a knee joint from a 15 years old patient affected by MO. Osteochondromas (indicated as "extra bone") develop as bony projections at the epiphyseal side of tibia and femur. (John Csongradi, National health museum). (C) Immunostaining with a Perlecan antibody. Strong staining is detected around control chondrocyte lacunae and minimal staining around the plasma membrane and the pericellular matrix (C: a). Staining in osteochondromas has no consistent pattern and the lacunae are not heavily stained (C: b-e)(Hecht et al., 2002, modified).

1.4.3 *Ext* genes in endochondral ossification and osteochondromas mouse models

In situ hybridization of *Ext1* and *Ext2* showed that both genes are strongly expressed in the developing mouse limb bud, with expression confined to the regions of proliferating and prehypertrophic chondrocytes in the growth plate (Stickens et al., 2000). In human osteochondromas *EXT* gene expression is reduced corresponding to their mutational status. As a consequence, HS seems to accumulate in the cytoplasm of the cell, instead of being transported to the cell

surface (Hameetman et al., 2007). In the attempt to study the role of EXT proteins *in vivo*, different mouse models have been generated. Homozygous *Ext1*$^{-/-}$ and *Ext2*$^{-/-}$ mice cannot synthesize HS and die around E9, before gastrulation is completed (Stickens et al., 2005; Lin et al., 2000). *Ext1*^{Gt} mice carry an insertion of a gene trap vector in the first intron of *Ext1* that leads to the generation of a non-functional truncated protein. *Ext1*$^{Gt/Gt}$ mutant survive until E16.5 (Koziel et al., 2004; Lin et al., 2000). In contrast to human MO patients, heterozygous *Ext1*$^{+/-}$, *Ext1*$^{+/gt}$ or *Ext2*$^{+/-}$ mutants do not develop exostoses at the appendicular skeleton. However *Ext2*$^{+/-}$ mice develop small exostoses at the costochondral cartilage of the ribs with low frequency (28%) (Stickens et al., 2005). Recent analyses of *Ext1*$^{Gt/Gt}$ mice helped to elucidate how the *Ihh* signal reaches the joint region to induce the expression of *PTHrP*. Initially, secondary factors have been hypothesized to mediate the *Ihh* signal. The phenotype of *Ext1*$^{Gt/Gt}$ mice strongly support a model in which heparan sulfate (HS) negatively regulates the propagation of Ihh in the cartilage anlagen, acting Ihh as a long range morphogen directly inducing the expression of *PTHrP*. Early stages of chondrocytes differentiation are perturbed in *Ext1*$^{Gt/Gt}$ mice, due to disturbed *Ihh* signaling. (Fig.3B)(Koziel et al., 2004).

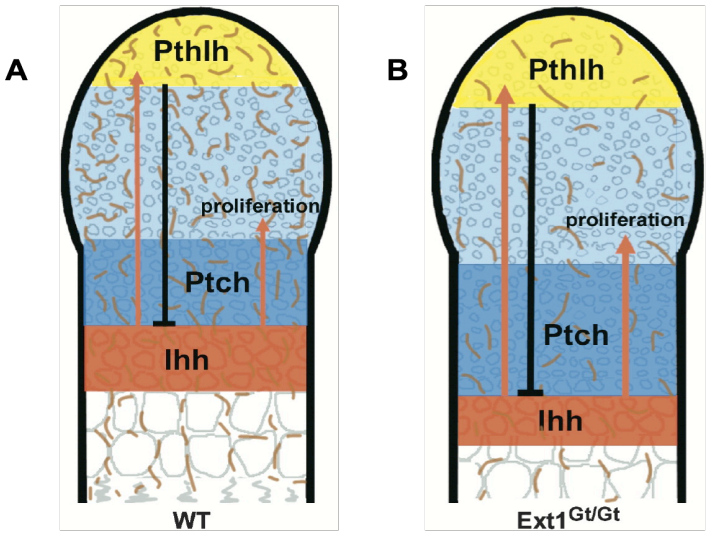

Figure 3. Ext1-Dependent HS regulates *Ihh* signaling. (A) Ihh, expressed in prehypertrophic chondrocytes (red), travels through the cartilage anlagen to directly activate the expression of *PTHrP* (*Pthlh*, yellow). *Ihh* signaling induces strong *Ptch1* expression (dark blue) in columnar chondrocytes flanking the *Ihh* expression domain and weaker *Ptch1* expression in distal chondrocytes including the periarticular, *PTHrP*-expressing cells (light blue and yellow) (Vortkamp et al., 1996). HS (brown) negatively regulates the propagation of the *Ihh* signal. (B) Reduced amount of HS in *Ext1*$^{Gt/Gt}$ mutants facilitates Ihh diffusion and leads to an increased domain of strong *Ptch1* expression and

upregulation of *PTHrP*. PTHrP in turn delays the onset of hypertrophic differentiation (Koziel et al., 2004).

The cellular origin of osteochondromas has not been identified yet and different cell types have been discussed. In human patients, homozygous loss of *EXT* function has been identified within the cartilage cap, suggesting a chondrogenic origin (Hameetman et al., 2007). Alternatively previous experiments have shown that an injury at the site of the perichondrium leads to the formation of solitary osteochondromas-like structures, pointing to a perichondrial cell as the origin of exostoses (Delgado et al., 1987). As a rival model the perichondrial groove of Ranvier acts as a reservoir for chondrocyte and osteoblast progenitors and cells from this structure have been discussed as candidate for the origin of cartilage tumors (Cormier et al., 2002; Gigante et al., 1996; Robinson et al., 1999, 2001)

1.4.4 Arthritis

About 14% of human patients affected by MO develop arthritis (Wicklung et al, 1995), which is the primary cause of degenerative joint diseases. It is characterized by breakdown and eventual loss of the cartilage at the articular surface due to trauma, infection or biochemical defects. The two most common types of arthritis are Osteoarthritis (OA) and Rheumatoid arthritis (RA). OA is caused by the breakdown of joint cartilage, which causes bone ends to grind against each other. Usually, OA affects a single joint. RA on the other hand, is a chronic, inflammatory type of arthritis, which affects multiple joints. It is also classified as an autoimmune disease, as immune cells attack the body's own healthy tissues (Roche Lexicon Medicine, 1987). The synovium is primarily affected by RA, but other organs can be affected as well (Hunziker, 2002; Solchaga 2001). OA is the most common human joint disorder, highly reducing quality of life and impairing movement by acute and chronic pain (Koopman, 1997; Resnick, 2002). Degradation of the cartilage matrix is associated with increased proteolysis of proteoglycan and collagen. A typical symptom of OA is the increased expression and synthesis of matrix degrading enzymes, like Mmps and aggrecanases, in synovial tissue and cartilage (Lark et al., 1997; van Lent et al., 2005; Valverde-Franco et al., 2006). This leads to the degradation of Agc1 of the articular cartilage into specific catabolic fragments, which accumulate in the extracellular matrix. These fragments can be detected by antibodies against

degradation specific epitopes, known as VDIPEN and NITEGE, referring to the amino acid sequence produced by Mmp or aggrecanase cleavage.

Agc1 degradation has been intensely studied during the past few years (Fosang et al., 1995; Lark et al., 1997; Mercuri et al., 1999; Valverde-Franco et al., 2006; Westling et al., 2002). Several transgenic models have been used to identify possible predisposition causes and to understand the mechanisms underlying the development of OA. An increase in *ColX* expression, apoptosis of chondrocytes, large lacunae and faint staining for proteoglycans are common symptoms of OA (Pirog-Garcia et al., 2007; Valverde-Franco et al., 2006; van Lent et al., 2005).

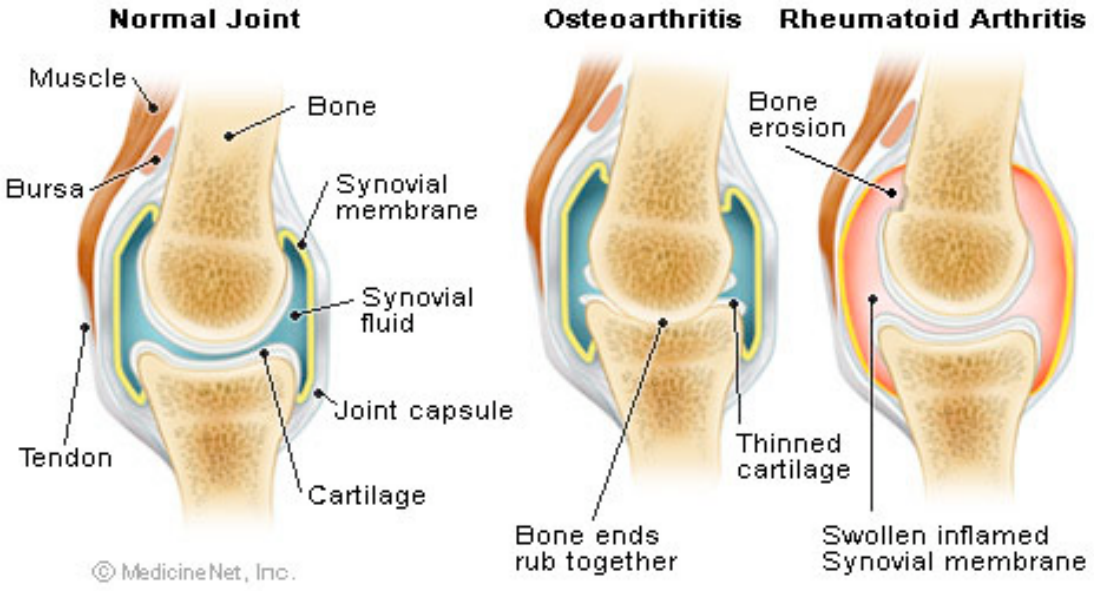

Figure 7. Healthy and arthritic joints. A normal, healthy joint allows movement by smooth sliding of the two articular surfaces, lubricated by a synovial fluid. Arthritis modifies the articular surface of bones. In Osteoarthritis loss of cartilage brings the two bone ends to rub against each other, causing friction. In Rheumatoid arthritis, chronic inflammation as consequence of autoimmunoresponse leads to the destruction of cartilage, bone, and ligaments, causing deformity of the joints (Medicinenet.com, retrieved on 11th November, 2009).

2. Aim of the study

'Multiple Osteochondromas' (MO) is an autosomal dominant inherited human disorder characterized by short stature and cartilaginous-capped benign bone tumors, also known as exostoses. These develop in juxta-epiphyseal position of the growth plate of actively growing bones and remain connected to the bony shaft (Bovée et al., 2008). In most MO patients (>90%) heterozygous mutations in the genes, Exostosin1 (*EXT1*) and *EXT2*, respectively, have been identified (Ahn et al., 1995; Stickens et al., 1996). Homozygous deletion of *Ext1* or *Ext2* in mice results in lack of HS biosynthesis. These mice die at E9.5 due to defects in mesoderm formation. In contrast to human MO patients, heterozygous $Ext1^{+/-}$ or $Ext2^{+/-}$ mutants do not develop exostoses in the appendicular skeleton.

The cellular origin and the molecular mechanism inducing osteochondroma development have been controversially discussed for many years and different studies came to different conclusions (Bovée et al., 1999; Hall et al., 2002).

In this study, two different transgenic mouse models will be analyzed to identify the origin of osteochondroma, $Ext1^{Gt/+}$ mice carrying a hypomorphic *Ext1* allele and produce reduced amounts of heparan sulfates. Homozygous mice survive until E16.5 (Yamada et al., 2004). Early stages of chondrocytes differentiation are disturbed in $Ext1^{Gt/Gt}$ mice, as Ihh protein traveling along the cartilage anlagen is facilitated by reduced amount of HS (Koziel et al., 2004). In addition to regulating chondrocyte differentiation, *Ihh* signaling also regulates osteoblast differentiation and vascularization of the cartilage elements (Joeng and Long, 2009; Kinto et al., 1997). Therefore, the effect of HS on the differentiation of osteoblasts and osteoclasts should be investigated in $Ext1^{Gt/Gt}$ mutants. As vascularization is an important step during endochondral ossification, the distribution of blood vessels and the migration of endothelial cells will be analyzed in the $Ext1^{Gt/Gt}$ mutants.

As mentioned previously, $Ext1^{-/-}$ mice die prior to bone formation and $Ext1^{Gt/+}$ mice do not develop exostoses. To investigate the molecular origin of osteochondromas, we used a mouse line carrying a conditional deletion of *Ext1* allele ($Ext1^{e2fl}$). Homozygous $Ext1^{e2fl/e2fl}$ mutants were crossed to mice carrying a Cre recombinase allele, which is expressed under the control of a doxycycline inducible *Col2* promoter (*Col2-rtTA-Cre*) (Grover and Roughley, 2006). To clarify if loss of heterozygosity or haploinsufficiency leads to osteochondromas

development small clones of cells will be isolated by laser microdissection and genetically analyzed for their allelic status and HS content to understand the role of HS during osteochondromas development.

3. Material and methods

3.1 Material

3.1.1 Chemicals

All chemicals, if not noted otherwise, were purchased from the companies Merck, Sigma or Roth.

- Acetic anhydride (Sigma)
- Agar (Difco)
- Agarose (Gibco BRL)
- Betaine (N,N,N –trimethylglycine) (Sigma)
- Chondroitinase ABC (Sigma)
- CTP, GTP, ATP, UTP (Roche)
- Dextran Sulfate (Sigma)
- DNAse (deoxyribonuclease), RNAse free (Roche)
- dNTPs (2'-Deoxynucleoside 5'-triphosphates) (Roche)
- Dream *Taq*-Polymerase (Fermentas (St. Leon-Rot))
- DPX Mountant for histology (Fluka)
- Ethidiumbromide (Serva, Heidelberg)
- Ficoll 400 (Pharmacia)
- Glass coverslips (Menzel-Glaeser, Germany)
- Glutaraldehyde (Sigma)
- Glycogen (Roche)
- Hyaluronidase I form bovine testis (Sigma)
- Kaisers Gelatine (Merck)
- Paraffin-paraplasts (Sherwood Medical Co, USA)
- PEG 4000: polyethylenglycol (MBI Fermentas)
- PFA (Paraformaldehyde) (Merck)
- Proteinase K (Roche)
- [P33]-UTP (radioactive Uridintriphosphat) (Hartmann Analytik (Braunschweig))
- Random primer: pd(N)6 Random Hexamer 5’-Phosphate (Invitrogen)
- Restriction endonucleases (NEB, Roche)
- Ribonuclease A, RNAse A (Roche)

- RNAse inhibitor (Roche)
- Superfrost plus slides (Menzel-Glaeser, Germany)
- Taq-DNA polymerase (Eppendorf)
- TEA, triethanolamine (Merck)
- Tissue culture dish 60x15 mm (Falcon)
- Toluidine Blue O (Sigma)
- Tryptone (Difco)
- T7, T3, SP6 RNA-polymerase (Roche)
- T4 DNA Ligase 400U/µl (New England Biolabs)
- (3-aminopropyl)triethoxysilane (Sigma)

3.1.2 Technical equipment

Technical equipment	Manufacturer
- 20°C-freezer	Liebherr, Bosch
- 80°C-freezer (HERAfreeze)	Thermo
-152°C	Sanyo
Agitator	VWR, Heidolph
Automatic tissue processor	Mikrom
Laboratory scales	Mettler Toledo
Bacteria agitator	Infors
Bacteria incubator	Memmert
Bench centrifuge	Eppendorf, Hettich
Beta/gamma (Geiger) counter (COMO)	S.E.A.
Camera for microscope	Visitron Systems
Cell culture microscope	Leica
Cryostat	Mikrom
Developing machine for film (Curix 60)	AGFA, Leverkusen

Electrophoresis chamber	Angewandte Gentechnologie Systeme
Embedding station	Leica
Gel imager	INTAS
Heat block	Eppendorf, HLC
Hotplate for sections	MEDAX
Hybridization oven	Unitherm
Incubator	Labotect
Luminometer (Centro LB 960)	Berthold Technologies
Magnetic stirrer	Heidolph
Microscope	Leica
Microtome	Mikrom
Microwave	Sharp
pH-Meter	Hanna Instruments
Nanodrop	Peqlab
Pipet-Boy	MATRIX
Pipettes	Eppendorf,
Powersupply	Biometra
Refrigerators	Bosch
Steril hood (HERA safe, MSC-Advantafe)	Thermo, BDK
Stereomicroscope	Zeiss
Thermocycler	Eppendorf, Biometra, Göttingen
Vortex shaker	Scientific Industries
Water system (Milli-Q System)	Millipore, Schwalbach
Water bath	GFL, Thermo

Waterbath for sections	MEDAX

Cell culture consumables were purchased from Corning and Falcon.

3.1.3 Software

CLC-bio Version 4.01
INTAS GDS
Microsoft Office2007 12.0
MicroWin 2000, Version 4.41
Spot Advanced Version 4.5.7

3.1.4 Buffers and Solutions

- 0.001% Fast Green (FCF) Solution: 0.01 g Fast green, 1000 ml Distilled water
- 0.1% Safranin O Solution: 0.1 g Safranin O, 100 ml Distilled water
- 0.1M Sodium Acetate Buffer, pH4.2: 1.36 g Sodium acetate, trihydrate, 100 ml Distilled water. Mix to dissolve and adjust pH to 4.2 using concentrated glacial acetic acid
- 1% Acetic Acid Solution: 1 ml Acetic acid, glacial, 99 ml Distilled water
- 1% Aqueous Silver Nitrate Solution: 1 g Silver nitrate, 100 ml Distilled water
- 5% Sodium Thiosulfate: 5 g Sodium thiosulfate, 100 ml Distilled water
- 25% EDTA: 250gr Triplex III, 60ml 10M NaOH, 1 liter distilled water, to pH7.4
- Alcian blue staining solution (Skeletal staining): 15 mg Alcian blue 8 GX (Sigma), 80 ml 95% Ethanol, 20 ml Glacial acetic acid
- Alizarin red staining solution (Skeletal staining): 50 mg Alizarin Red (Sigma), 1 liter 1% KOH
- Alcian blue solution (Micromasses): 0.05% Alcian blue 8 GX (Sigma), in 75% EtOH: 0.1M HCl (4:1)
- Collagenase digestion solution: 0.3 U/ml Collagenase NB4 (Serva) in sterile 1XPBS containing 5% FCS and 0.05% Trypsin-EDTA (Invitrogen).
- Endothelial cell medium: Endothelial basal medium MCDB 131 (PAA U15-011) was supplemented with 20%FCS (Invitrogen-Gibco), 50U/ml Penicillin/50µg/ml Streptomycin (Invitrogen-Gibco), 10µg/ml Hydrocortisone (Sigma, water soluble H-0396), 80µg/ml endothelial cell growth supplement (ECGS from bovine pituitary Sigma E0760).

- Gel-loading-buffer (10x): 15% Ficoll (Type 400); 0,25% Bromphenolblue; 6 mM EDTA,pH 8.0
- Hybridization buffer: 50% Formamid; 3 M NaCl; 20 mM Tris-HCl; pH 7.4; 5 mM EDTA;
- Kodak-developer D-19 (Kodak, USA)
- Kodak-fixer (Kodak, USA)
- Kodak Scientific Imaging Film (Kodak, USA)
- LB medium (Luria Bertrani): 1% tryptone; 0,5% yeast extract; 1% NaCl, pH 7.0
- LB agar: 15g agar per 1L LB-medium
- Methyl Green Solution (0.5%): 0.5 g Methyl green (ethyl violet free from Sigma), 100 ml 0.1M Sodium acetate buffer, pH4.2
- MACS Cell isolation buffer: 1xPBS supplemented with 0.5% BSA and 2mM EDTA
- Micromass culture medium: DMEM/F12 (Invitrogen (Gibco)) supplemented with 10%FCS and 50U/mlPenicillin/50µg/mlstreptomycin
- Paraformaldehyde 4% (w/v) in PBS
- PBS (Phosphat Buffered Saline): 1.5 mM KH2PO4; 140 mM NaCl; 3 mM KCl; pH 7.4
- Photoemulsion (autoradiography emulsion type NTB2) (Kodak, USA)
- Proteinase K: 10mg/ml resuspended in 50 mM Tris-HCl, pH 8,0; 1 mM CaCl2,
- RNAse free water (DEPC water) 0.1% DEPC (Diethylpyrocarbonat)
- Scott's buffer (10g MgSO4, 2g Natriumbicarbonate in 1000 ml H2O)
- SOC medium: 2% tryptone; 0.5% yeast extract; 10 mM NaCl, 2.5 mM KCl, 10 mM
MgCl2 and 20 mM glucose
- SSC (standard saline citrate, 20x): 300 mM Sodium citrate; 3 M NaCl; pH 7.0
- TAE-buffer (50x): 2 M Tris, pH 7,5 - 8,0; 50 mM EDTA
- Transcription buffer (10x): 0.4M Tris-HCl, pH 8,0; 60 mM MgCl2; 100 mM dithiothreitol,
- Toluidine Blue: 1 g Toluidine Blue O, 2 g Sodium Borate (Borax), 100 ml Distilled Water
20 mM spermidine (Roche)
- Washing buffer (10x): 4 M NaCl; 0.1M Tris-HCl; 0,05 M EDTA; pH 7.5
- Weigert's Iron Hematoxylin Solution: Mix equal parts of stock solution A and B (ready to use).

- Y-Eosin: 100ml Eosin; 0.5ml Glacial acetic acid

3.1.5 Kits

- DAB-staining kit (Pierce)
- EVA Green PCR Master Mix (Bio Budget)
- Nucleospin-RNA isolation (Macherey Nagel)
- Plasmid Midiprep kit (Qiagen)
- qRT-PCR-Kit: Superscript III (Invitrogen)

3.1.6 Protein names and their synonyms

PTHLH, parathyroid hormone-like hormone: PTH-like; parathyroid hormone related protein (PthrP); parathyroid hormone-related peptide; PTH-related peptide
PTHR1, parathyroid hormone receptor: PPR/PTH-related peptide receptor; PTH/PTHrPR
BGLAP1, bone Gla protein: Osteocalcin mOC-A/ OG1
VEGF: vascular endothelial growth factor: VEGF-A splice variant A
VEGFR1, VEGF receptor 1: Flt1, fms-like tyrosine kinase receptor1
VEGFR2, VEGF receptor 2: KDR, kinase insert domain-containing receptor, Flk-1, fetal liver kinase 1
NRP1, neuropilin 1

3.1.7 Bacterial strain

Escherichia coli DH5aTM. Genotype : F-f80dlacZDM15 D(lacZYAargF)U169 deoR recA1 endA1 hsdR17(rk-, mk +) phoA supE44 1-thi-1 gyrA96 relA1(Gibco BRL, Karlsruhe).

3.1.8 Mouse lines

Ext1$^{Gt/Gt}$ mice (official designation, *Ext1Gt*(*pGT2TMpfs*) *064Wcs*) were provided by Olivia G. Kelly and William C. Skarnes (Mitchell et al., 2001). *Ext1*$^{e2neofl/\ e2neofl}$ (official designation, *Ext1*$^{tm1.1Kjns}$) were provided by Kevin B. Jones (Jones et al., 2010).

3.1.9 Mouse and rat DNA probes for in situ transcription

Probe, Vector, Insert size (basepairs: bp), DNA Endonuclease (for antisense), RNA polymerase (for antisense), Reference

rCol2, pGEM-3Z, 550 bp, *Hind* III, T7, (Kohno et al., 1984)

mCol X, pBSK+, 400 bp, *Cla* I, T3, (Jacenko et al., 1993)

Mmp13, pCR-TOPO21, 1000 bp, *Hind* III, T7, (Yamagiwa et al., 1999)

Bglap1, pBSK, 500 bp, *Xba* I, T3, (Celeste et al., 1986)

mIhh, pBSK, 1800 bp, *Xba* I, T7, (Bitgood and McMahon, 1995)

mPtch1, pBSK, 5000 bp, *BglII*, T7, (Goodrich et al., 1996)

Ucma pBSK, 417 bp, Not I T3, (Tagariello et al., 2008)

Vegf-A pCR-TOPO21, 300 bp, Hind III, T7 (Stricker et al., 2002)

Flt-1 pBSK+, 1.6Kb, BAM HI, T7 (Finnerty, 1993)

Flk-1 pBSK+, 1 KB, BAM HI, T7 (Quinn, 1993)

Nrp1 pCR-TOPO21, 831 bp, Hind III, T7 (was a kind gift of Dr. Elazar Zelzer)

3.2 METHODS

3.2.1 Doxycycline administration

Expression of Cre-recombinase in Col2-rtTA-Cre mice was induced either by administration of 4 mg/ml doxycycline in 5% sucrose through the drinking water of the lactating mother at P8 for 8 days or by intraperitoneal injection of doxycycline (80 µg/gram body mass) in 1xPBS into lactating mothers at P8.

3.2.2 Quick preparation of genomic DNA for mouse genotyping

Small pieces of mouse tails were incubated in 200 µl Viagen direct PCR-Tail (PeqLab Biotechnology GmbH) with 0.2 mg/ml Proteinase K at 55 °C overnight. After inactivation at 85°C for 45 minutes, PCR was performed directly on lysate.

3.2.3 PCR-Methods

The polymerase chain reaction method allows the amplification of DNA fragments with specific oligonucleotide primers The PCR products can be fragmented by gel electrophoresis, purified and used for cloning (Mullis et al., 1986; Saiki et al.,

1985). For a standard PCR reaction the reaction mixture consisted of the following components: 10 ng of plasmid or 100 ng of genomic DNA; 2,5 µl 10x PCR-buffer; 0,25 µl 25 mM dNTPs, 1,25 µl of each primer (10µM) and 0,5 µl of 5U/µl Taq-polymerase. Amplification conditions were: 94°C for 5 minutes; 30 cycles of 94°C for 30 seconds, an appropriate annealing temperature for 30 seconds, 68°C for 1 minute and 72°C for 7 minutes. The PCR-products were analyzed in a 1% agarose gel.

3.2.3.1 Genotyping of mice by PCR

For genotyping of mice the standard PCR protocol was used, if not otherwise indicated.

Primers for *Ext1Gt/Gt* mice (ascertained by inverse PCR):

*Ext1*fw: 5'-CACATCAGGTGCCTCACAAC-3'

*Ext1*rv: 5'-CTCCCAGCACTTTTCCTGAC-3'

5'pgto: 5'-TACATAGTTGGCAGTGTTTGGG-3'

PCR conditions for genotyping of *Ext1*$^{Gt/Gt}$ mice were: 94°C for 5 minutes; 30 cycles

of 94°C for 45 seconds, 60°C for 45 seconds, 72°C for 1 minute; and 72°C for 7 minutes.

The resulting 800 bp fragment indicated the transgenic allele and a 600 bp fragment indicates the wild-type allele.

For *Ext1*^{e2neofl} allele routine genotyping was done with a panel of primers used to detect recombination as indicated in Fig. 8. In addition, presence or absence of Cre-recombinase was confirmed by PCR in each mouse.

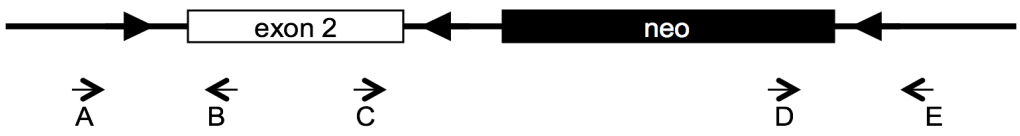

Figure 8. Genotyping primers for *Ext1*^{e2neofl} mice

Ext1 recombination genotyping

Primer A: GAGTCCATCCTGCTCTGCAT

Primer B: TTGTTGCATGGGAAAGACAA

Primer C: CCAAACTGGTTTCAAGCTTT

Primer D: CGTTGGCTACCCGTGATATT
Primer E: CTCCCAATTCTGGCTCTTCA
Cre-recombinase genotyping
Forward: ACCAGCCAGCTATCAACTCG
Reverse: TTACATTGGTCCAGCCACC

3.2.3.2 Nested PCR

First round of nested PCR was performed in single reaction with three primers (A, B and C Outer) with an annealing temperature of 58°C. Second round of nested PCR was performed with two separated reactions (primers A and B inner and A and C inner) with an annealing temperature of 62°C.

Laser-capture microdissection clone genotyping
A-Outer: ACCAGCTACAGATCAACA (both alleles)
B-Outer: CTCACCTTCCCATTTAGT (*Ext1*^{e2fl})
C-Outer: AGGCTTAGTTATTTGGGG (*Ext1*^{e2flinv})
A-Inner: ACCCCTCCCCCACCTGATTTA (both alleles)
B-Inner: GCGCACGCCTTTAATCCCA (*Ext1*^{e2fl})
C-Inner: ACTTTCTGTCTGGTTCCTCGT (*Ext1*^{e2flinv})

3.2.3.3 RNA isolation and cDNA synthesis

The reverse transcription polymerase chain reaction is the most sensitive method for the detection of low-abundance mRNA. Total RNA was isolated from micromasses of *Ext1*$^{Gt/Gt}$, *Ext1*$^{Gt/+}$ and wild-type embryos with Nucleospin kit (Macherey-Nagel) following manufacturer instructions. The quantity and quality of the isolated total RNA was determined by photometric measurement.
The cDNA was generated by reverse transcription with Superscript III kit (Invitrogen) using random primers.

3.2.3.4 Quantitative Real time PCR

Direct detection of the PCR product can be monitored by measuring the increase in fluorescence caused by the binding of SYBR Green dye to double stranded DNA. For PCR the following primers were used:

m*Col2*-Fw: 5´- CGAGTGGAAGAGCGGAGACT -3´
m*Col2*-Rv: 5´- AACTTTCATGGCGTCCAAGGT -3´
m*ColX*-Fw: 5´- ACGGCACGCCTACGATGT -3´
m*ColX*-Rv: 5´-CCATGATTGCACTCCCTGAA -3´
m*VEGF*-A-Fw: 5´- GCTGTGCAGGCTGCTGTAAC -3´
m*VEGF*-A-Rv: 5´- CCTATGTGCTGGCTTTGGTG -3´
m*Bglap*-Fw: 5´- ACCCTGGCTGCGCTCTGTCTCT -3´
m*Bglap*-Rv: 5´-GAT GCGTTTGTAGGCGGTCTTCA -3´
cDNAs were normalized against transcript levels of ß2Microglobulin :
m*ß2M*-Fw: 5'- GCTCGGTGACCCTGGTCTTT -3' and
m*ß2M*-Rv 5'- GAGGCGGGTGGAACTGTGTT-3'
One PCR reaction mixture consisted of: 10 µl cDNA (diluted 1/10 V), 5 µl primer (final concentration 7.5 pM in 5 µl) and 15 µl SYBR Green Master Mix. PCR conditions were: 95°C for 10 minutes, followed by 40 cycles of 95°C for 15 seconds and 60°C for 1 minute. After the last PCR cycle the melting curves for the amplification products were measured from 60°C to 95°C. The results were analyzed with the SDS software (Applied Biosystems). The quantification of the PCR product is based on the calculation of the fluorescence threshold value (CT-value). The CT-value is that PCR-cycle in which the reporter-fluorescence exceeds the background-fluorescence. After the CT-value is reached the kinetics of the amplification reaction should be exponential. The CT-values of different templates can be compared with each other (relative quantification) or to a CT-value of a known template concentration using a standard curve (absolute quantification).

3.2.4 Gel electrophoresis

Agarose gel electrophoresis was carried out for analytical purposes and for isolation of specific DNA-fragments. Corresponding to the size of the DNA-probes 0.8% to 2% agarose gels were prepared with TAE buffer. To visualize the DNA fragments, 0.5 µg/ml ethidiumbromide was added to the liquid agarose. Ethidiumbromide intercalates into the stacked bases of the DNA molecule and emits orange light when illuminated with ultraviolet light (254 nm). For loading the DNA and to estimate the running time of the gel, gel- loading buffer was added to the DNA solution and standard size markers were used to determine the size of

the isolated bands. For cloning DNA fragments were excised from the gel and extracted with glass milk according to the manufacturer instructions. Gel electrophoresis of total RNA was performed in 1x TAE buffer.

3.2.5 Laser capture microdissection.

Sections for single cells or cell clones isolation from postnatal tissues were prepared as described above. Six-micrometer paraffin sections were transferred to PALM Membrane Slides (1mm glass slides covered with a 1.35 µm thin Polyethylene-naphthalate membrane) and let dry overnight at room temperature. Slides were deparaffinized, rehydrated and stained with Mayers Hematoxylin and Eosin Y as suggested from manufacturer. Cells were then captured with P.A.L.M. Microbeam System (Carl Zeiss MicroImaging GmbH) and digested in 20µl of buffer containing 50 mM Tris HCl pH8, 0.5 % Tween20 and 0.1µg/µl Proteinase K for one hour at 60°C. Proteinase K was then inactivated for 30 minutes at 85°C and PCR reaction was performed directly on the cell lysate.

3.2.6 Sequencing

Sequencing was carried out by GATC Biotech.

3.2.7 Determination of the concentration of nucleic acids

To quantify the amount of DNA or RNA, the optical density of probes was measured with a photometer at a wavelength of 260 nm. For DNA (double strand) the OD260= 1 corresponds to a concentration of 50 µg/ml, for RNA the OD260= 1 corresponds to a concentration of 40 µg/ml. The relation of the absorption at 260 nm and 280 nm describes the purification grade of the nucleic acids and should not exceed 2.0.

3.2.8 Cell culture

3.2.8.1 Endothelial cell isolation

To distinguish endothelial cells from the micromass cultures I used endothelial cells expressing *green fluorescent protein* (GFP). Using an antibody against

VEGFR2 and MACS magnetic beads (Miltenyi Biotech) GFP endothelial cells were isolated from B5/EGFP mice between E12.5 and E13.5, which express GFP under the control of the *β*-actin promoter (Hadjantonakis et al 1998). Embryos were isolated, dissected and digested for 45 minutes with 2mg/ml Collagenase at 37°C, flipping tubes every 10 minutes. Each embryo was processed singularly. Cells were passed through a cell strainer (40µm) and seeded on a 75cm^2 and let adhere O/N. On the next day cells were washed with 1X PBS and trypsinized. Cells were then washed in cell isolation buffer, centrifuged 10 minutes at 4°C at 1000rpm and then incubated in 200µl isolation buffer with anti-mouse Flk1 (BD Pharmingen) diluted 1:40 for 30 minutes at 4°C with agitation. Cells were again washed in cell isolation buffer, centrifuged 10 minutes at 4°C at 1000rpm and then resuspended in 80µl isolation buffer and 20µl goat anti-rat IgG microbeads (MACS Miltenyi) were added. After incubation at 4°C for 30 minutes on agitation, cells were washed again, resuspended in 500µl isolation buffer and applied onto a mini Macs column (Miltenyi) for magnetic separation. Columns were washed 3 times with 500µl isolation buffer and eluted with 1ml buffer. Cells were then seeded onto 25cm^2 flask (Corning) pre-coated with Collagen I from rat tail. For coating 0.5mg/ml Rat tail collagen type I (BD bioscience) diluted in 1XPBS (Invitrogen (Gibco)) was incubated at 37°C overnight.

3.2.8.2 Micromass culture

Micromass cultures are high density culture of limb mesenchymal cells. These undergo condensation giving rise to aggregates that later become cartilage nodules, mimicking chondrocyte differentiation in vivo. All four limb buds of E12.5 mice were collected and washed in sterile 1xPBS. Each embryos was processed singularly and digested with 500µl/4limbs 1U/ml dispase(Neutral protease, Serva) in 1xPBS for 15 minutes at 37°C. Limbs were then washed 3 times with 1X PBS to remove the ectoderm and digested for 30 minutes with collagenase digestion solution for 30 minutes at 37°C. Cells were then passed through a cell strainer (40µm), washed with 10ml medium, counted with a Neubauer chamber, and centrifuged 5 minutes at 1000rpm. Cells were then resuspended at a concentration of 2x10^7/ml in DMEM/F12, 20µl were seeded on 12 well plates and incubated 2 hour at 37°C. Cells were then fed with 1.5 ml micromass medium and changed every second day for 5 weeks.

3.2.8.3 Boyden chamber assay

Boyden chamber assay is used to test chemotactic behavior in the presence of different chemoattractants. It consists of two compartments separated by a pore filter. The chemotactic factor is placed in one compartment and the gradient develops across the thickness of the filter. Cell movement into the filter is measured after an incubation period less than the time taken for the gradient to decay. In my experiment I used as chemoattractant source micromasses from *Ext1*$^{Gt/Gt}$ mutants and control littermates.

Both micromasses and endothelial cells were starved for 24 hours in basal medium supplemented only with pen strep. Endothelial cells were then trypsinized, resuspended in DMEM/F12 at a concentration of $2x10^4$ /ml and 500µl were seeded onto a cell culture insert (BD falcon353182) which was placed directly on the micromass cultures. DMEM/F12 and DMEM/F12 supplemented with 20ng/ml VEGF (Human VEGF-A Peprotech) were used as negative and positive controls. Boyden chamber were incubated for 24 hours (as previously described Sansone et al. 2007) at 37°C and inserts were then placed in a new 12 well plate. Non migrated cells from the upper side on the membrane were wiped off and GFP positive cells were counted at fluorescent microscope at a wavelength of 488nm. Ten fields at 20x magnification for each well and each insert were counted. Cells were then fixed in ice cold methanol for 10 min and methanol was replaced with sterile water and stored at 4°C.

3.2.8.4 Alcian blue staining of micromasses

Alcian blue is a cationic dye, which stains acid mucopolysaccharides and glycosaminoglycans. Micromass cultures were washed with 1xPBS, fixed for 10 minutes with 4%PFA and stained with Alcian blue staining solution overnight at RT. Next day cells were then washed 3 times and stored in sterile water at 4°C.

3.2.9 Histology and skeletal staining

3.2.9.1 Skeletal staining

Mice were killed by asphyxiation with CO2, skin and inner organs were removed. Full skeleton were then fixed with 100% EtOH for 2 days and placed in Alcian blue to stain proteoglycans for 24 hours. Then shortly washed with EtOH to remove rest of Alcian blue and cleared in 2%KOH for 24 hours. Skeleton were then placed in Alizarin red staining solution, to detect calcium deposits for at least 6 hours and then again in 2%KOH. Skeletons were then embedded in 100% Glycerol, after ascending series of KOH-glycerol mixture (2%KOH:Gly v/v: 80:20, 60:40, 40:60, 20:80)

3.2.9.2 Harvesting and processing of murine tissue

Limbs were either fresh frozen in OCT embedding medium at -60°C for cryosectioning, or fixed in 4% PFA at 4°C overnight for embedding into paraffin. Tissue was rinsed three times with PBS for 5 minutes. Tissue of E14.5 and E16.5 limbs was dehydrated for 10 minutes in 30%, 50%, 75%, 80%, 95% and 100% ethanol and subsequently incubated twice in 100% xylol. Then three changes of 100% paraffin for 2 hours each followed. Limbs were embedded into paraffin and sectioned into 5 µm slices for 4-5 parallel sections, which were placed on silanized slides. Mice at embryonic stage 7.0 were dissected together with the maternal decidua out of the uterus, fixed overnight at 4°C in 4% PFA, included in paraffin and sectioned at 5µm.

Knees from postnatal stages were harvested fixed in 4% PFA in PBS and decalcified in 25% EDTA (pH 7.4) at 37°C. Samples were processed to be embedded into paraffin as described above. Five- to 10-µm sections from paraffin-embedded tissue were used for histology, *in situ* hybridization, immunohistochemistry and LCM.

3.2.9.3 Hematoxylin/Eosin staining

This histological staining method stains nuclei blue (Hematoxylin) and the cytoplasm red (Eosin). Sections were deparaffinized, rehydrated and subsequently

incubated for 45 seconds in Harris Hematoxylin (Sigma), rinsed shortly with tab water and then incubated for 2 to 3 minutes in Y Eosin (Sigma). Finally slides were rinsed with tab water, dehydrated by an increasing ethanol series, transferred into Xylol and embedded in DPX mounting medium.

3.2.9.4 Tartrate resistant acid phosphatase (TRAP) staining

Osteoclasts are characterized by the production of the enzyme tartrate resistant acid phosphatase (TRAP). Sections were deparaffinized, rehydrated and incubated 15 min at RT with TRAP staining solution washed twice with bidest water and mounted with water based mounting medium, Kaiser Gelatin.

3.2.9.5 Von Kossa staining

This technique is for demonstrating deposits of calcium or calcium salt so it is not specific for the calcium ion itself. In this method, tissue sections are treated with a silver nitrate solution and the silver is deposited by replacing the phosphates reduced by the strong light, and thereby visualized as metallic silver. Sections were deparaffinized, rehydrated and incubated 5 minutes in 1%AgNO3 under UV light. Slides were then washed 3 times in 5% sodiumthiosulfate and 3 times in bidest water. Slides were counterstained with Methyl green, dehydrated by short incubation in ascending alcohol series and transferred in xylol and embedded in DPX mounting medium.

3.2.9.6 Toluidine blue staining

Toluidine blue should stain proteoglycans red-purple and the background blue.
Sections were deparaffinized, rehydrated and incubated in 0.2% Toluidine blue for 5 minutes and dehydrated in ethanol solutions 30%, 50%, 75%, 80%, 95% and 100%. The sections were incubated in 100% xylol and then covered with glass coverslips using minimal volume of mounting medium (DPX mountant for histology).

3.2.9.7 SafraninO staining

This method is used for the detection of cartilage, mucin, and mast cell granules on formalin-fixed, paraffin-embedded tissue sections. The cartilage and mucin will be stained orange to red, and the nuclei will be stained black. The background is stained green.

Sections were deparaffinized, rehydrated and stained with Weigert's iron hematoxylin working solution for 10 minutes. Sections were washed in running tap water for 10 minutes and then stained with fast green (FCF) solution for 5 minutes. Slides were rinsed quickly with 1% acetic acid solution for no more than 10 –15 seconds and then stained in 0.1% safranin O solution for 5 minutes. Sections were dehydrated and cleared with 95% ethyl alcohol, absolute ethyl alcohol, and xylol, using 2 changes each, 2 minutes each and mounted using DPX medium.

3.2.9.8 CD31 immunohistochemistry.

CD31 is a 130 KDa integral membrane protein, also known as platelet endothelial cell adhesion molecule 1 (PECAM1). CD31 is expressed constitutively on the surface of adult and embryonic endothelial cells (Huss et al., 2001; Vecchi et al.,1994; Vanzulli et al., 1997; Delisser et al., 1997). Limbs were sectioned at 5µm with a Microm cryostat. Sections were then fixed for 10 minutes in ice cold acetone and rehydrated for 5 minutes in 1xPBS. Endogenous peroxydase was blocked by incubation with 0.2% H2O2 in 1xPBS for 5 minutes. After washing in 1xPBS containing 0.5% BSA for 5 minutes primary antibody rat anti-mouse CD31 (PECAM) (BD Pharmingen) diluted 1:70 in 1xPBS/0.5%BSA was incubated for 1 hour at RT. After washing 3 times for 5 minutes with 1xPBS/0.5%BSA slides were incubated with secondary antibody rabbit anti-rat HRP, diluted 1:70 1xPBS/0.5%BSA for 45 minutes at RT. After washing section were incubated 5 minutes with diaminobenzidine (DAB) substrate and embedded with Kaiser Gelatin.

3.2.9.9 Heparan sulfate immunohistochemistry

Heparan sulfate can be detected with different antibodies which recognize specific patterns of differentially sulfated motives. The 10E4 antibody recognize (GlcA-

GlcNS)/(GlcA-GlcNAc) mixed sequences and the HepSS1 antibody recognize (GlcA-GlcNS)-rich sequences.

Sections were deparaffinized, rehydrated and washed 5 minutes in 1XPBS pH 7.4. Slides were then incubated in a humified chamber for 30 min at 37°C with 10000 U/ml hyaluronidase I (from bovine testis SIGMA) in 1XPBS pH7.4. After washing 3 times 5min in 1XPBS pH7.4 endogenous peroxydase was inactivated for 30 min at RT with 3% H2O2 in 1xPBS. After washing 3 times 5min in 1xPBS pH7.4 unspecific binding was blocked for 30 min at RT in Blocking solution (10% goat serum in 1x PBS). Primary antibody 10E4/HepSS1 (Seikagaku, Japan) diluted 1:100 in blocking solution was incubated O/N at 4°C. On the next day slides were washed 3 times for 5min in 1xPBS pH7.4. Incubation followed with Goat biotinylated secondary antibody against mouse IgM (Vector Laboratories) diluted 1:100 in blocking solution for 30 min at RT. After washing slides were incubated 30 min with Streptavidin-HRP (Perkin-Elmer) diluted 1:100 in 1xPBS. Slides were washed 3 times for 5 minutes in 1xPBS and then incubated with DAB for 5 minutes. Sections were then counterstained with methyl green or directly mounted with Kaiser Gelatin.

3.2.9.10 Methyl green staining

Methyl green is used a counterstaining for immunohistochemistry or other special stains. After section were deparaffinized and rehydrated, they were stained in methyl green solution for 5 minutes at room temperature. After rinsing in distilled water slides were dehydrate quickly through 95% alcohol (10 dip), 2 changes of 100% alcohol (10 dips each). Then sections were cleared in xylol and mounted with DPX.

3.2.9.11 VDIPEN immunohistochemistry

Degradation of the articular aggrecan leads to production of specific catabolic fragments, which accumulate in the matrix. Specific epitopes are generated, which are better known as VDIPEN and NITEGE, referring to the aminoacidic sequence produced from Mmps or aggrecanases cleavage. Aggrecan degradation have been intensely studied during the past few years (Lark et al., 1997, Westling et al., 2002, Valverde-Franco et al.,2006, Fosang et al., 1995, Mercuri et al., 1999).

Sections were deparaffinized, rehydrated and digested with 0,25 U/ml chondroitinase ABC (Sigma) in 0.1M Tris-HCl, pH8.0 for 1 hour at 37°C to remove chondroitin sulfate from the proteoglycans. Endogenous peroxydase was inactivated for 30 min at RT with 3% H2O2 in 1xPBS. And then washed for 5min in 0.1% Triton X-100 (v/v) in 1XPBS pH7.4. After blocking for 30 min at RT in Blocking solution (10% goat serum in 1X PBS), slides were then incubated O/N with VDIPEN primary antibody (kindly provided from Amanda J. Fosang) at a concentration of 2µg/ml in blocking solution at 4°C. On the next day slides were washed 3times for 5min in 1xPBS pH7.4. Incubation followed with rat-HRP anti rabbit secondary antibody (DAKO) diluted 1:200 in PBS for 3 hours at RT. After washing slides were incubated with DAB for 5 minutes. Sections were directly mounted with Kaiser Gelatin.

3.2.10 In situ Hybridization

3.2.10.1 Preparation of DNA template for in vitro transcription

Plasmid DNA was isolated from *E.coli* DH5 cells using QIAprep Plasmid Miniprep or Midiprep Kits according to the manufacturer instructions. 5 µg plasmid DNA was linearized with 5 U of the appropriate restriction endonuclease for 2 hours at 37°C. Efficiency of the digestion was analyzed on a 1% agarose gel. For purification phenol/chloroform extraction was performed twice. The final supernatant was transferred to a clean tube and was precipitated with 2.5V of 100% ethanol. The mixture was centrifuged at 14.000 rpm for 15 minutes at room temperature (RT). The DNA pellet was washed with cold 80% ethanol and resuspended in 10 µl of RNAse free water.

3.2.10.2 Labeling of antisense riboprobes

Transcription reaction was performed in 20 µl with the following components: 500 ng linearized DNA template for *in vitro* transcription, 1x transcription buffer, 0.5 mM NTP mix, 5 U RNAse inhibitor, RNAse free water, 40 U RNA-polymerase and 80 µCi [P33]-UTP. The transcription reaction was carried out for 1.5 hours at 37°C. To remove the DNA template, 10 U DNAse (RNAse- free) were added to the transcription mixture and incubated for 30 minutes at 37°C. The transcription

mixture was then diluted with 4 V of RNAse free water, containing 20 ng/ml glycogen and 0.5 M LiCl, and precipitated with 2.5 V of 100% ethanol. Probes were incubated at -20°C for 30 min and then centrifuged at 14.000 rpm for 15 minutes at 4°C. The RNA pellet was washed twice with cold 80% ethanol, resuspended in 50 µl RNAse free water, and diluted 1: 20 with hybridization buffer. Before use the riboprobe was heated for 5 minutes at 95°C and chilled on ice.

3.2.10.3 Prehybridization and in situ hybridization

All solutions for the prehybridization procedure were prepared with RNAse free water. The sections were incubated in xylol for 30 minutes to remove the paraffin. To rehydrate the tissue, the sections were incubated in a descending ethanol series (100%, 95%, 80%, 75%, 50%, 30%) each for 2 minutes, followed by 0.85% NaCl for 5 minutes and PBS for 5 minutes. After rehydration the tissue was fixed in 4% PFA for 30 minutes. The sections were then incubated for 5 minutes in following solutions: PBS, 0.2N HCl and RNAse free water. The tissue was digested for 5 minutes with 0.02 mg/ml Proteinase K and rinsed with PBS for 5 minutes. Subsequently the sections were refixed in 4% PFA with 0.2% glutaraldehyde for 10 minutes and rinsed with PBS for 5 minutes. The sections were acetylated by 0.25% acetic anhydride (freshly added) to 0.2% Triethanolamine for 10 minutes, then rinsed with PBS for 5 minutes and additionally incubated in 0.85% NaCl for 5 minutes. Sections were dehydrated with the following ethanol solutions: 30%, 50%, 75%, 100%. The sections dried at RT for 15 minutes. A minimal volume of labeled riboprobe (50µl) was distributed evenly on the slide and the sections were covered with plastic coverslips to prevent evaporation. Hybridization was performed at 70°C overnight.

After hybridization the sections were washed in 5xSSC for 30 minutes and coverslips were removed. The sections were washed in 2xSSC for 30 minutes and treated with 0.02mg of RNAse A in 1x Washing buffer for 30 minutes. Stringent washing took place in 2xSSC with 50% formamide for 30 minutes and then twice in 2xSSC for 30 minutes. The sections were dehydrated in an ascending ethanol series (30%, 50%, 75%, 80%) containing 0.3M ammonium acetate. Finally the sections were incubated in 100% ethanol for 15 minutes and dried for 10 minutes at RT. The slides were exposed to a X-ray film (Kodak Scientific Imaging Film) overnight at RT to estimate the intensity and strength of each probe. The sections

were dipped in photoemulsion NTB2 at 40°C in the darkness. Dried sections were stored at 4°C in darkness for the time predicted from the developed X-ray film. The dipped sections were developed in Kodak-developer for 5 minutes at 15°C, rinsed in water and fixed in Kodak- fixer for 15 minutes at RT. The sections were counterstained with 0.2% Toluidin blue O for 5 minutes and dehydrated in ethanol solutions 30%, 50%, 75%, 80%, 95% and 100%. The sections were incubated in 100% xylol and then covered with glass coverslips using minimal volume of mounting medium (DPX mountant for histology). The sections were analyzed by dark- field microscopy.

4. Results

4.1 Endochondral ossification in *Ext1*$^{Gt/Gt.}$

4.1.1 Osteoblast and osteoclast invasion are perturbed in *Ext1*$^{Gt/Gt}$ mutants.

Mutations in the human *EXT1* and *EXT2* genes lead to the formation of human osteochondromas. However, the cellular and molecular causes of the disease have yet to be identified. These include the cell type that gives rise to the osteochondromas and the allelic status of *EXT1* in the cells, which will form the tumor. Previous studies based on morphological investigations of early human osteochondromas biopsies pointed to either chondrocytes of the growth plate or osteoblast progenitors of the perichondrium/periosteum as potential candidates (Delgado et al., 1987; Hameetman et al., 2007; Robinson et al., 1999). Analysis of a hypomorphic allele of *Ext1* in mice revealed that chondrocyte differentiation is severely delayed (Koziel et al., 2004) in homozygous mutants indicating that osteochondromas might originate in proliferating/differentiating chondrocytes. However, preliminary investigations revealed that the ossification process and the invasion of blood vessels seem to be disturbed in the mutant skeletal elements. To investigate if disturbed ossification or vascular invasion might contribute to osteochondroma development we first investigated the role of *Ext1* in regulating these processes in detail.

As targeted deletion of *Ext1* (*Ext1*$^{-/-}$) is lethal during gastrulation (Lin et al., 2000; Stickens et al., 2005) I analyzed mineralization and vascular osteoclast invasion in a mutant mouse carrying a hypomorphic allele of *Ext1* (*Ext1*$^{Gt/Gt}$). These mice survive until E16.5, the stage at which primary ossification centers have formed in wild type (wt) mice (Fig. 9). The deletion of *Ext1* in these mice has been generated by the insertion of a gene trap vector into the first intron of *Ext1*, creating a truncated Ext1 protein fused to the *ß-geo* reporter of the vector (Leighton et al., 2001) (Fig. 9). *Ext1*$^{Gt/+}$ mice show no obvious phenotype, develop normally and are viable (Koziel et al., 2004). Therefore in the present study *Ext1*$^{Gt/+}$ mice have been used as control littermates, and are referred to as wt.

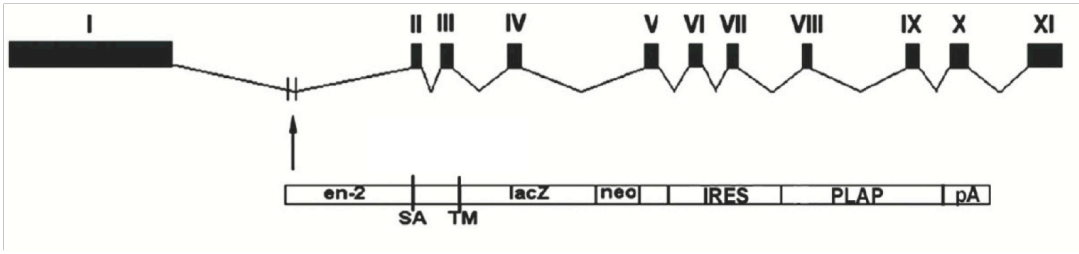

Figure 9. Hypomorphic allele of *Ext1.* Schematic representation of the *Ext1* gene and the gene trap vector. The product of the hypomorphic allele is a truncated, non functional Ext1 protein.

In wt mice the ossification process starts at E13.5 to E14.5 when chondrocytes in the center of the cartilage anlagen differentiate into *ColX* expressing hypertrophic chondrocytes. In parallel cells of the perichondrium differentiate into osteoblasts, secreting a Col1 rich mineralized matrix. Subsequently, the ColX rich cartilage matrix is degraded by multinucleated, bone resorbing cells, the osteoclasts, allowing blood vessels and osteoblasts to invade the skeletal anlagen.

4.1.2 Expression of osteoblast markers and chondrogenic matrix degrading enzymes are not significantly delayed in *Ext1*$^{Gt/Gt}$ mice.

To analyze the role of *Ext1* during osteoblast differentiation, changes in the expression patterns of osteoblast markers were investigated by *in situ* hybridization in *Ext1*$^{Gt/Gt}$ mice (Fig. 10). At E14.5, before the primary ossification center forms, chondrocytes turn into hypertrophic and terminal hypertrophic cells expressing *ColX* and matrix metalloprotease 13 (*Mmp13*). In parallel, osteoblasts starting to differentiate in the perichondrium/periosteum express bone gamma-carboxyglutamate protein (Bglap), a secreted protein implicated in bone mineralization and calcium homeostasis (Lee et al., 2000). At E16.5 a proportion of wt hypertrophic chondrocytes has differentiated into terminal hypertrophic cells resulting in two zones of *Mmp13* expression separated by the bone marrow cavity (Fig. 10 B, D). Osteoblasts start to differentiate and deposits mineralized matrix, as shown by *Bglap* expression in the ossified center of the bone and the perichondrium/periosteum flanking the hypertrophic cells (Fig.10 F). *ColX* expression in the E16.5 mutant anlagen reveals hypertrophic differentiation of the chondrocytes. However the narrow distance between the two expression domains

in the *Ext1*$^{Gt/Gt}$ mutants (Fig. 10 A) indicates a severe delay, as also *Ext1*$^{Gt/Gt}$ mutants show only one zone of terminal hypertrophic chondrocytes expressing *Mmp13*, while *Bglap* expression is restricted to the perichondrium/periosteum (Fig.10 C, E). In summary, cartilage matrix resorption and osteoblast differentiation are both taking place in the anlagen of E16.5 *Ext1*$^{Gt/Gt}$ mutants, but both are delayed compared to wt embryos. This delayed expression of osteoblast markers in *Ext1*$^{Gt/Gt}$ mutants can be explained as a consequence of the general delay in chondrocyte differentiation, which has been described before (Koziel et al, 2004).

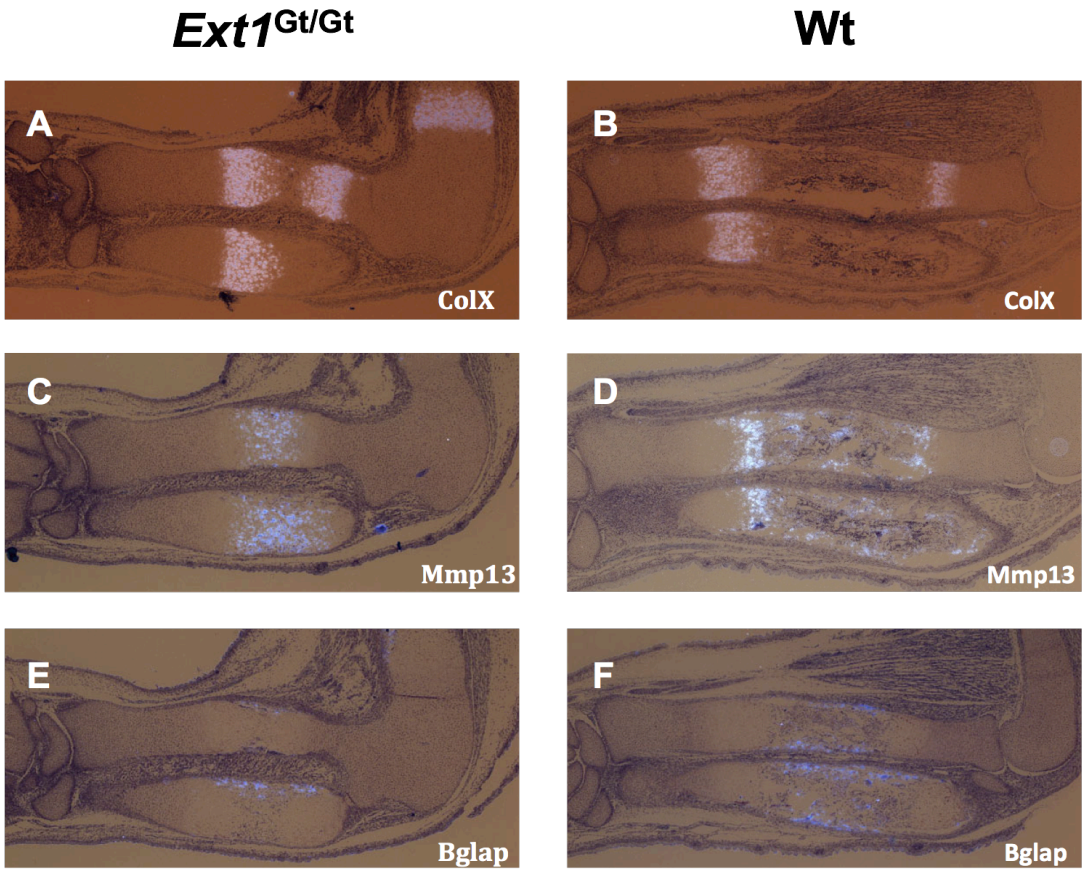

Figure 10. Ossification is delayed in E16.5 *Ext1*$^{Gt/Gt}$ forelimb. In situ hybridization of *ColX*, *Mmp13* and *Bglap* on wt (B, D, F) and *Ext1*$^{Gt/Gt}$ skeletal anlagen (A, C, E) revealed extended domains of hypertrophic chondrocytes (*ColX* and *Mmp13* expression). *Bglap* expression demonstrates that ossification is restricted to the perichondrium/periosteum flanking the hypertrophic region in *Ext1*$^{Gt/Gt}$ mutant (E). Magnification 50X.

4.1.3 Endochondral ossification and osteoclast invasion are defective in *Ext1*$^{Gt/Gt}$ mice.

Ext1$^{Gt/Gt}$ mice show delayed expression of osteoblast and hypertrophic differentiation markers compared to wt. Nonetheless gene expression can be considered normal in relationship to hypertrophic chondrocytes differentiation and delayed as a consequence of the primary delay, due to disturbed *Ihh* signaling (Koziel et al., 2004). Ossification and osteoclast invasion were morphologically analyzed in relationship to hypertrophic differentiation in *Ext1*$^{Gt/Gt}$ mutant and wt littermates at different stages, from E14.5 to E16.5 (Fig. 11).

At E14.5 osteoblasts start to differentiate in the perichondrium/periosteum, secreting a Col1 rich mineralized matrix, which can be detected by von Kossa staining. In wt mice first mineralization of the perichondrium/periosteum can be detected at E14.5 (Fig. 11 B) and at E15.5 (Fig. 11 D) a few mineralized trabeculae have replaced the cartilage matrix. At E16.5 the zone of endochondral bone has expanded and wider mineralized trabeculae can be detected (Fig. 11 F). At E14.5 in *Ext1*$^{Gt/Gt}$ anlagen chondrocytes have not turned hypertrophic yet and mineralization has not started (Fig. 11 A). In *Ext1*$^{Gt/Gt}$ mutants first mineralization of the perichondrium/periosteum can be detected at E15.5 (Fig. 11 C, red arrow). At E16.5 the perichondrium/periosteum surrounding the hypertrophic zone is strongly mineralized and more mineralized trabeculae have substituted the cartilaginous matrix surrounding the hypertrophic chondrocytes (Fig. 11 E).

Osteoclasts are characterized by the production of the enzyme tartrate resistant acid phosphatase (TRAP). In wt mice, first osteoclast invasion can be detected at E14.5 in the perichondrium surrounding the diaphyses of the skeletal elements (Fig. 11 H). At E15.5 osteoclasts have invaded the primary ossification center (Fig. 11 J) and at E16.5 the zone of endochondral bone has expanded and more osteoclasts can be detected (Fig. 11 L). The *Ext1*$^{Gt/Gt}$ mutants show delayed osteoclast invasion at the primary ossification center. At E14.5 and E15.5 the *Ext1*$^{Gt/Gt}$ mutant skeletal anlagen is devoid of osteoclasts (Fig. 11 G, I). Only at E16.5 single osteoclasts can be detected that start to invade the diaphyses of *Ext1*$^{Gt/Gt}$ mutants (Fig. 11 K, red arrows). In summary osteoclast invasions and mineralization are delayed in *Ext1*$^{Gt/Gt}$ mutants.

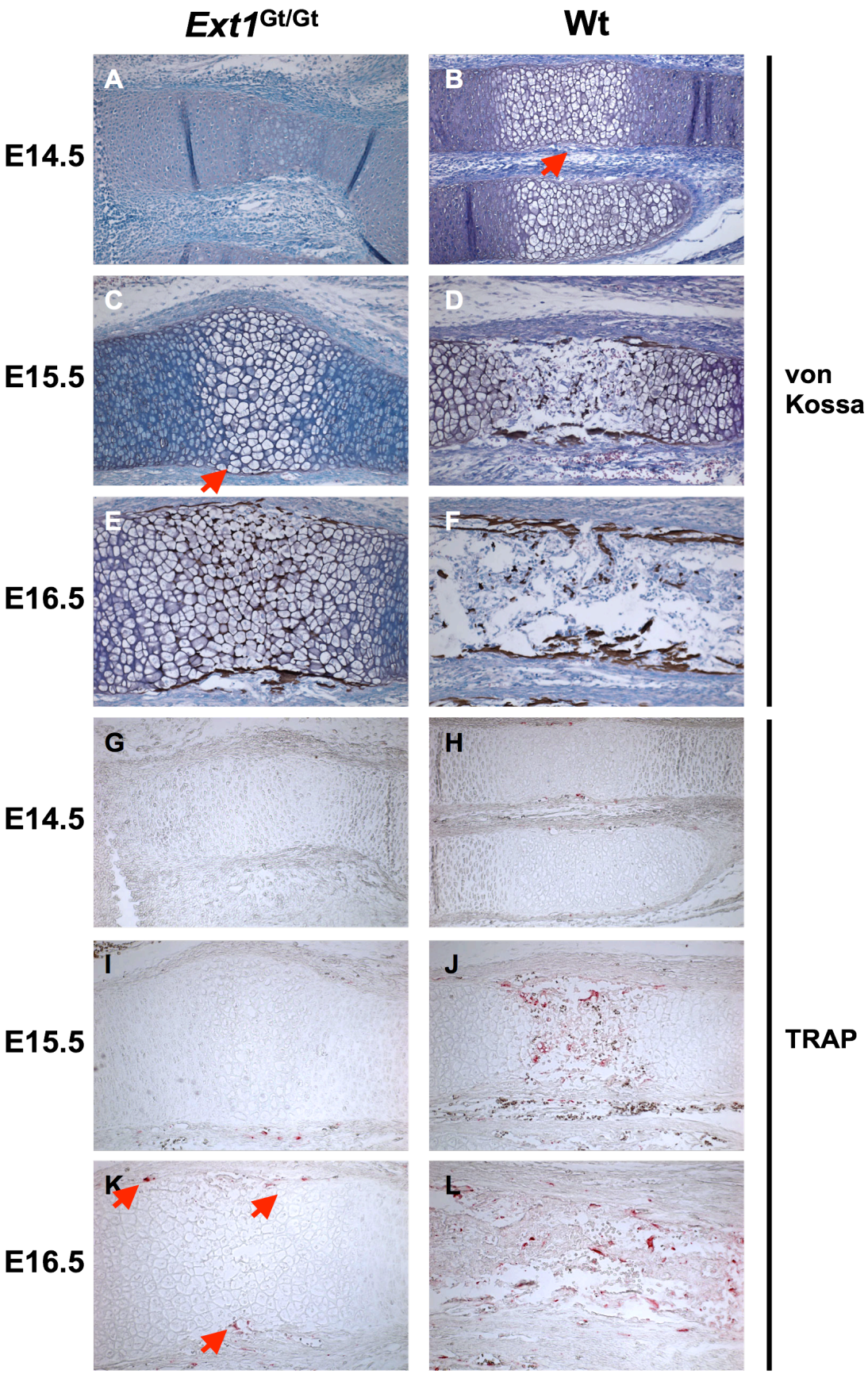
Ext1Gt/Gt
Wt
E14.5
E15.5
E16.5
A
B
C
D
E
F
von Kossa
E14.5
E15.5
E16.5
G
H
I
J
K
L
TRAP

Fig. 11. Osteoblast differentiation and osteoclast invasion are delayed in *Ext1*$^{Gt/Gt}$ skeletal elements. Von Kossa staining of *Ext1*$^{Gt/Gt}$ and wt skeletal elements (A-F) reveals that the mineralization of *Ext1*$^{Gt/Gt}$ mutant radii (A, C and E) is severely delayed compared to wt radii (B, D and F). At E15.5 and E16.5 the wt elements (D, F) show mineralized bone matrix and a bone marrow cavity between two zones of hypertrophic chondrocytes. At E15.5 the *Ext1*$^{Gt/Gt}$ mutant (C) shows no mineralization except of a weak staining of the perichondrium/periosteum (C, red arrow). At E16.5, hypertrophic cells are still surrounded by a mineralized matrix In the *Ext1*$^{Gt/Gt}$ mutants and skeletal elements are lacking a bone marrow cavity, which in wt mice is has started to form at E15.5 (D). TRAP staining (G-L) of E14.5 to E16.6 *Ext1*$^{Gt/Gt}$ mutant radii (G, I, K) show no osteoclast invasion compared to wt radii (H, J, L). At E14.5 wt skeletal elements show osteoclast invasion of the perichondrium/periosteum (H). At E15.5 and E16.5 (J, L) a high number of osteoclasts can be detected in the center of the wt anlagen. E14.5 and E15.5 *Ext1*$^{Gt/Gt}$ mutants show no osteoclast invasion (G, I). Although chondrocytes have turned hypertrophic in the mutant skeletal elements at E16.5 (K) only a few TRAP positive osteoclasts can be detected in the perichondrium/periosteum (K, red arrows). Magnification 200X.

4.1.4 Development of the vascular plexus is disturbed in *Ext1*$^{Gt/Gt}$ mutants

During the first stages of endochondral ossification the cartilage template is an avascular structure, which develops into a hollow and highly vascularized element, the marrow cavity (Karsenty and Wagner, 2002). Hypertrophic chondrocytes start to produce angiogenic factors, inducing the first capillary invasion of the cartilage template (Colnot and Helms, 2001; Zelzer et al., 2001). The vasculature supplies the template with cells belonging to the osteoblast and osteoclast lineage (Colnot et al., 2004; Zelzer et al., 2002). VEGF-A have been shown to directly enhance the resorption activity and survival of mature osteoclasts (Nakagawa et al., 2000). Osteoclasts express *Flt-1* and *Vegf-A* from hypertrophic chondrocytes has been shown to be a chemoattractant for osteoclasts to invade the developing bone (Blavier and Delaisse, 1995; Engsig et al., 2000; Henriksen et al., 2003). The delay in gene expression observed in *Ext1*$^{Gt/Gt}$ mutants likely results from the delay in chondrocyte differentiation. Although osteoblast differentiation and cartilaginous matrix resorption in E16.5 *Ext1*$^{Gt/Gt}$ mutants have started, bone marrow cavity formation and osteoclast invasion of the cartilage anlagen are defective in *Ext1*$^{Gt/Gt}$ mutants. As a similar phenotype has been correlated to defective vascularization and disturbed VEGF-A protein distribution (Blavier and Delaisse1995; Engsig et al., 2000; Henriksen et al., 2003; Vu et al., 1998) I decided to investigate blood

vessels formation in the *Ext1*$^{Gt/Gt}$ mutants. Homozygous *Ext1*$^{Gt/Gt}$ embryos are characterized by an edematous appearance (Koziel et al., 2004; Lin et al., 2000) suggesting that blood vessels formation is also disturbed in these mutants. Vascularization was analyzed at E14.5 and E16.5 in wt and *Ext1*$^{Gt/Gt}$ mice, using an anti-CD31/PECAM antibody that specifically detects endothelial cells of the blood vessels (Fig. 12). In E14.5 wt embryos, blood vessels can be detected in the limb mesenchyme and in the perichondrium/periosteum surrounding hypertrophic chondrocytes (Fig. 12 B). In *Ext1*$^{Gt/Gt}$ mutants of the same stage, endothelial cells can be identified in the limb mesenchyme. However, they appear disorganized and proper vessels do not form (Fig. 12 A). Furthermore no invasion of the perichondrium/periosteum can be detected. At E16.5 a highly vascularized perichondrium/periosteum and bone marrow cavity have formed in wt embryos (Fig. 12 D, F). In contrast in *Ext1*$^{Gt/Gt}$ mutants no bone marrow cavity has formed and no invasion of the periosteum by endothelial cells can be detected (Fig. 12 C, yellow lines indicate borders of the anlagen). As revealed by Hematoxylin/Eosin staining *Ext1*$^{Gt/Gt}$ mutant blood vessels do not invade the mutant anlagen although at E16.5 chondrocytes have turned hypertrophic (Fig. 12 E).

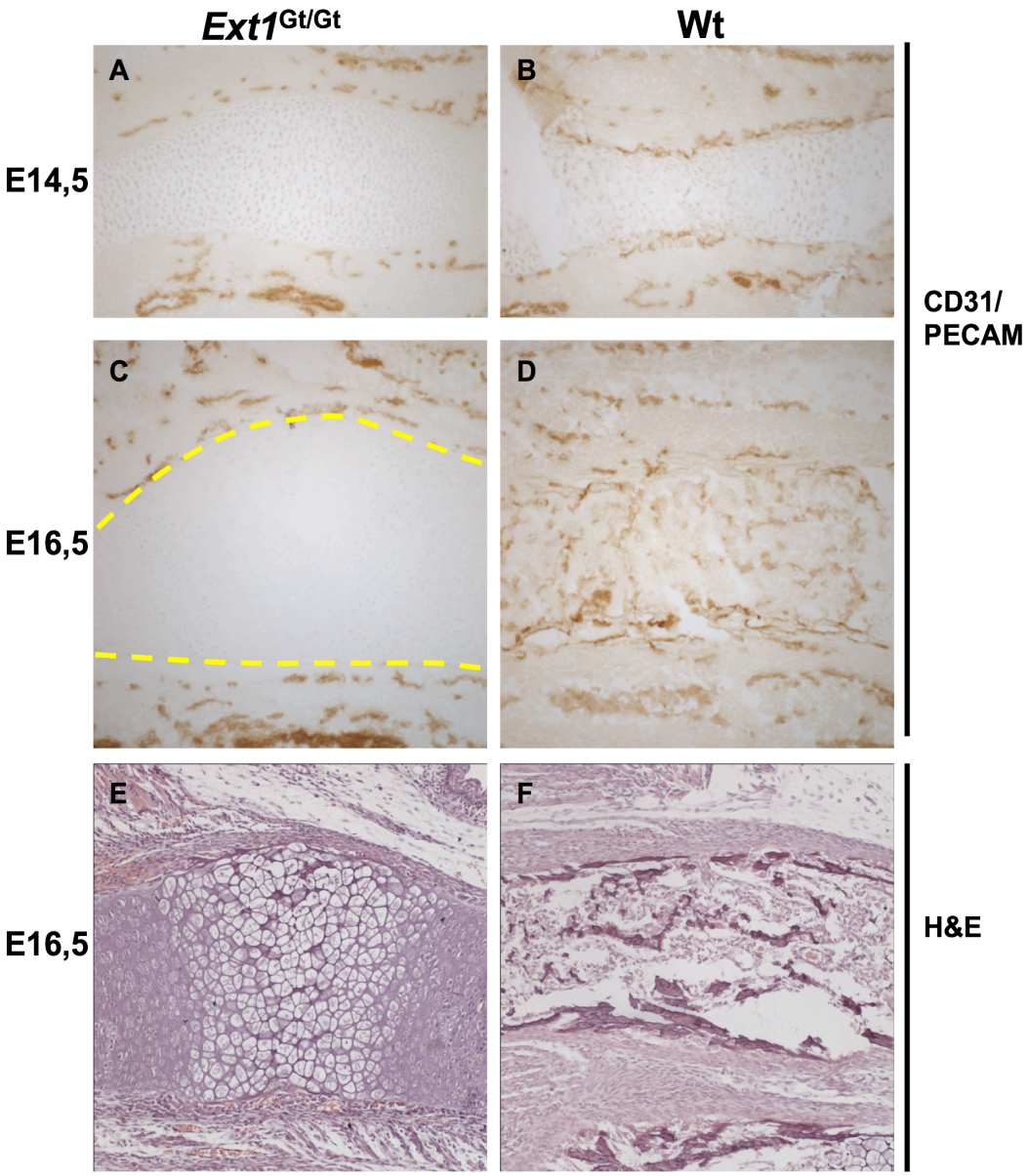

Figure 12. Blood vessel formation is disturbed in *Ext1*$^{Gt/Gt}$ mutants. Cryosections of wt and *Ext1*$^{Gt/Gt}$ mutant radii at E14.5 and E16.5 were immunostained using an antibody against CD31/PECAM, a marker for endothelial cells and analyzed by H&E (A and C). Parallel sections of E16.5 *Ext1*$^{Gt/Gt}$ mutants (E) and wt radii (F) were stained with Hematoxylin/Eosin. In E14.5 wt embryos the periosteum is invaded by blood vessels (B). At E16.5 a highly vascularized region has developed in the center of the wt skeletal anlagen (D, F). Endothelial cells in the *Ext1*$^{Gt/Gt}$ mutant (A and C) do not form a proper vasculature. At E14.5 and E16.5 no invasion of the periosteum can be detected and the endothelial cells invasion has not taken place in the mutant skeletal element is devoid of blood vessels (A) and no blood vessel invasion can be observed at E16.5, although hypertrophic differentiation has taken place (C, E). Magnification 200X.

4.1.5 Expression of angiogenic markers is not disturbed in *Ext1*$^{Gt/Gt}$ mutant

Blood vessel invasion of the periosteum is induced by the expression of angiogenic growth factors in hypertrophic chondrocytes. These factors signal to their receptors on endothelial cells in the surrounding tissue, inducing their migration into the ossifying perichondrium/periosteum. To examine if the defective angiogenesis results from changes in the expression of vascular endothelial growth factor A (VEGF-A) and its receptors *Flt-1*, *Flk-1*, and *Nrp1*, I analyzed the expression of these genes by *in situ* hybridization in E14.5 to E16.5 *Ext1*$^{Gt/Gt}$ mutant and wt forelimbs (Fig. 13 and 14). It has previously been shown that hypertrophic chondrocytes express *Vegf-A* and *Nrp1*, while the receptors *VegfR2/Flk1* and *VegfR1/Flt1* are expressed on endothelial cells in the surrounding tissue starting at E14.5. Upon formation of the periosteum at E15.5 both receptors can be detected on EC invading the ossified region. At E16.5 the expression of both receptors is additionally increased in the bone marrow and at the interface between bone marrow and terminal hypertrophic chondrocytes, while *Vegf-A* and *Nrp1* expression remains unchanged (Zelzer et al., 2002). Consistent with published data, overlapping expression of *Vegf-A* and *ColX*, is found in hypertrophic chondrocytes of E14.5 wt mice (Fig. 13 B, D). At this stage *Nrp1* expression cannot be detected in the cartilage anlagen of radius and ulna but is strongly expressed in the joint interzone of the digits (Fig. 13 J, red arrow). *Flk1* and *Flt1* are strongly expressed in the tissue surrounding the skeletal elements and in the perichondrium (Fig. 13 F, H). In *Ext1*$^{Gt/Gt}$ mutants only few chondrocytes express *ColX* and *Vegf-A*, in relation to the delay in hypertrophic differentiation (Fig. 13 A, C). In contrast to the wt, *Nrp1* is not expressed in the mutant digits (Fig. 13 J, I), while *Flk-1* and *Flt-1* are expressed in the surrounding mesenchymal tissue, similar to the wt (Fig. 13 E, F and G, H). In wt mice at E16.5 *Vegf-A* and *Nrp1* are strongly expressed from hypertrophic chondrocytes (Fig. 14 B, D, J), while *Flk-1* and *Flt-1* are still expressed in the limb mesenchyme but strong expression can also be detected in the bone marrow cavity (Fig. 14 F, H). At E16.5 *Ext1*$^{Gt/Gt}$ mutants show a strong overlapping expression of *ColX*, *Vegf-A* and *Nrp1*, delayed compared to wt littermates as a consequence of the delay in hypertrophic differentiation (Koziel et al., 2004) (Fig. 14 A, C, I and B, D, J). *Flk-1* and *Flt-1*

expression is restricted to the perichondrium/periosteum in the *Ext1*$^{Gt/Gt}$ mutants and expression in the center of the anlagen is missing (Fig. 14 E, G).

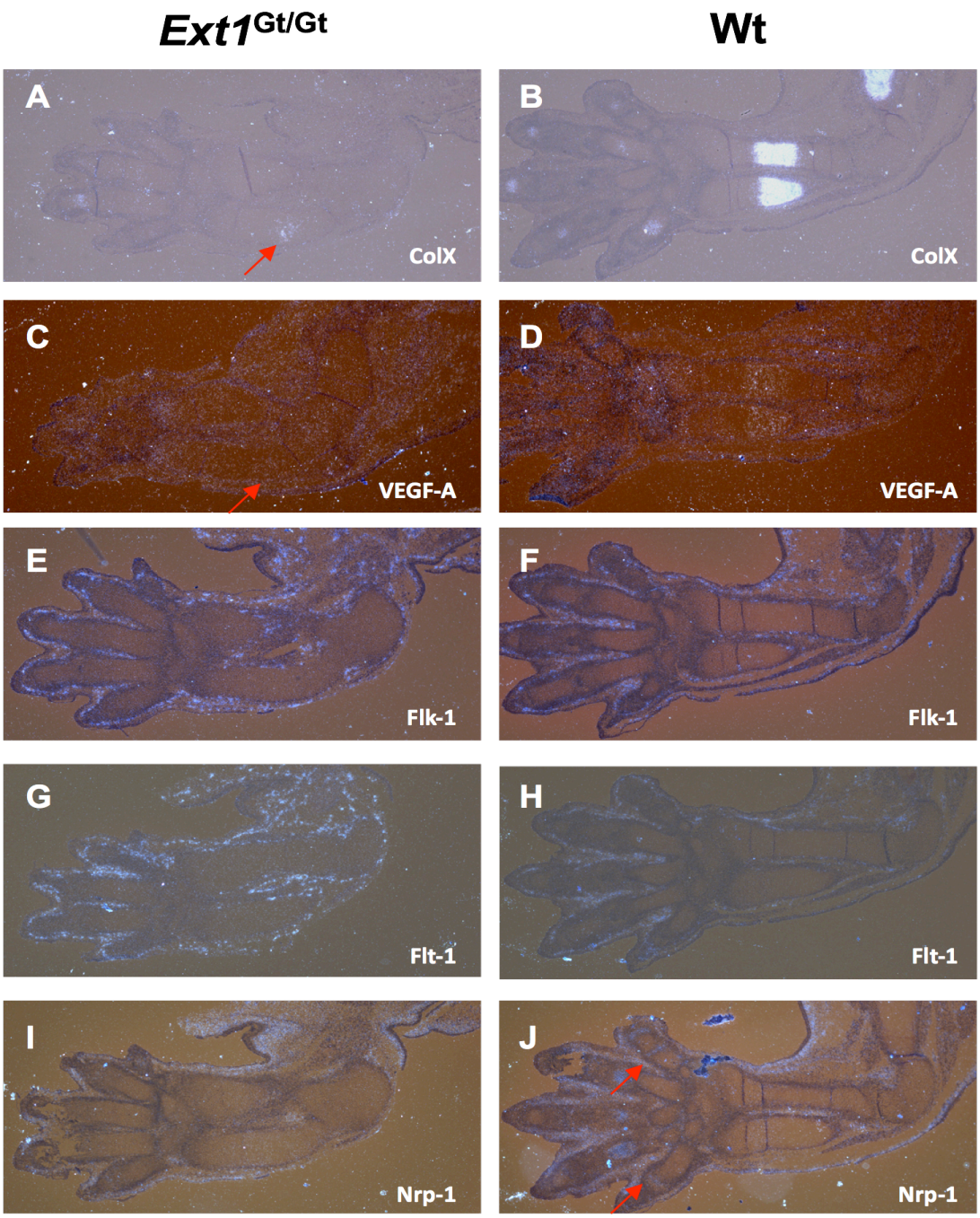

Figure 13. Expression of vascularization markers is not disturbed in *Ext1*$^{Gt/Gt}$ mutant forelimb at E14.5. Wt and *Ext1*$^{Gt/Gt}$ forelimbs were hybridized with riboprobes for *ColX* (A, B), *Vegf-A* (C, D) and the VEGFRs, *Flk-1* (E, F), *Flt-1* (G, H) and *Nrp1* (I, J). *Ext1*$^{Gt/Gt}$ skeletal anlagen (A, C, E, G, I) show delayed expression of all markers expressed by hypertrophic chondrocytes (A, C, I), compared to wt mice (B, D, J). Furthermore *Nrp1* is only expressed in the skin in the mutant (I) while it is expressed in the skin and in the joint interzone of the digits of the wt embryos (J, red arrows). VEGF-A receptors, *Flk-1* and *Flt-1* are normally expressed in the mesenchymal tissue of the *Ext1*$^{Gt/Gt}$ mutants (E, G) similar to wt limbs (F, H). Magnification 50X.

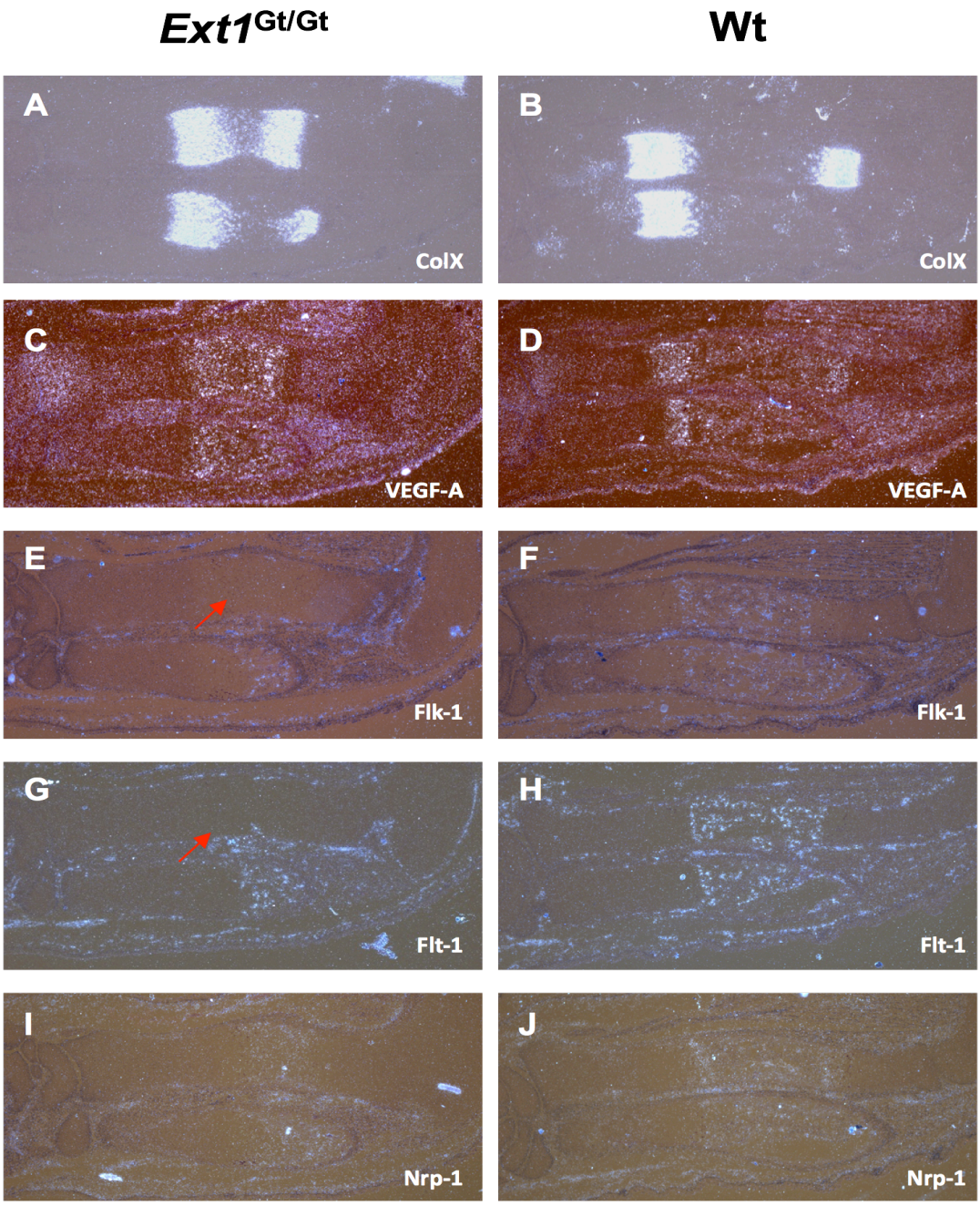

Figure 14. Expression of vascularization markers in E16.5 *Ext1*$^{Gt/Gt}$ forelimbs is not disturbed. *In situ* hybridization of wt and *Ext1*$^{Gt/Gt}$ forelimbs with riboprobes for *ColX* (A, B), *Vegf-A* (C, D) and the VEGFRs, *Flk-1* (E, F), *Flt-1* (G, H) and *Nrp1* (I, J). Expression of *ColX*, *Vegf-A* and *Nrp1* (A, C, I) are expanded in *Ext1*$^{Gt/Gt}$ skeletal anlagen with two distinct *ColX* expression domains (A). However, expression in the mutant is still delayed compared to wt (B, D, J). *Flk-1* and *Flt-1* (F, H) are strongly expressed in the wt bone marrow cavity, while their expression is still lacking in the center of the *Ext1*$^{Gt/Gt}$ mutant anlagen (E, G, red arrows). Magnification 50X.

In summary, *Ext1*$^{Gt/Gt}$ mutants show disturbed blood vessels formation and no vascular invasion of the cartilage anlagen, although expression of angiogenic markers is not considerably delayed. This suggests that either the stabilization or the binding of VEGF-A might be altered by loss of HS.

4.1.6 *Ext1*$^{Gt/Gt}$ chondrocytes induce increased migration of endothelial cells *in vitro*.

Although in *Ext1*$^{Gt/Gt}$ mutants hypertrophic chondrocytes express *Vegf-A* and endothelial cells express the proposed receptors, blood vessel invasion of the differentiating periosteum flanking the hypertrophic region is severely delayed. As HS has been shown to mediate VEGF-A binding to its receptor the delay might be due to the reduced signal reception in the endothelial cells. In addition the release of VEGF-A by the chondrocytes might be altered to the reduced levels of HS in the *Ext1*$^{Gt/Gt}$ chondrocytes. To analyze the capacity of *Ext1*$^{Gt/Gt}$ mutant chondrocytes to induce endothelial cell migration a modified Boyden chamber assay was established. High density micromass cultures of primary limb mesenchymal cells ($4x10^5$ cells) were seeded in the bottom of the well of a 12-well culture plate. In such micromass cultures mesenchymal cells condense and differentiate into chondrocytes, forming so called “cartilage nodules”. The chondrocytes in these nodules have been shown to undergo the critical stages of differentiation including differentiation into hypertrophic chondrocytes thereby mimicking the *in vivo* chondrocyte differentiation process (Ahrens et al., 1977; Solursh et al., 1978). Micromass cultures differentiated for 5 weeks before Boyden chamber assay was performed.

To distinguish endothelial cells from cells of the micromass cultures I isolated primary endothelial cells of a mouse line expressing *green fluorescent protein* (GFP) under the ubiquitous *β*-actin promoter (B5/EGFP mice) (Hadjantonakis et al 1998). Using an antibody against VEGFR2 and MACS magnetic beads (Miltenyi Biotech) endothelial cells were isolated from E12.5 and E13.5 B5/EGFP mice. After one week of culture, endothelial cells were subjected to 24 hours of serum starvation. Then 10^4 GFP endothelial cells were seeded on the transwell plate filter, situated on top of the micromass cultures and let migrate through the filter toward the bottom of the well.

Migration towards the micromass cultures was analyzed after 24 hours by counting the number of cells found on the bottom side of the filter and on the micromass cultures (Fig. 15 A, B). As positive control migration towards 30ng of VEGF-A protein as attractive signal was analyzed.

Interestingly migration towards the *Ext1*$^{Gt/Gt}$ mutant chondrocytes was significantly increased by 30% compared to wt (unpaired students T-test: n=7; p<0.0001) (Fig. 15C). A Boyden chamber assay with 30ng of VEGF-A protein as attractive signal was used as positive control. Comparing the Boyden chamber assay for VEGF-A and *Ext1*$^{Gt/Gt}$ micromasses I can conclude that endothelial cells have migrated 60% more towards *Ext1*$^{Gt/Gt}$ mutant cells than to VEGF-A in 24 hours. In contrast the control micromasses induce an increased migration up to 45% in 24hours compared to VEGF-A protein.

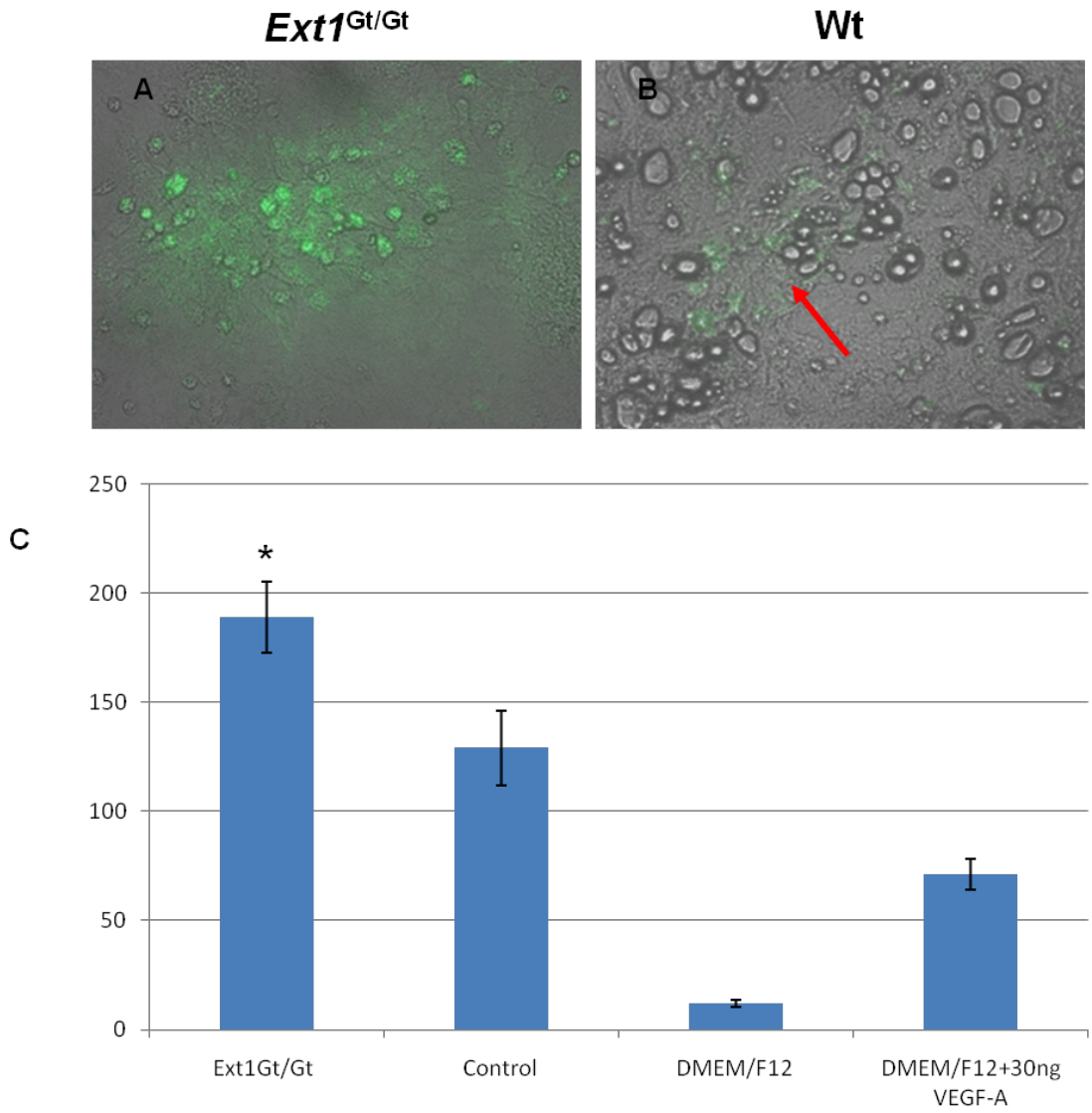

Figure 15. Increased migration of endothelial cell towards *Ext1*$^{Gt/Gt}$ mutant micromasses. 24 hours Boyden chamber assay with endothelial cells expressing GFP. Representative pictures of migrated GFP-endothelial cells on micromass cultures of *Ext1*$^{Gt/Gt}$ mutant (A) or wt micromasses (B). Red arrow in B shows an adherent endothelial cell on wt culture. Magnification 100X. (C) Endothelial cell migration showed a 30% increase toward *Ext1*$^{Gt/Gt}$ micromass cultures compared to wt cultures. (Y axis: number of migrated endothelial cells) (n=7; *: $p < 0.02$ unpaired student's t test).

In order to test if the increased migration of endothelial cells is a consequence of an increased *Vegf-A* expression in the mutant micromass cultures, quantitative reverse transcription PCR (qRT-PCR) was performed using cDNA of the same micromass cultures. No significant alterations in the expression levels of *Vegf-A*, *ColX* and *Bglap* (*Osc)* could be detected (unpaired Student t-test: n=7 $p>0.05$) (Fig. 16C), indicating that the increase in endothelial cell migration towards the

Ext1$^{Gt/Gt}$ mutant chondrocytes is not due to an increase in VEGF-A transcript. Alcian blue staining on micromass cultures show high number of chondrogenic nodules in the mutant micromasses, while the wt cultures show few nodules and presence of hypertrophic cells (Fig.16 A, B). The expression analyses revealed a significant increase in *Col2* expression in *Ext1*$^{Gt/Gt}$ micromasses ($p<0.05$; $n=7$) which correlate with the strong Alcian blue staining that reflects the presence of cartilaginous nodules.

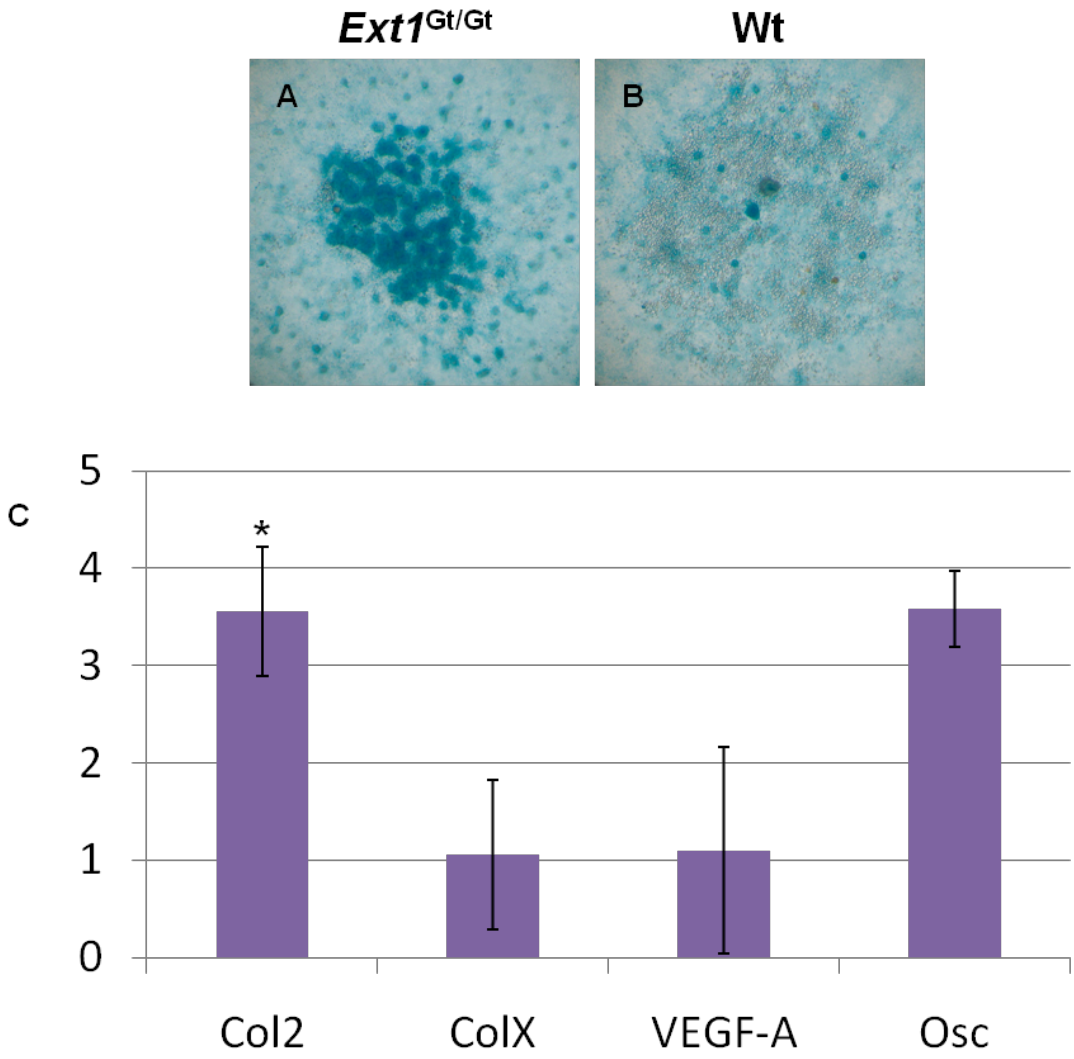

Figure 16. Increase in endothelial cell migration is not due to increase in VEGF-A expression in *Ext1*$^{Gt/Gt}$ mutant micromasses. Alcian blue staining of *Ext1*$^{Gt/Gt}$ mutant (A) and wt micromasses (B). Strong Alcian blue staining of the *Ext1*$^{Gt/Gt}$ mutant micromasses (A) reveals high number of chondrogenic nodules. In contrast wt micromasses show only few nodules and hypertrophic chondrocytes (B). Gene expression analyses by quantitative real time PCR (qPCR) (C). qPCR evaluation shows that *Ext1*$^{Gt/Gt}$ mutant cultures express similar level of *ColX*, *Vegf-A* and *Bglap* (*Osc*) compared to wt micromasses ($p>0.05$; n=7). However *Col2* expression is upregulated in the *Ext1*$^{Gt/Gt}$ mutant cultures. (*; $p<0.05$; n=7)(Y axis represent increase fold values). (Magnification 40X).

4.2 Analysis of an *Ext1* mouse models for Multiple Osteochondromas

4.2.1 Gene targeting strategy and disruption of *Ext1* function

The early lethality of *Ext1*$^{Gt/Gt}$ mice limits their use as a model for studying osteochondroma development. In order to investigate the generation of exostoses, I analyzed a mouse model in which the *Ext1* gene can be conditionally inactivated, kindly provided by Dr. Kevin B. Jones (University of Utah). These mice carry two trans orientated loxP sites flanking the second exon of the *Ext1* gene, and a NEO cassette, flanked by an additional loxP site cis-orientated to the second loxP site (*Ext1*$^{e2neofl/e2neofl}$) (Fig. 17). Cre-induced recombination of the allele generated 8 different allelic recombinations of the transgene. To establish a mouse line lacking the NEO cassette, *Ext1*$^{e2neofl/e2neofl}$ males were crossed to *Prx1-Cre* females, which express Cre recombinase in the germ line (Logan et al., 2002). Twenty litters were genotyped by PCR to identify mice that had lost the neo cassette and retained the second exon in either wt (*Ext1*$^{e2fl/+}$) or inverted orientation (*Ext1*$^{e2flinv/+}$) (Fig. 17). 36 out of 127 mice carried the wt allele and 26 the inverted. These two mouse lines were crossed to C57BL6/J wt mice for two generations, to verify stable germ line transmission of the targeted allele. Both *Ext1*$^{e2fl/+}$ and *Ext1*$^{e2flinv/+}$ mice are born at the expected Mendelian ratios.

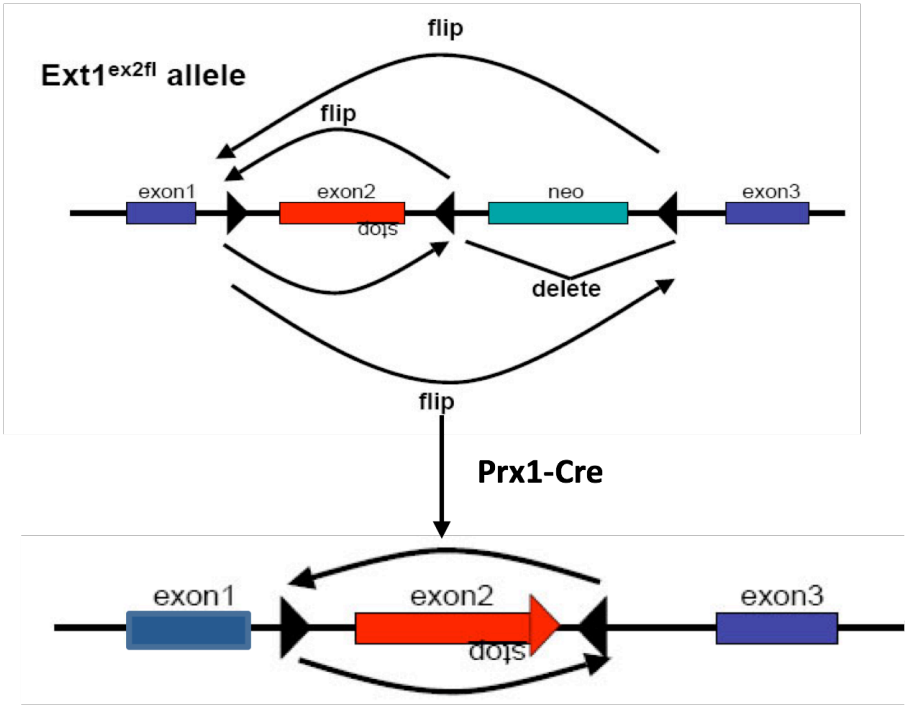

Figure 17. Generation and characterization of head-to-head floxed *Ext1* allele: deletion of the neomycin resistance gene and generation of a non functional *Ext1* allele. *Ext1*$^{e2neofl/e2neofl}$ mice carry two loxP sites, trans-orientated, flanking the second exon of the *Ext1* gene, and a NEO cassette, flanked by a third loxP site cis-orientated to the second loxP site. The neomycin resistance gene was deleted by crossing *Ext1*$^{e2neofl/e2neofl}$ males to *Prx-1 Cre* females expressing Cre recombinase in the germ line.

In order to confirm that the inversion of exon 2 results in a loss of *Ext1* function allele sections of homozygous *Ext1*$^{e2flinv/e2flinv}$ embryos, derived from crosses of *Ext1*$^{e2flinv/+}$ mutants, were analyzed at embryonic stage E7,0 (Fig. 18) with Hematoxylin/Eosin staining. Four out of 10 embryos were smaller and failed to undergo gastrulation, consistent with the phenotype previously described for *Ext1*$^{-/-}$ and *Ext2*$^{-/-}$ null mutant mice (Stickens et al., 2005; Lin et al., 2000). Genotyping, performed by nested PCR on carefully dissected embryonic tissues, confirmed that these embryos were homozygous *Ext1*$^{e2flinv/e2flinv}$ mutants. In wt embryos the structures typical for this stage of development can be subdivided into the extra embryonic compartment and structures of the embryo proper (Fig.18 B). The posterior end of the primitive streak (ps) bulges into the proamniotic cavity (pc) forming the posterior amniotic fold. In the mesoderm of the posterior amniotic fold, small cavities coalesce to form a single cavity, the exocoelom (ec). In the 4 *Ext1*$^{e2flinv/e2flinv}$ mutant embryos it was not possible to distinguish between extra embryonic structures and the embryo proper (Fig. 18 A). To exclude that these mutants produced functional Ext1 protein, the amount of HS was analyzed by

immunohistochemistry using an antibody for the 10E4 epitope, which recognize alternating D-glucuronic acid and *N*-acetyl-D-glucosamine residues of HS (Fig. 18 C, D). Wt and heterozygous mice showed strong staining of HS in all embryonic and extra embryonic tissues (Fig. 18 D), while no HS sulfate could be detected in the homozygous *Ext1*$^{e2flinv/e2flinv}$ mutants. 10E4 staining was however detected in the surrounding placenta (Fig. 18 C), which partly consists of heterozygous maternal tissue and can be considered as internal positive control.

In summary, these results show that when exon 2 of *Ext1* is inverted, it results in a loss of function of *Ext1* allele and abolishes the production of HS.

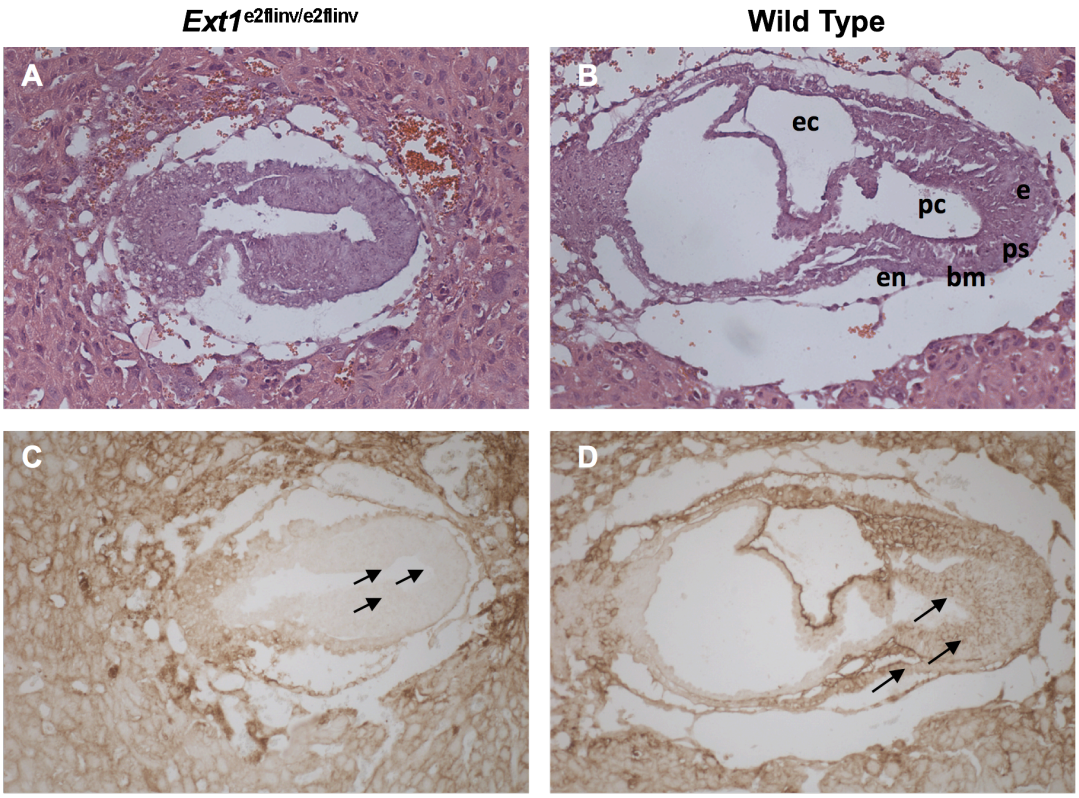

Figure 18. Inversion of exon2 of *Ext1* generates a loss of function of the *Ext1* allele. Hematoxylin/Eosin staining (A and B) and immunohistochemistry with the 10E4 antibody (C and D) of E7.0 frontal sections of wt (B and D) and *Ext1*$^{e2flinv/e2flinv}$ embryos (A and C) demonstrated failing gastrulation and reduced HS in the embryonic tissue (A and C, arrows) of *Ext1*$^{e2flinv/e2flinv}$ mice, whereas placental tissues showed intensive staining for HS (ec, exocoelomic cavity; pc, proamniotic cavity; e, ectoderm; ps, primitive streak; bs, basement membrane; en, endoderm). Magnification 200X.

4.2.2 Postnatal inactivation of *Ext1* generates exostoses.

To investigate if clonal somatic loss of *Ext1* leads to osteochondroma formation, the *Ext1* gene was deleted in proliferating chondrocytes by crossing homozygous *Ext1*$^{e2fl/e2fl}$ mutants to mice carrying a *Cre* recombinase allele under the control of a tetO heptad minimal cytomegalovirus (CMV) promoter and a *rtTA* (tetracycline reverse transcriptional activator) gene under the control of a *Col2* promoter *(Col2-rtTA-Cre*; Grover and Roughley, 2006). In the resulting *Col2-rtTA-Cre;Ext1*$^{e2fl/e2fl}$ mice doxycycline treatment activates the rtTA reverse repressor that is expressed in *Col2* expressing cells. The activated rtTA in turn induces the expression of *Cre* recombinase by binding the tetO/CMV promoter. Consequently, exon 2 of the *Ext1* gene is inverted in *Col2* expressing chondrocytes after administration of doxycycline (Fig. 19).

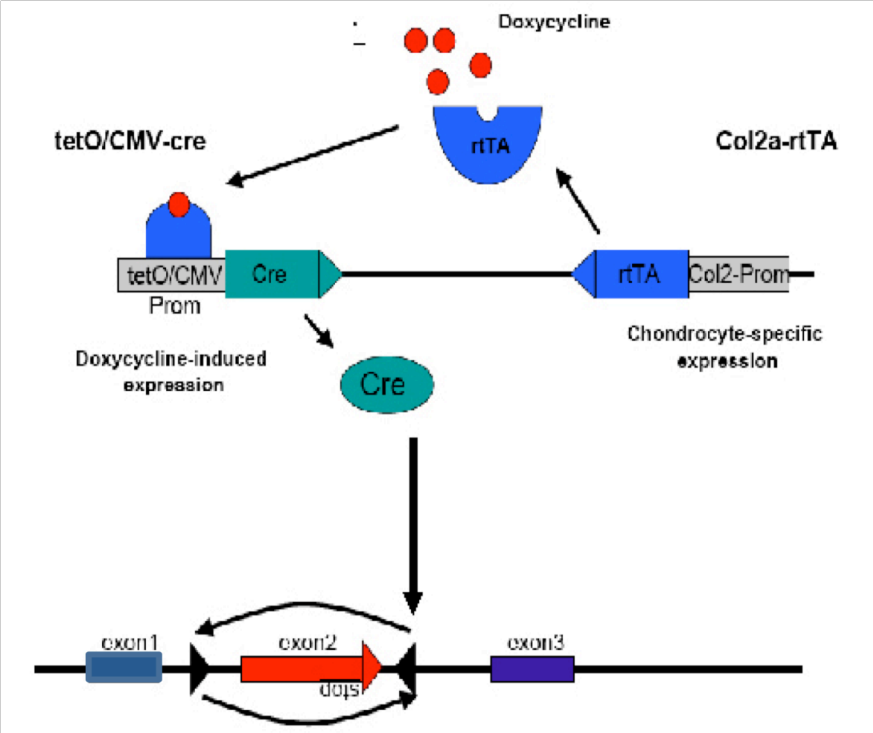

Figure 19 Somatic inactivation of *Ext1* in proliferating chondrocytes. *Ext1*$^{e2fl/e2fl}$ mice were crossed to a mouse line carrying a doxycycline inducible Cre recombinase gene under the control of the *Col2* promoter (*Col2-rtTA-Cre*). Doxycycline binds to the reverse transcriptional tetracycline repressor (rtTA), which is produced in *Col2* expressing chondrocytes. The activated rtTA binds to the tetO/CMV promoter and activates the expression of *Cre* recombinase. This enzyme recombines the trans-orientated loxP sites resulting in an inversion of the genomic sequence flanked by the two loxP sites.

In previous experiments 4mg/ml doxycycline in drinking water has been administrated to lactating mothers starting at postnatal day 8 (P8) over a period of 8 days. Using this protocol, massive exostoses were generated at all metaphyses of the long bones, leading to severe bone malformations (K. B. Jones personal observations). In order to induce a controlled, less severe phenotype I established a protocol to induce reduced numbers of osteochondromas with 100% penetrance. The following treatment strategies were compared:

1) 4 mg/ml doxycycline in 5% sucrose through the drinking water for 8 days

2) 4 Intraperitoneal (IP) injections of 80µg doxycycline /gram body weight (gbw)

3) 2 IP injections of 80µg doxycycline /gbw

4) 1 IP injection 80µg doxycycline /gbw

Histological analyses of sections through hindlimbs of 8 weeks old mice after induction revealed that all treatment strategies resulted in the reproducible induction of the exostoses in all cases investigated. As the malformations of the long bones seemed to be less severe in the shortest treatment period a single IP injection of 80µg doxycycline/gbw was used in all further experiments (Fig. 20).

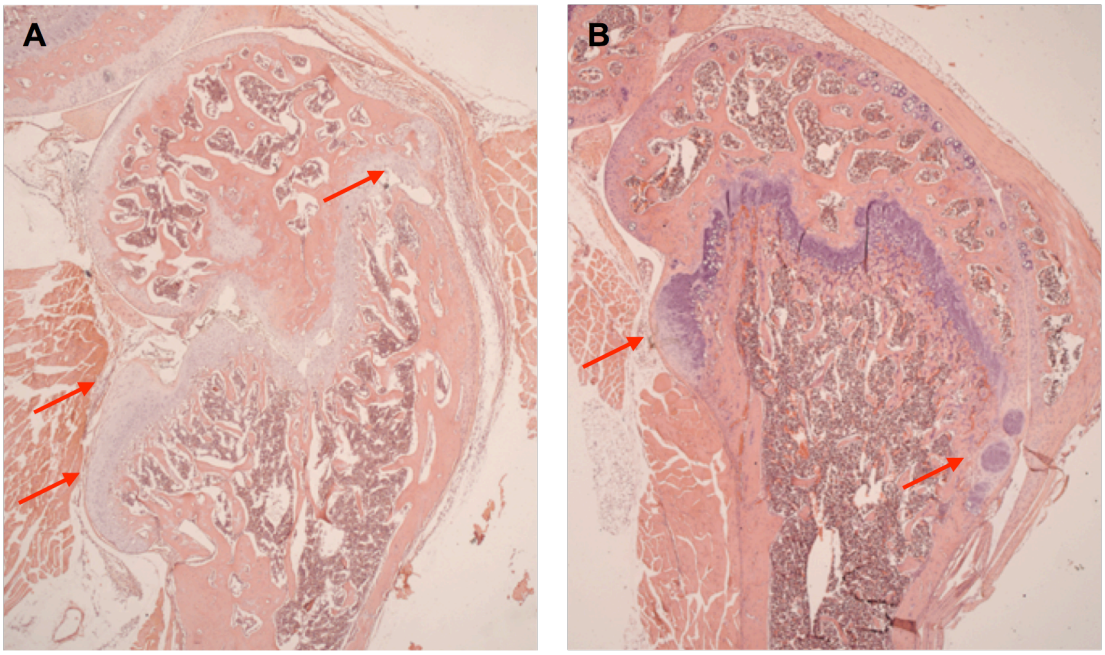

Figure 20. Histological analyses of femurs of *Col2-rtTA-Cre;Ext1*$^{e2fl/e2fl}$ mice induced with different doxycycline administrations. *Col2-rtTA-Cre;Ext1*$^{e2fl/e2fl}$ mice treated 8 days with 4 mg/ml doxycycline, administered through drinking water, (A) or one IP injection of 80µg doxycycline/gbw (B) were sacrificed at 8 weeks of age. Both treatment strategies resulted in the development of ostechomdromas. Red arrows indicate exostoses arising at the side of the growth plate. Magnification 25X.

To analyze the development of osteochondromas animals were sacrificed at different time points after the doxycycline treatment (4, 5, 6 and 8 weeks old mice). In the course of the study knees were collected and processed for further analyses. Histological anaysis on H&E stained serial sections of the knees shows development of osteochondromas in homozygous *Ext1*$^{e2fl/e2fl}$ mice, which carry the *Cre* recombinase under the *Col2* promoter (*Col2-rtTA-Cre*) with a frequency of 100%. None of the animals that did not carry the Cre-recombinase allele or were not homozygous for the *Ext1*^{e2fl} allele did show any sign of osteochondroma development (Table 1 and Jones et al., 2010).

Table 1. Frequency of osteochondromas development after doxycycline induction.

Genotype	N° of mice showing exostoses					
	4 Weeks of age	5 Weeks of age	6 Weeks of age	8 Weeks of age	15 Weeks of age	Total
Col2-rtTA-Cre; Ext1$^{e2fl/e2fl}$	7/7	4/4	5/5	10/10	2/2	28/28
Ext1$^{e2fl/e2fl}$	0/4	0/1	0/1	0/8	0/1	0/15

4.2.3 Murine osteochondromas resemble the human phenotype

As already shown by morphological staining mutants at eight weeks of age have developed exostoses of considerable size, that can easily be depicted at the side of the femur (Fig. 20). To investigate if, as in human patients, osteochondromas are formed on all endochondral bones skeletal preparation were stained with Alizarin red, which detects calcium deposits of the mineralized matrix. In induced *Col2-rtTA-Cre;Ext1*$^{e2fl/e2fl}$ animals at the age of eight weeks, osteochondromas are not restricted to the extremities, but developed on all endochondral bones including the vertebrae, (Fig.21 C, D, C1, D1) as well as the pelvic bone (Fig.21 A, B, A1, B1), thus mimicking the human phenotype. Moreover, similar as in human patients, bones severely affected by osteochondromas are frequently reduced in size compared to control bones (Fig. 21 C, D)

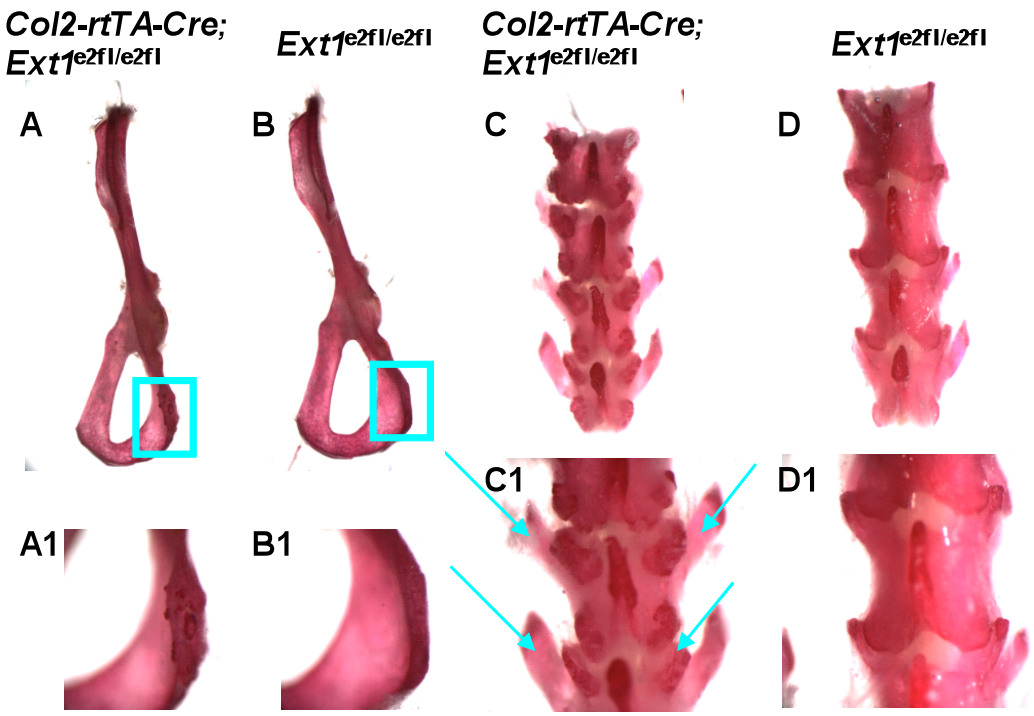

Figure 21. Doxycycline treated *Col2-rtTA-Cre;Ext1*$^{e2fl/e2fl}$ mice show exostoses at many sites of the endochondral skeleton. Alizarin red staining of the pelvic bone (A, B, A1, B1) and vertebrae (C, D, C1, D1). *Col2-rtTA-Cre;Ext1*$^{e2fl/e2fl}$ pelvic bone (A1 higher magnification of A) develop osteochondromas. Furthermore, mutant vertebrae (C1 higher magnification of C) are shorter compared to the control (D1 higher magnification of D) and show several exostoses (blue arrows in C1).

To test if *Col2-rtTA-Cre;Ext1*$^{e2fl/e2fl}$ osteochondromas display a similar cellular organization as the human tumors, *in situ* hybridization with markers for different chondrocyte populations were performed (Fig. 22 B-E). Morphologically human osteochondromas have a bony stalk in contact with the cortical bone and the bone marrow and are covered by a cartilage cap at the outside. The organization of chondrocyte populations in the cartilage cap resembles the organization of the growth plate (Wicklund et al., 1995; Gordon et al., 1981; Peterson, 1989). *In situ* hybridization revealed that *Col2-rtTA-Cre;Ext1*$^{e2fl/e2fl}$ osteochondromas cells distribute similar as in human osteochondromas. The chondrocytes in murine osteochondromas express the typical differentiation markers of the embryonic growth plate: *ColX*, *Ihh*, *Ptch1*, and *Col2*. Hypertrophic, *ColX*-expressing chondrocytes are in contact with the mineralized bone, adjacent to prehypertrophic *Ihh*-expressing and columnar *Ptch1*-expressing chondrocytes. These are surrounded by proliferating *Col2*-expressing chondrocytes.

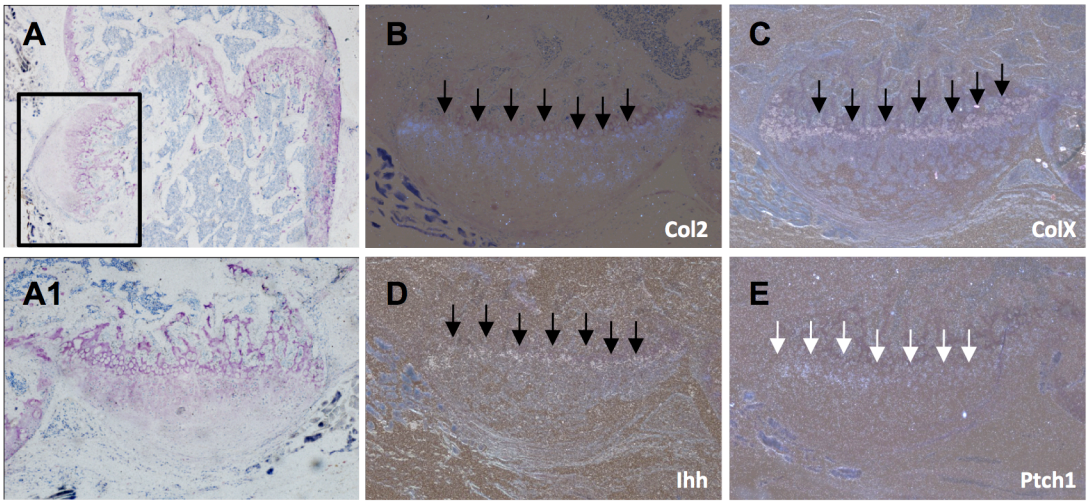

Figure 22. The cellular organization of *Col2-rtTA-Cre;Ext1*$^{e2fl/e2fl}$ osteochondroma resembles a growth plate. Parallel sections of 8-week-old mice were stained with Toluidine blue (A and A1) and hybridized with antisense riboprobes for *Col2* (B), *ColX* (C), *Ihh* (E), and *Ptch1* (F). *In situ* hybridization demonstrates that osteochondroma chondrocytes mimic the organization of the physis, with *Col2* expressing proliferating chondrocytes followed by *Ihh*- and *ColX*-expressing hypertrophic chondrocytes (F). Similar to the growth plate *Ptch1* is expressed in proliferating chondrocytes, flanking the *Ihh* expression domain. (Fig. A shows higher magnification of boxed areas in A1). Magnification 50X (A); 100X (A1, B-E).

4.2.4 A physeal proliferative chondrocyte is the cellular origin of osteochondromas

To understand the initiation of osteochondroma formation and to identify the cell type in which they originate, the relative position of the tumor to the growth plate was carefully investigated. Femurs of *Col2-rtTA-Cre;Ext1*$^{e2fl/e2fl}$ mice at different ages were compared (4, 5, 6 and 8 weeks old mice) starting with 8 weeks old mice (Fig. 23). At this stage mice have reached their sexual maturity, comparable to the end of puberty in humans. Osteochondromas usually stop growing at the end of puberty when the growth plate itself closes and cells cease to proliferate (Legeai-Mallet et al., 1997; Schmale et al., 1994; Wicklund et al., 1995; Gordon et al., 1981; Peterson, 1989). Morphological staining revealed that 8 weeks old *Col2-rtTA-Cre;Ext1*$^{e2fl/e2fl}$ mutants display massive exostoses at the distal end of the femur which occasionally are still in contact with the proliferative zone of the growth plate (Fig. 23D). In order to define at which stage osteochondroma formation is initiated, femurs of younger mice, between 4 and 6 weeks of age were analyzed. 4, 5 and 6 weeks old *Col2-rtTA-Cre;Ext1*$^{e2fl/e2fl}$ mice revealed smaller osteochondromas,

which are less differentiated than in the 8 weeks old mutants. In most cases, especially in the younger tumors, the clones consist exclusively of chondrocytes (Fig. 23 B, C), which are surrounded by a highly developed extracellular matrix (Fig. 23 C1).

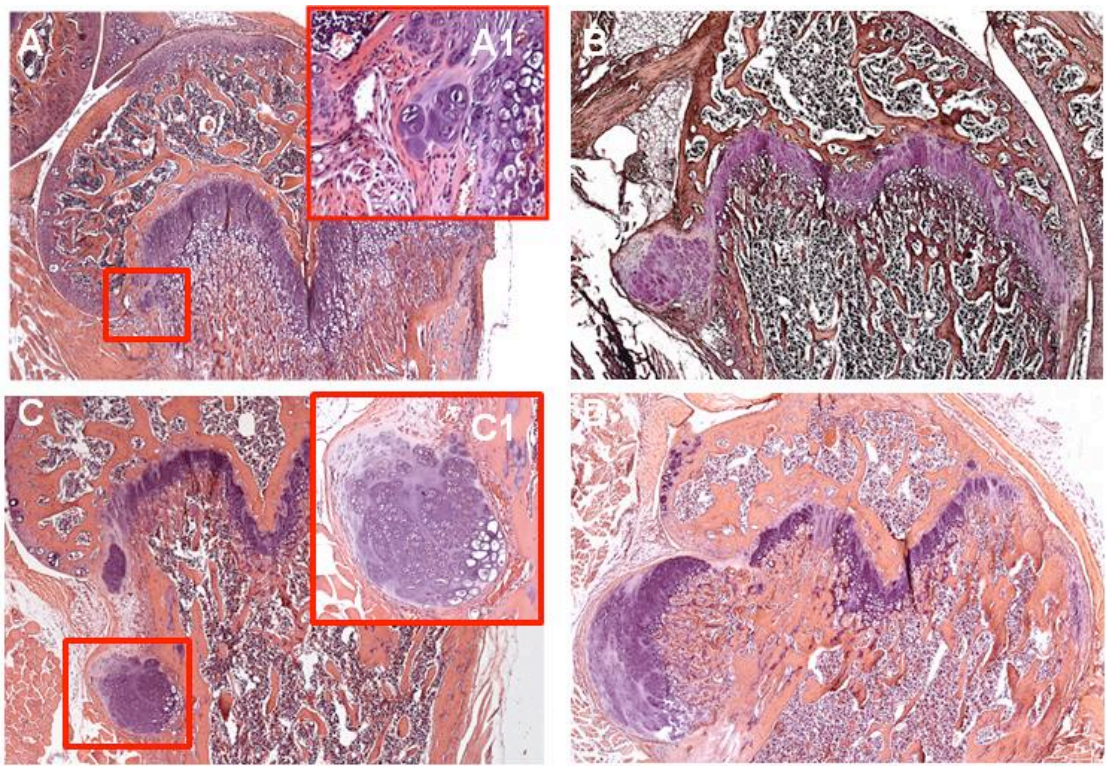

Figure 23. Osteochondromas develop from growth plate chondrocytes into massive tumors at femur epiphyses. Hematoxyline/Eosin staining of femur sections at 4, 5, 6 and 8 weeks of age (A to D). In 4 weeks old *Col2-rtTA-Cre;Ext1*$^{e2fl/e2fl}$ mice few cells disrupt the growth plate organization (A, A1 higher magnification of the red box in A), to proliferate and expand at the side of the femur growth plate (B, C, D), developing into massive, differentiated osteochondromas in 8 weeks old mutants. Higher magnification of osteochondromas from 6 weeks old mice (C1 and C) show clustered organization of chondrocytes. Magnification 100X (A, B, C, D) and 20X (A1, C1).

Interestingly at 4 weeks of age *Col2-rtTA-Cre;Ext1*$^{e2fl/e2fl}$ mice show very small clones of chondrocytes, located at the upper side of the growth plate where it is connected to the articular cartilage (Fig. 23A) that are clearly separated from the growth plate by the extracellular matrix To confirm the morphological observation that these early osteochondromas consist of chondrocytes I analyzed the expression of chondrocyte markers (Fig. 24). *In situ* hybridization revealed that these early osteochondroma cells express *Col2* and *Ucma*, a matrix protein typical for early proliferating chondrocytes (Tagariello et al, 2008) (Fig.24 B, D). The same cells lacked of *ColX* and *Ihh* expression (Fig.24 C, E), demonstrating that in 4

week old *Col2-rtTA-Cre;Ext1*$^{e2fl/e2fl}$ mice the osteochondromas consist of early proliferative chondrocytes which have not differentiated into pre– or hypertrophic chondrocytes, yet. In summary gene expression analyses confirmed the morphological observations that a chondrocyte is likely the cellular origin of osteochondromas in *Col2-rtTA-Cre;Ext1*$^{e2fl/e2fl}$ mice. The location of these clones in or on close proximity to the growth plate strongly indicates that osteochondromas in *Col2-rtTA-Cre;Ext1*$^{e2fl/e2fl}$ mice develop from physeal chondrocytes, which proliferates and further differentiates into a more complex structure resembling the human osteochondromas.

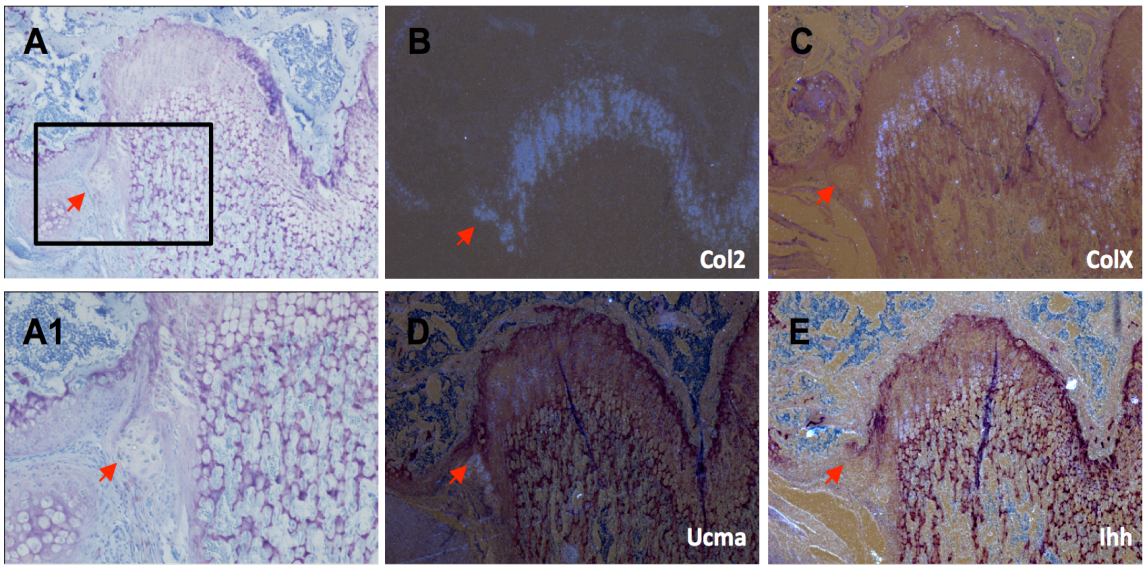

Figure 24. Gene expression analyses confirm a growth plate chondrocyte as cellular origin of osteochondromas in *Col2-rtTA-Cre;Ext1*$^{e2fl/e2fl}$ mice. Parallel sections of distal femurs from 4-week-old mice were stained with Toluidine blue (A and A1) and hybridized with antisense riboprobes for *Col2* (B), *ColX* (C), *Ucma* (E), and *Ihh* (F). These early osteochondromas express no *Ihh*, or *ColX*, but strongly express *Col2* and *UCMA*, markers for early proliferating chondrocytes. A1 shows higher magnification of boxed area in A. Magnification 100X (A, B-E); 200X (A1)

4.2.5 Loss of heterozygosity is required for development of osteochondromas

One controversially discussed question is the allelic status of the human osteochondromas. It has not been clarified yet if haploinsufficiency of *EXT* genes is sufficient to disturb cell signaling in the growth plate or a complete loss of function is necessary. To further investigate the etiology of MO syndrome, clones of 1 to 10 mutant cells were isolated from sections of *Col2-rtTA-Cre;Ext1*$^{e2fl/e2fl}$

osteochondromas at different developmental stages by laser capture microdissection (LCM) (Fig. 25 A). In order to amplify small amounts of DNA representing 1-10 genomes (8pg DNA/genome) nested primer pairs were designed detecting the wt and the inverted allele respectively. To amplify a single genome the first amplification round was performed in a single reaction using one forward primer detecting both alleles and two reverse primers, for the wt and the inverted allele respectively. As the difference in size between the two nested PCR products was too small to be detected on an agarose gel (54 base pairs) the second amplification round was performed in separated reactions (Fig. 25 B).

128 out of 183 clones analyzed, about 70%, were not successfully amplified by PCR. This failure rate matches the technical success rate of other studies in which LCM analyses were performed on paraformaldehyde-fixed, paraffin embedded tissues (Becker et al., 1997; Ohno et al., 1997). The results of our genotyping analyses revealed that of the remaining 55 successfully analyzed clones, 38 were homozygous for the inverted allele *Ext1*$^{e2flinv/e2flinv}$, 14 were homozygous for the wt allele (*Ext1*$^{e2fl/e2fl}$) and three were heterozygous (*Ext1*$^{e2fl/e2flinv}$.) indicating that in our mouse model osteochondroma cells carried all possible genomic rearrangements of the *Ext1* transgene. Approximatively 70% of the clones of osteochondromas tissue carried a homozygous mutation (Fig. 25 C). This result supports the hypothesis that loss of heterozygosity happens in a small cluster of cells, which eventually proliferate and expand, possibly including wt cells into its structure.

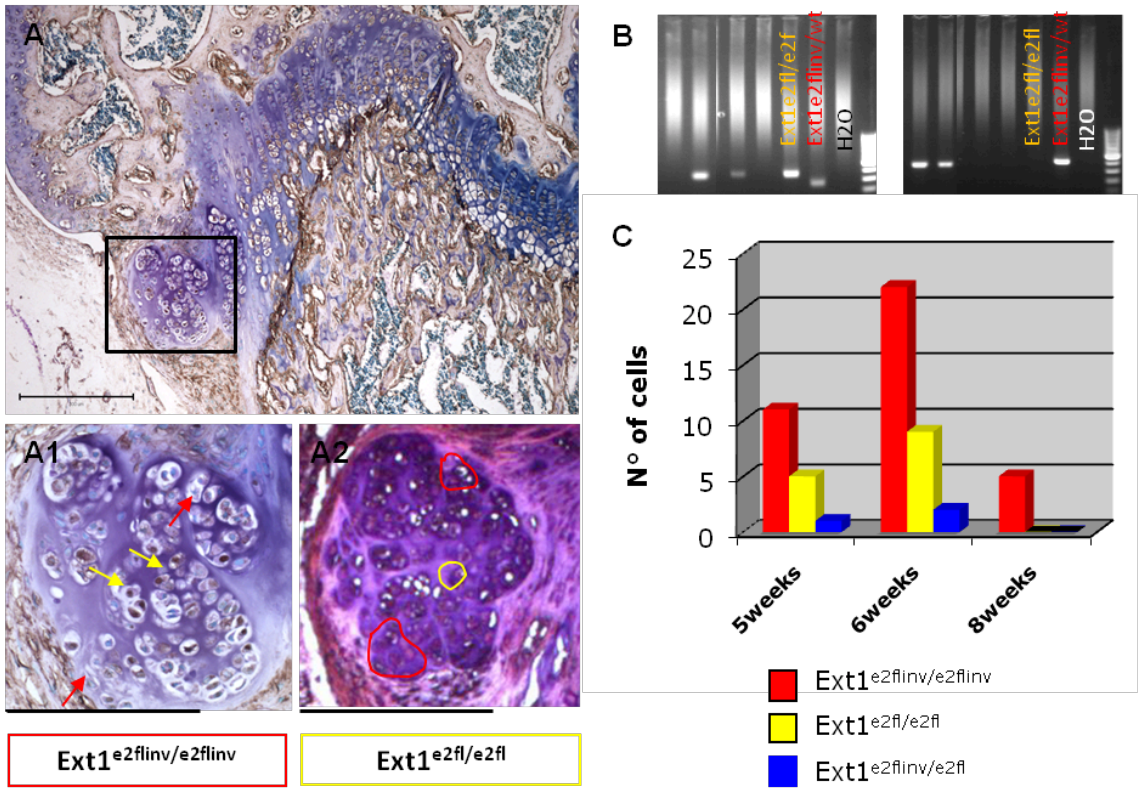

Figure 25. Osteochondromas chondrocytes are mostly homozygous for the inversion of exon 2 of *Ext1*. (*A*) Immunohistochemistry with 10E4 antibody on osteochondroma of a 6-week-old *Col2-tTA-Cre;Ext1*$^{e2fl/e2fl}$ shows that loss of HS correlated with homozygosity for the inverted allele in parallel sections (red-encircled clones in A2, red arrows in A1). HS-positive chondrocytes demonstrated the *Ext1*$^{e2fl/e2fl}$ (yellow-encircled clones in A2, yellow arrows in A1) genotype. Nested PCR on cell lysate after laser microdissection (LCM) was used to identify forward or reverse orientation of exon 2 (B). Genomic DNA was used as positive controls for the wt and the inverted allele as indicated. Water control was used to confirm lack of contaminations (H2O). The distribution of 55 LCM-identified clone genotypes from osteochondroma chondrocytes demonstrates a strong majority of *Ext1*$^{e2flinv/e2flinv}$ genotypes at all ages (C). Bar in A=300µm; Bar in A1-A2=150µm.

4.2.6 HS staining confirms loss of heterozygosity in *Col2-tTA-Cre;Ext1*$^{e2fl/e2fl}$ osteochondromas

To further confirm the spatial distribution of genotypes within the osteochondromas parallel sections were analyzed by LCM genotyping and 10E4 immunohistochemistry (Fig. 25 A, 26). Femurs of 8 and 4 old weeks mice (Fig. 26 A and B) show a strong HS staining in growth plate chondrocytes, while osteochondromas cells are depleted of HS synthesis. No HS is detected on 6 out of 10 osteochondromas and 4 osteochondromas display a minority of clones still

producing small amounts of HS. Genetic analyses confirm that HS-negative areas consistently were *Ext1*$^{e2flinv/e2flinv}$ and that osteochondromas containing *Ext1*$^{e2fl/e2fl}$ cells displayed small discrete regions of HS synthesis. The observation that most of the osteochondroma tissue is depleted of HS (Fig. 26) support the morphological observation that osteochondromas develop from a growth plate chondrocyte, which is not able to produce HS, and develop into a structure mostly composed of cells that do not produce any functional Ext1 protein.

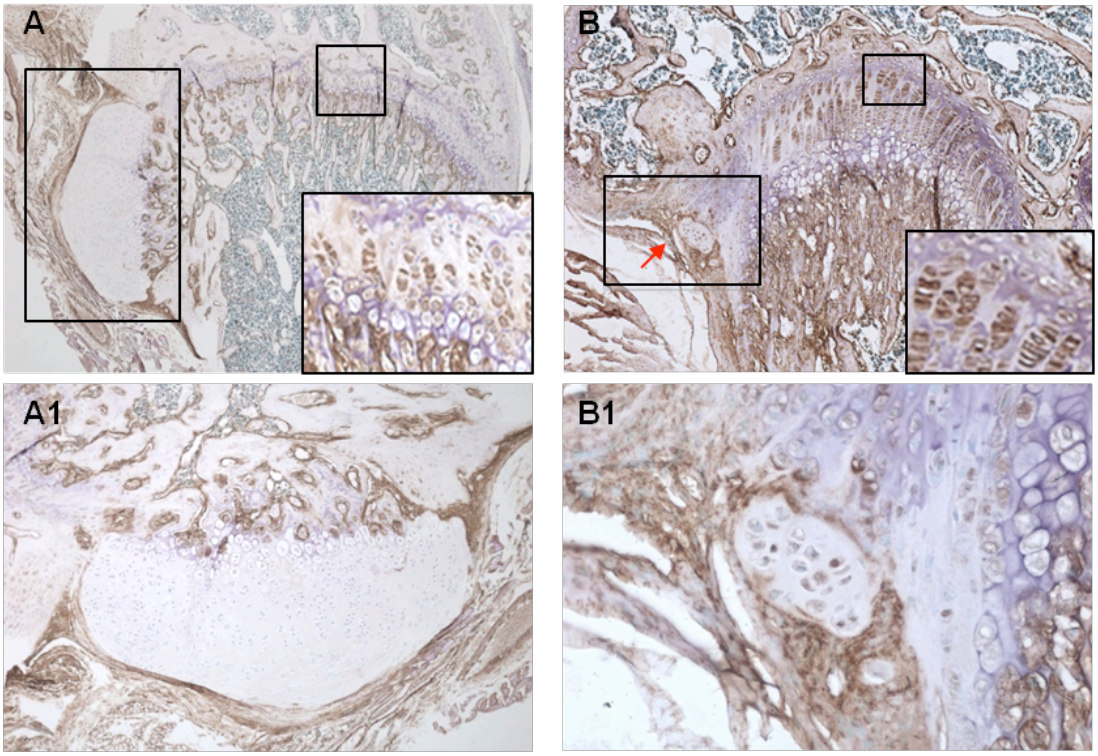

Figure 26 HS staining of osteochondromas supports loss of heterozygosity theory. Parallel sections of 8 and 4 week-old mice were analyzed by immunohistochemistry using the 10E4 antibody and counterstained with Methyl Green (A and B). HS staining demonstrates normal HS distribution in physeal chondrocytes (A and B, right Insets) but absence of HS in osteochondroma chondrocytes (A1 and B1). Magnification 100X (A and B); 200X (A1 and B1).

As reported previously, HS plays an important role in chondrocyte differentiation (Koziel et al., 2004). To investigate whether a chondrocytes lacking HS production can still differentiate into different chondrocyte subtypes, the distribution of HS on sections of *Ext1*$^{Gt/Gt}$ mice was analyzed by immunohistochemistry using the 10E4 and HepSS1 antibodies, which recognize different patterns of GlcNAc or GlcNS sequences. Wt mice show a strong staining for both epitopes in the mesenchymal tissue surrounding the cartilage anlagen, in the carpal bones and in proliferating and hypertrophic chondrocytes of the skeletal elements (Fig.27 D and F). *Ext1*$^{Gt/Gt}$

mutants show severely reduced 10E4 staining (Fig.27 C) in all chondrocytes, while strong HepSS1 staining is detectable in proliferating chondrocytes (Fig. 27 E). *Ext1*$^{Gt/Gt}$ mutants still produce a 20% of the amount of wt HS and the distribution of the two different epitopes is consistent with previous biochemical analyses (Yamada et al. 2004). The epitope recognized by the HepSS1 antibody was shown to be represented in *Ext1*$^{Gt/Gt}$ mutants in an amount comparable to wt mice, while the sequence that reacts with the 10E4 antibody is less represented in *Ext1*$^{Gt/Gt}$ mutants than in wt embryos. In contrast to *Ext1*$^{Gt/Gt}$ immunohistochemistry for 10E4 and HepSS1 on parallel sections of *Col2-tTA-Cre;Ext1*$^{e2fl/e2fl}$ femurs reveals that osteochondroma cells show a reduced staining for both antibodies further confirming a complete loss of HS synthesis in osteochondromas (Fig. 27 A and B).

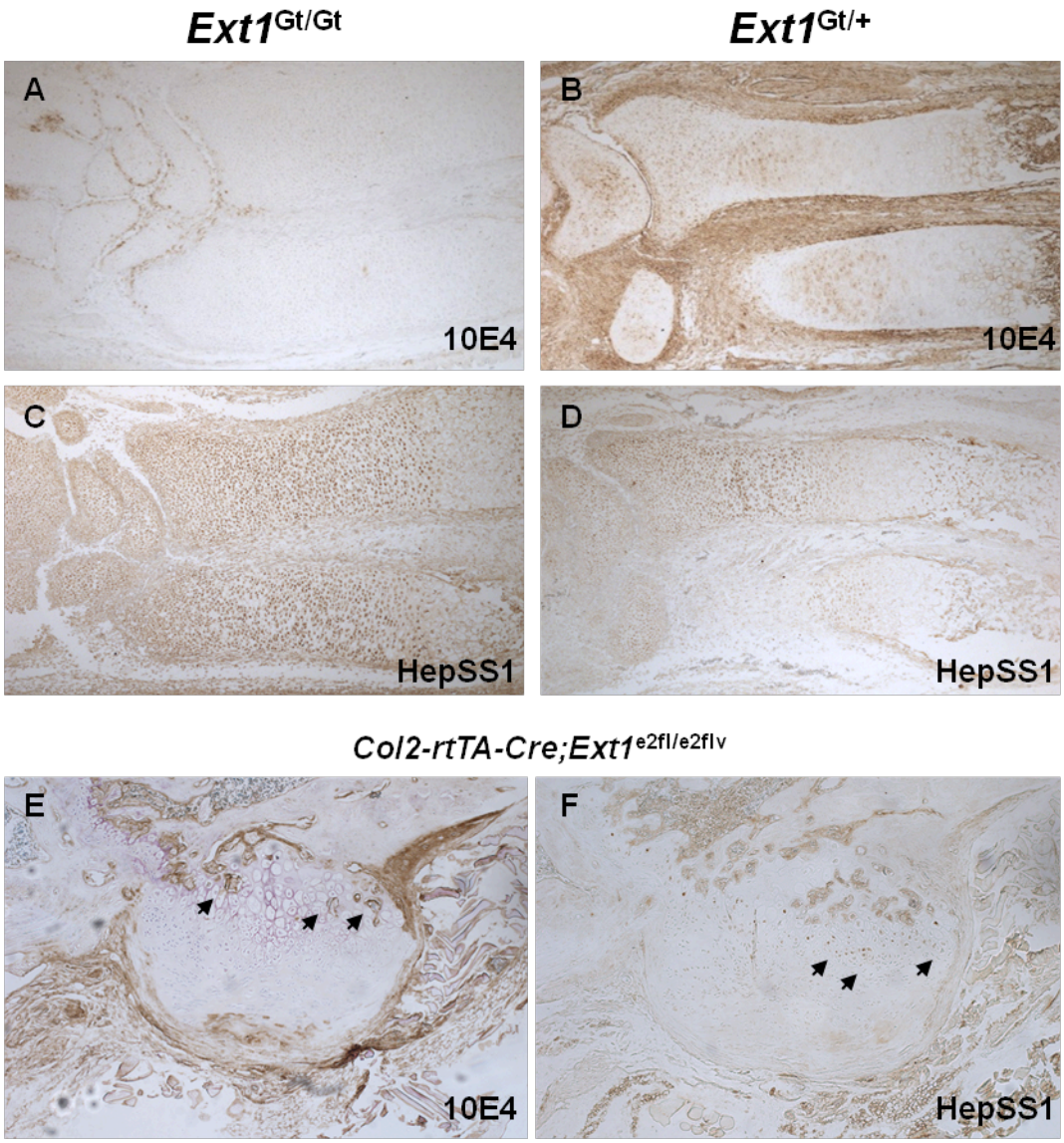

Figure 27. *Ext1*$^{Gt/Gt}$ mutants show different HS staining patterns for different epitopes, while osteochondromas lack HS. 10E4 and HepSS1 immunohistochemistry was carried out on E16.5 *Ext1*$^{Gt/Gt}$ mutant (A and C), control forelimbs (B and D) and osteochondromas (E and F). *Ext1*$^{Gt/+}$ show strong staining with both antibodies in proliferating and hypertrophic chondrocytes and in carpal bones (B, D). *Ext1*$^{Gt/Gt}$ mutants show severely reduced 10E4 staining (A), compared to wt (B) but are positive for HepSS1 staining (C). In osteochondroma tissue no HS could be detected with either antibodies (E and F). Magnification 200X (A and B), 100X (C-F).

4.2.7 *Col2-tTA-Cre;Ext1*$^{e2fl/e2fl}$ mice display signs of early osteoarthritis.

Osteoarthritis (OA) is a degenerative joint disease characterized by loss of proteoglycans in the articular surface of the bones, which affects about 14% of MO

human patients (Wicklund et al., 1995). To investigate if *Col2-tTA-Cre;Ext1*$^{e2fl/e2fl}$ mice develop signs of proteoglycan loss, section of knee joints were stained with Safranin O and Toluidine blue. Safranin O uniformly stains the articular surface (Fig. 28B) of wt mice at 8 weeks of age. In contrast, mutant knee joints at the same age show an increased number of chondrocytes with lacunae and irregular proteoglycan distribution (Fig. 28A, yellow arrows). In addition many cells in the articular surface appear to be hypertrophic. *In situ* hybridization revealed that in wt mice *ColX* expression is restricted to hypertrophic chondrocytes in the growth plate (Fig. 28D, yellow arrow) while strong expression of *ColX* in both, the growth plate and in the articular region, (Fig. 28C, yellow arrows) can be detected in *Col2-tTA-Cre;Ext1*$^{e2fl/e2fl}$ mice (Fig. 28E, F, yellow arrows). Since expression of *ColX* in the articular chondrocytes belongs to the symptoms of early OA, older mice were analyzed in order to investigate the progression of OA during aging.

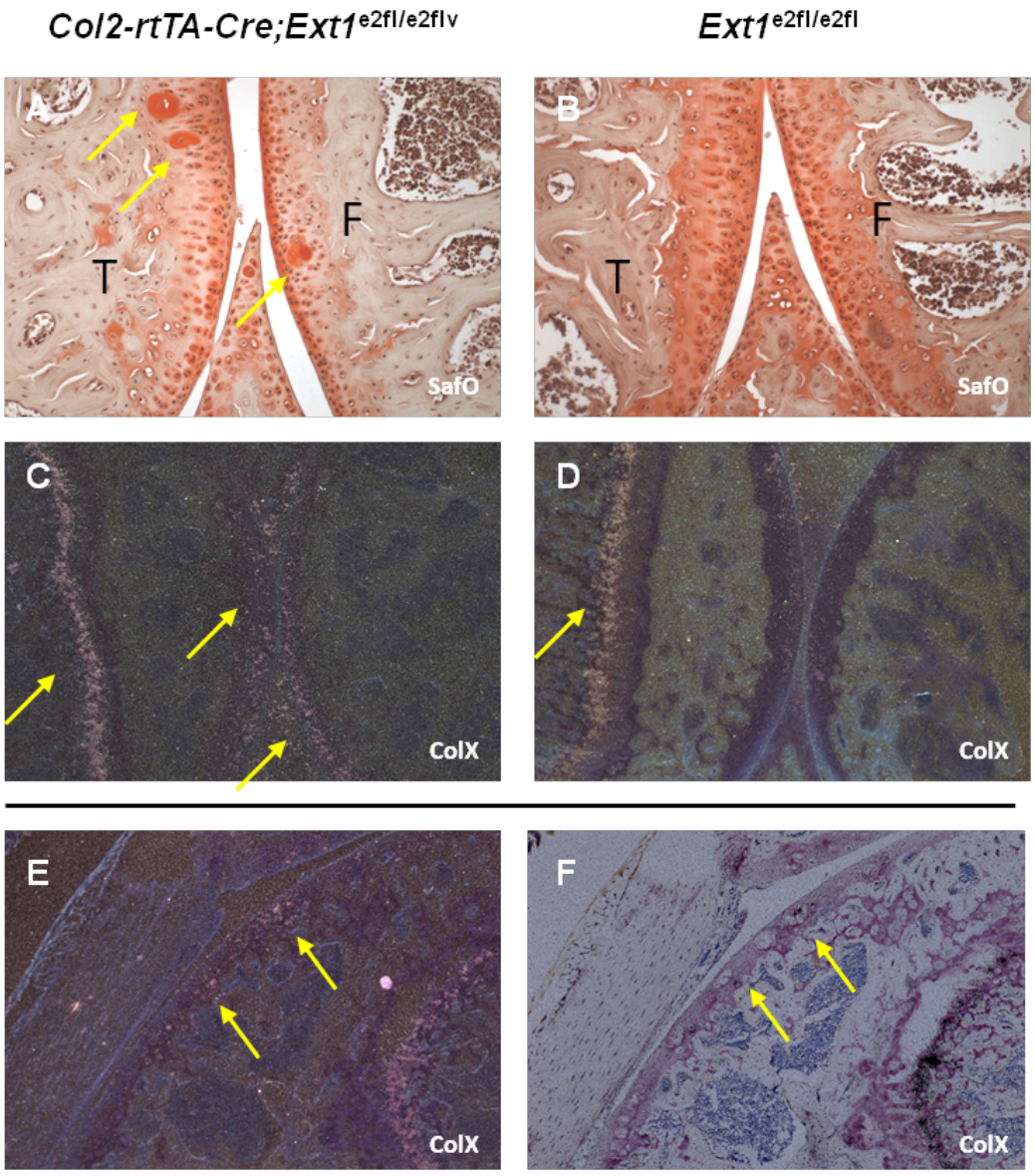

Figure 28. *Col2-tTA-Cre;Ext1*$^{e2fl/e2fl}$ joints display symptoms of early osteoarthritis. Safranin O (A, B) staining reveals chondrocytes with atypical morphology in the articular surface and irregular proteoglycan distribution in 8 weeks old *Col2-tTA-Cre;Ext1*$^{e2fl/e2fl}$ mice (A, yellow arrows) while control mice show uniformly distributed proteoglycan staining (B). *In situ* hybridization (C-F) confirms that chondrocytes turn hypertrophic in the mutant, shown by strong *ColX* expression in the articular cartilage (C, yellow arrows). The control shows normal *ColX* expression in the growth plate, but not in the articular surface (D, yellow arrow). Higher magnification confirms that *ColX* expression is consistent with hypertrophic morphology (E, F yellow arrows). (T: tibia; F: femur). Magnification 100X (C and D); 200X (A, B, E and F).

Mice were sacrificed at 3, 6 and 8 months of age. In wt mice chondrocytes of the articular surface are distributed in three typical zones, superficial (SZ), middle (MZ) and deep zone (DZ), and a strong proteoglycan staining is present in all layers. Cells in the superficial zone are small, flattened and orientated parallel to the

articular surface. Cells of the middle zone are rounder and do not show a specific orientation relative to the surface. Deep zone cells are organized in groups of three or more cells, which arrange in columns perpendicular to the surface and are surrounded by an extensive pericellular matrix (Tyyni and Karlsson 2000; Grogan et al., 2009; Youn et al., 2006). In the mutant joints distribution and orientation of cells through the three zones is disturbed. Articular cartilage in *Col2-tTA-Cre;Ext1*$^{e2fl/e2fl}$ mutant joints display loss of cellularity and the chondrocytes of the superficial zone fail to align parallel to the joint surface (Fig. 29 A, B). Moreover, big lacunae are detectable in the articular surface, most likely generated after hypertrophic chondrocytes undergo apoptosis (Fig 29 A, A1, red arrows). Enzymatic degradation of aggrecan, one of the main components of the articular ECM by Mmps, resulting in the generation of the epitope VDIPEN, is one of the symptoms of OA. In order to confirm that loss of proteoglycan staining was due to proteolytic degradation of aggrecan VDIPEN immunohistochemistry was performed. While healthy knees do not react with the VDIPEN antibody, the VDIPEN epitope could clearly be detected in regions that show loss of proteoglycan staining (Fig. 29C, D red arrows) confirming that *Col2-rtTA-Cre;Ext1*$^{e2fl/e2fl}$ mice spontaneously develop OA. Interestingly, the cartilage cap of osteochondromas is also strongly positive for VDIPEN staining (Fig. 28E, F, red arrows), suggesting that Mmp activation could be associated to *Ext1* loss of function.

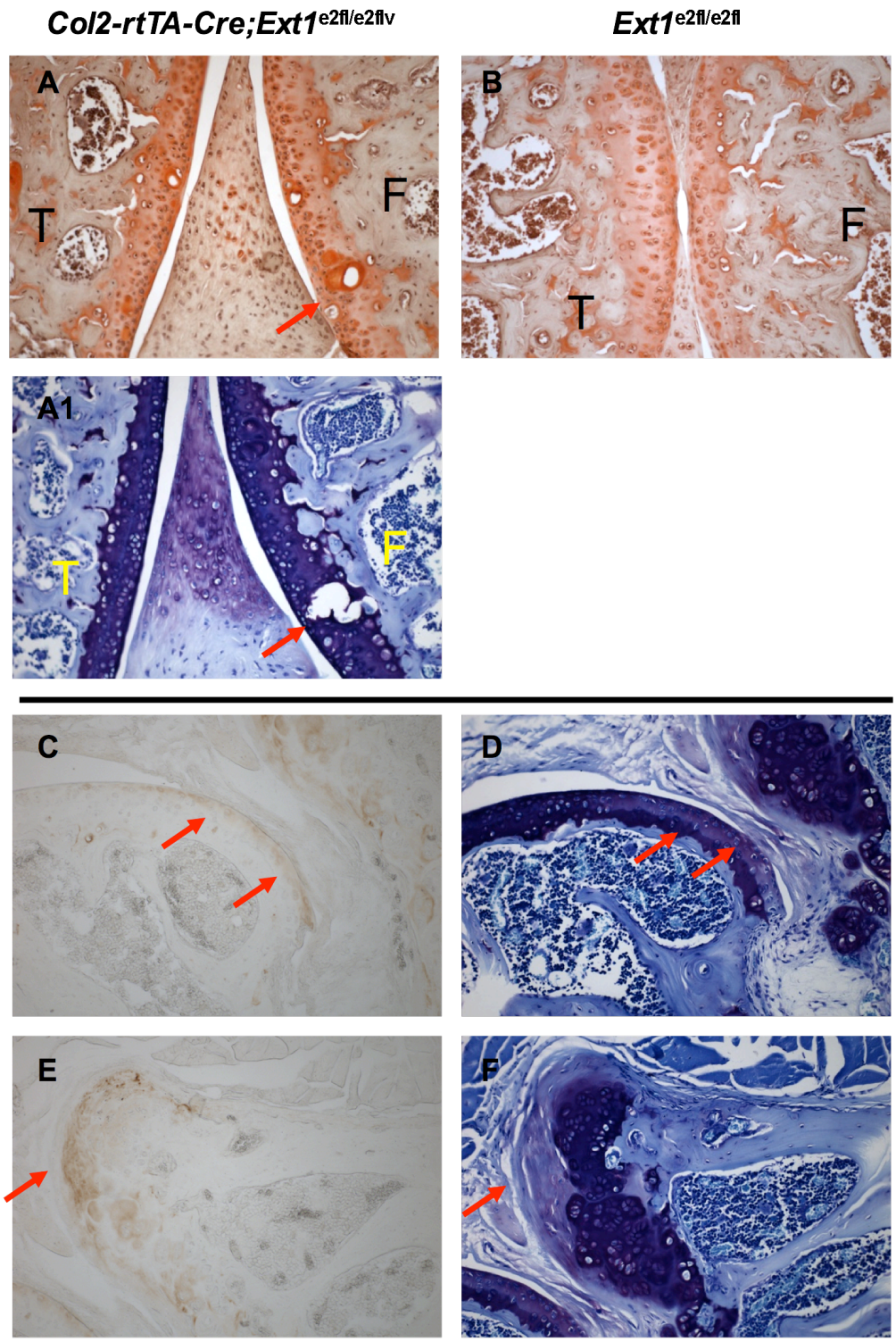

Figure 29. *Col2-tTA-Cre;Ext1*$^{e2fl/e2fl}$ develop osteoarthritis during aging. Safranin O (A, B) and Toluidine Blue (A1) staining on 3 months old *Col2-tTA-Cre;Ext1*$^{e2fl/e2fl}$ knees show a non-homogeneous distribution of proteoglycan in the articular cartilage. Big lacunae can be detected (A, A1 red arrows), in the mutant articular surface. VDIPEN immunohistochemistry (C, E) and Toluidine Blue staining (D, F, red arrows) of 8 months old *Col2-tTA-Cre;Ext1*$^{e2fl/e2fl}$ mice show that cartilage loss is due to Mmp13-mediated proteolytic degradation of aggrecan. Strong VDIPEN staining can be detected in the cartilage cap of osteochondromas (E, red arrow). (T: tibia; F: femur). Magnification 200X.

5. Discussion

5.1 Role of HS during the ossification process

Multiple osteochondroma (MO) syndrome, previously known as hereditary multiple exostoses (HME) syndrome, is a human autosomal dominant disorder characterized from the formation of benign bone tumors at the metaphysis of endochondral bones.

MO has been associated with loss of function mutations in *EXT* genes, with a more severe phenotype associated with *EXT1* mutations rather than *EXT2* (Lüdecke et al., 1995; Porter et al., 2004; Wuyts et al., 1995). *EXT1* and *EXT2* encode glycosysltransferases, which are essential for heparan sulfate (HS) synthesis.

Many theories about the etiology of osteochondromas have been suggested and two vital questions remained open. First, which cell type is the origin of MO? The two principal suspects are an epiphyseal plate chondrocyte or an osteoblastic cell from the adjacent perichondrium. Second, which is the genetic event that initiates the development of osteochondromas? Is haploinsufficiency of *EXT* genes followed by disturbed cell signaling in the growth plate or is a complete loss of function due to loss of heterozygosity in somatic cells necessary?

5.1.1 HS has no direct influence on osteoblast and osteoclast differentiation in Ext1Gt/Gt mice

In order to understand the mechanisms underlying osteochondroma formation, several mouse models have been generated so far. Homozygous deletion of *Ext1* and *Ext2* genes in mice, which are deficient for HS, die prior to bone formation, thus precluding analysis of MO (Lin et al., 2000; Stickens et al., 2005). Only $Ext2^{+/-}$ mice develop small exostoses at the costochondral cartilage of the ribs with low frequency (28%; Stickens et al., 2005).

In another mouse model, the $Ext1^{Gt/Gt}$ mutants produce 20% of the wild type (wt) HS content and survive until E16.5 (Koziel et al., 2004; Yamada et al., 2004). In $Ext1^{Gt/Gt}$ HS has been shown to play a key role in chondrocyte differentiation, regulating the distribution of the morphogen Ihh along the longitudinal axis of

cartilage anlagen.

Ihh regulates chondrocytes proliferation and differentiation, interacting in a negative feedback loop with the secreted growth factor Parathyroid hormone (PTH) related protein (PTHrP). Ihh is produced by prehypertrophic and early hypertrophic chondrocytes and signals through its receptor Patched-1 (Ptch1) to upregulate PTHrP in the distal periarticular chondrocytes. PTHrP signals back to its receptor, the shared PTH/PTHrP receptor (PPR), expressed by proliferating and prehypertrophic chondrocytes, thereby inhibiting the differentiation of proliferating cells into prehypertrophic chondrocytes. HS negatively regulates the propagation of Ihh in the cartilage anlagen. Early stages of chondrocytes differentiation are perturbed in *Ext1*$^{Gt/Gt}$ mice, as Ihh protein can travel further upregulating PTHrP in the distal chondrocytes. PTHrP in turn delays the onset of hypertrophic differentiation (Koziel et al., 2004).

Ihh also regulates osteoblast differentiation and vascular invasion of the cartilage anlagen. It has been shown that *Ihh* deficient mice exhibit severe defects in cartilage vascularization and osteoblast development during endochondral ossification (St-Jacques et al., 1999). Moreover, targeted deletion of Smoothened (*Smo*$^{n/n}$), which results in ablation of all Hh signals, reveals that in these mice formation of normal bone collar and development of the primary spongiosa was abolished (Long et al., 2003). While ablation of *Ihh* signaling pathway inhibits osteoblast differentiation and blood vessel formation, its activation can accelerate ossification and induce vascularization (Kinto et al., 1997). Furthermore, activation of signaling downstream of *Ihh* is sufficient to induce vascularization of the hypertrophic cartilage *in vivo* in the absence of *Ihh* (Joeng and Long, 2009). Preliminary investigations revealed that the ossification process could be disturbed in the *Ext1*$^{Gt/Gt}$ mutant skeletal elements. Therefore, the effect of HS on osteoblast and osteoclast differentiation was investigated in *Ext1*$^{Gt/Gt}$ mutants. *In situ* hybridization analyses show that cartilage matrix resorption and osteoblast differentiation are both delayed compared to wt embryos but both are taking place in the anlagen of E16.5 *Ext1*$^{Gt/Gt}$ mutants, and seem to be normal in relation to hypertrophic differentiation (Fig. 10). Gene expression analysis revealed delayed osteoblast and osteoclast differentiation in *Ext1*$^{Gt/Gt}$ mutants as a consequence of delayed chondrocyte differentiation (Koziel et al, 2004), but not as a direct effect of the reduced amount of HS (Fig. 10 and 11). HS might thus have different effects on the distribution of Ihh in chondrocytes and in the surrounding periosteum.

5.1.2 HS regulates vascularization by influencing the distribution of VEGF-A

When chondrocytes turn hypertrophic they start to produce a calcified extracellular matrix (ECM) and angiogenic stimulators, such as VEGF-A, thereby inducing the first vessel invasion of the cartilage anlagen. The vasculature in turn supplies the bone template with cells belonging to the osteoblast and osteoclast lineage necessary for deposition of a mineralized bone matrix and resorption of the chondrogenic matrix.

The fundamental role of VEGF-A signaling during endochondral ossification has been confirmed by experiments where disturbed blood vessel formation impaired correct development of the growth plate. It has been shown that VEGF-A is produced by hypertrophic chondrocytes and that inhibition of VEGF-A by administration of soluble Flt1 impaired growth plate vascular invasion (Gerber et al., 1999). Defects in blood vessel formation have also been associated to reduced release of VEGF from the hypertrophic cartilage matrix which is mediated by Mmps. *Mmp9* deficient mice show a massive and transient enlargement of the hypertrophic zone, due to delay in chondrocyte apoptosis, capillary invasion and ossification (Vu et al., 1998). This phenotype is similar to that generated by inhibition or conditional deletion of VEGF-A, suggesting a possible role of Mmp9 for VEGF-A release (Gerber et al., 1999; Haigh et al., 2000). Furthermore, VEGF-A has been suggested to have a direct role in osteoclastogenesis and therefore in cartilage resorption. *In vitro* experiments show that VEGF-A can directly enhance the resorption activity and survival of mature osteoclasts (Nakagawa et al., 2000). Recombinant VEGF-A can induce osteoclast recruitment, survival and activity in a mouse model for osteopetrosis, a rare inherited disorder, characterized by harder and denser bones (Niida at al., 1999). Osteoclasts express *Flt-1* and *Vegf-A* from hypertrophic chondrocytes has been shown to be a chemoattractant for osteoclasts invading the developing bone (Blavier and Delaisse, 1995; Engsig et al., 2000; Henriksen et al., 2003). These observations correspond to the phenotype of *Ext1*$^{Gt/Gt}$ mutant mice. In these mice mineralization occurs at E16.5, concomitantly to hypertrophic differentiation (Fig. 10 A, E and 11 E), while ColX matrix is not degraded, although *Mmp13* is expressed (Fig. 10 C). Also osteoclasts invasion is inhibited at E16.5 in *Ext1*$^{Gt/Gt}$ mutant anlagen (Fig.11 K). *Ext1*$^{Gt/Gt}$ mice show an edematous aspect and have severe defects in heart formation, indicating

defects in vascular development. As cartilage resorption and osteoclasts invasion are disturbed similar to phenotype in which VEGF signaling is impaired I investigated if blood vessels development is disturbed in *Ext1*$^{Gt/Gt}$ mice. In these mice, distribution of endothelial cells in E14.5 and E16.5 forelimbs is disorganized (Fig.12). *Ext1*$^{Gt/Gt}$ mice show delayed expression of vascularization markers, which is normal in relation to hypertrophic differentiation, as for ossification markers, therefore most likely due to delayed chondrocyte differentiation (Fig. 13 and 14) (Koziel et al., 2004). HS mediates binding of VEGF-A to its receptors, thereby activating the signaling pathways which promote rearranging and development of the blood vessel net. *In vitro* experiments of embryonic stem cell cultures chimeric for either HS production or VEGFR2 synthesis reveal that HS can mediate activation of VEGF-A signaling *in trans* in endothelial cells (Jakobsson et al., 2006). In zebrafish, knock-down of Perlecan, which belongs to the family of HS, caused an abnormal increase and redistribution of VEGF-A, suggesting a role for HS in generating a VEGF gradient and providing an instructive signal for endothelial cells during angiogenesis (Zoeller et al., 2009). Similarly, a VEGF-A splice variant with low affinity for HS has been shown to activate VEGFR2 in a weak and transient way, while VEGF-A^{165} induced a strong and sustained response (Cebe-Suarez et al., 2006).

As gene expression of vascularization markers is normal in relation to hypertrophic differentiation but morphological analyses revealed that vascular invasion is disturbed in *Ext1*$^{Gt/Gt}$ mutant I analyzed if reduced amounts of HS can be responsible for defects in the VEGF-A protein distribution. *In vitro Ext1*$^{Gt/Gt}$ chondrocyte cultures, producing reduced levels of HS, attract endothelial cells more efficiently than wt cultures (Fig. 15). Since the level of *Vegf-A* transcript is similar in *Ext1*$^{Gt/Gt}$ mutant and control cultures, the increased migration of endothelial cells towards the *Ext1*$^{Gt/Gt}$ mutant culture does not seem to depend on *Vegf-A* upregulation (Fig. 16). Instead, these results indicates a function for HS in regulating VEGF-A protein distribution, as the reduced amount of HS chains decorating the surface of *Ext1*$^{Gt/Gt}$ chondrocytes might be responsible for an increased release of VEGF-A protein from the cell surface. This results in enhanced levels of freely diffusible protein in the medium, which is more accessible to endothelial cells.

In vivo, this would not only perturb blood vessel invasion but also reception of the VEGF-A signal by osteoclasts from the surrounding perichondrium. Hence, these

cells would not invade the primary ossification center, thereby impairing resorption of the cartilage matrix. This hypothesis fits to the phenotype observed in this study. *Ext1*$^{Gt/Gt}$ chondrocytes are able to express *Vegf-A* (Fig. 13 C and 14 C), but endothelial cells are disorganized and not able to invade the primary ossification center (Fig. 12 A and C). Since HS regulates VEGF-A distribution as well as binding of VEGF-A to its receptors, both protein distribution and activation of the vascularization signaling pathway at the site of the primary ossification center might be disturbed in *Ext1*$^{Gt/Gt}$ mutants. This hypothesis is in agreement with the phenotype of *Ext1*$^{Gt/Gt}$ mutants, where blood vessel formation and osteoclast invasion are both impaired (Fig. 11 and 12), but gene expression of osteogenic and vascularization markers is not considerably delayed, as revealed by *in situ* hybridization (Fig.10, 13 and 14). Western blot analysis of VEGF-A release as well as immunohistochemistry to reveal the activation status of VEGF receptors will be necessary to elucidate how HS influences vascularization of the growth plate.

5.2 Development of osteochondromas

5.2.1 Strategy to model loss of heterozygosity and disruption of *Ext1* function

In the past few years, the MO syndrome has been intensively studied in the attempt to understand how osteochondromas arise. Data collected from human patients suggested different controversial hypotheses. The hypothesis that osteochondromas originate from the chondrocyte lineage is supported by animal studies in which transplantation of a growth plate at a 90° angle to the longitudinal axis of the normal growth plate can generate exostoses (D´ambrosia et al., 1968). Furthermore, in human patients a second somatic mutation was found only in the cartilaginous cap indicating a chondrocyte as the origin of MO (Bovée et al., 1999, Hameetman et al., 2007). Additionally these studies support the hypothesis that loss of heterozygosity (LOH) of the *EXT1* and *EXT2* genes is essential for MO formation, defining them as tumor suppressor genes (Bovée et al., 1999; Hameetman et al., 2007). In this scenario human patients are in a heterozygous state and clonal expansion of cells carrying a second somatic mutation would lead to the generation of exostoses. However, a second mutation could not be identified in all human osteochondromas. Cells with only one functional *EXT1* or

EXT2 allele might not be 100% efficient in HS production, thereby causing misregulation of HS-dependent cell signaling (Bovée et al., 1999; Hameetman et al., 2007).

Finally, the observation that late stage human osteochondromas are usually in continuity with the cortical and medullary bone is indicating possible defects in bone collar differentiation. Moreover, animal experiments have shown that injury of the perichondrial groove of Ranvier leads to formation of solitary osteochondromas (Delgado et al., 1987).

As neither *Ext1*$^{+/-}$, *Ext2*$^{+/-}$ or *Ext1*$^{Gt/+}$ mice develop osteochondromas and *Ext1*$^{Gt/Gt}$ mice die around E16.5, not allowing to study later stages of endochondral bone development and more importantly formation of osteochondromas, I analyzed a mouse model that carries a conditionally targeted *Ext1* allele either in the wild type (*Ext1*$^{e2fl/e2fl}$) or in the inverted orientation (*Ext1*$^{e2flinv/e2flinv}$). Homozygous mice for the inverted allele showed the same phenotype as the null allele, with extraembryonic and embryonic structures morphologically not distinguishable. More importantly, *Ext1*$^{e2flinv/e2flinv}$ tissue did not produce any HS, as shown by immunohistochemistry.

The analysis of these mice is useful as a model to induce somatic *Ext1* loss of function to study osteochondroma development.

To mimic the events that are suspected to generate exostoses I crossed *Ext1*$^{e2fl/e2fl}$ mice into a mouse line, which expresses *Cre* recombinase under the *Col2* promoter, active in proliferating chondrocytes.

5.2.2 Loss of heterozygosity in a chondrocyte is generating osteochondromas

5.2.2.1 Osteochondromas generate by loss of heterozygosity

Which the first event is that lead to generate osteochondromas has been for a long time disputed. Osteochondromas have been first thought to be the consequence of skeletal dysplasia. After the founding that osteochondromas development is linked to mutation in *EXT1* and *EXT2* genes (Ahn et al., 1995; Bovée et al., 1999; Lüdecke et al., 1997; Wuyts et al., 1998, Wuyts and Van Hul, 2000) it is now generally accepted that exostoses are neoplastic. As mutations are autosomal dominant inherited, the *EXT* genes belong to the category of tumor suppressor genes. Although loss of heterozigozity has been demonstrated in the cartilage cap

of osteochondromas of MO patients (Bovée et al, 1999, Hameetman et al., 2007), this second mutation could not be detected in all MO patients, raising the question for the initial event in the development of the disease. Several evidences I collected during my analyses suggested that LOH is necessary for the development of osteochondromas. First, *Col2-rtTA-Cre;Ext1*$^{e2fl/e2fl}$ mice developed osteochondromas with 100% penetrance when induced with doxycycline, while none of the other genotypes that were induced with doxycycline showed exostoses, including *Col2-rtTA-Cre;Ext1*$^{e2fl/+}$. This supports the theory that *Ext1* haploinsufficiency is not enough to generate osteochondromas and that a second mutation is necessary (Bovée et al., 1999; Hameetman et al., 2007). After induction at 8 weeks of age mice show big osteochondromas, resembling the human phenotype in cellular organization (Fig. 20-22). Late stage osteochondromas are still in contact with the cortical bone and the bone marrow and chondrocytes are organized in different population with hypertrophic and prehypertrophic chondrocytes surrounded by a cartilage cap, as confirmed by morphological analyses and *in situ* hybridization (Fig. 22). Genotyping analyses of small chondrocyte clones isolated by laser microdissection revealed that at least 70% of the cells isolated from osteochondromas were homozygous for the inverted allele (Fig. 25). Furthermore, most of the osteochondromas did not synthesize HS. Immunohistochemistry revealed that when HS was produced, it was confined to discrete regions within the tumor tissue (Fig. 25-27). A similarly abnormal and decreased distribution of HS was observed in human osteochondromas (Hecht et al., 2002; Trebicz-Geffen et al., 2008). Interestingly, genotyping analyses revealed that osteochondromas of *Col2-rtTA-Cre;Ext1*$^{e2fl/e2fl}$ mice diplay a mixed genotype similar to that observed in humans (Fig. 25). This could be explained by the fact that wt cells can be included in the osteochondromas during its growth and therefore cells isolated from late stage human osteochondromas diplay a mixed genotype. However, osteochondromas of *Col2-rtTA-Cre;Ext1*$^{e2fl/e2fl}$ mice diplay also a mixed genotype but the results presented in this study strongly indicate that osteochondromas develop by clonal expansion of a small cluster of chondrocytes, which are deficient for HS (Fig. 26). As I have shown that lack of HS can be correlated with loss of function of both alleles of *Ext1* (Fig. 25) a plausible conclusion is that LOH in a small clone of chondrocytes is the initial event for generation of osteochondromas.

5.2.2.2 A chondrocyte is the cell of origin of osteochondromas

As for the cellular origin of MO at least two different cell types have been proposed to be the first to mutate. Both chondrocyte or osteoblast progenitor cells have been suggested to be eligible candidates (Bovée et al., 1999; D´ambrosia et al., 1968; Delgado et al., 1987; Hameetman et al., 2007). To induce generation of osteochondromas *Ext1*$^{e2fl/e2fl}$ mice were crossed to an inducible *Cre* recombinase line, which expression is driven under the *Col2* promoter. The *Col2* promoter has previously been shown to drive expression in both chondrocytes and cells of the perichondrium/periosteum embryonically (Long et al., 2001). Therefore a recent study analyzed and compared the activity of inducible Cre recombinase under the *Col2* promoter (*Col2-rtTA-Cre*) and the Osterix promoter (*Osx-CreERT*) (Maes et al., 2007), a transcriptional factor essential for osteoblast differentiation and bone formation (Nakashima et al., 2002). Mice carrying either of these two *Cre* lines were crossed to *Rosa26*$^{LacZ/+}$ mice and relative expression were compared by β-Galactosidase (β-gal) staining. Analyses of knee sections of *Col2-rtTA-Cre;Rosa26*$^{LacZ/+}$ and *Osx-CreERT;Rosa26*$^{LacZ/+}$ mice sacrificed at P16, which have been induced at P8, revealed that the *Col2* promoter drive expression of the allele in about 50% of proliferating growth plate chondrocytes and rarely in cells of the periosteum and cortical bone and bone marrow, while the *Osx* promoter revealed expression in the osteoblasts of the perichondrium/periosteum and the cortical bone and bone marrow. Expression was also detected in hypertrophic chondrocytes of the growth plate, but was excluded from the proliferative zone (Jones et al., 2010).

In the present study, I could show that HS has no direct influence on osteoblast differentiation (Fig. 10). Moreover, mice in which somatic *Ext1* inactivation under the *Osx* promoter were induced demonstrated mild aberrations in hypertrophic chondrocytes, but no osteochondromas (Jones et al., 2010). These evidences indicate that a cell from the osteoblastic lineage is likely not the origin of MO syndrome.

Observations in *Ext2* deficient zebrafish show that HS deficient proliferative chondrocytes lose their ability to respond to polarity signals and cannot organize into columns (Clement et al., 2008). As previously shown in *Ext1*$^{Gt/Gt}$ mutants, reduced amounts of HS inhibits chondrocyte differentiation and increase the proliferative potential (Koziel et al., 2004). Here, I provide evidence that somatic

inactivation of *Ext1* in proliferative chondrocytes leads to development of osteochondromas in mice. Tumors in *Col2-rtTA-Cre;Ext1*$^{e2fl/e2fl}$ mice arise at the side of the growth plate, often still in contact with it, and show a stratified distribution of different chondrocytes population similar to the growth plate (Fig.22). Morphological observations and gene expression analyses suggest that chondrocytes with a early less differentiated character are the cell type to first detach from the growth plate, thereby generating osteochondromas (Fig.23 and 24). Mutant chondrocyte clusters disrupt the columnar organization at the side of the growth plate, where this connects to the articular surface (Fig. 24). The clones proliferate by clonal expansion (Fig. 23) and differentiate further into columnar, prehypertrophic and hypertrophic chondrocytes, forming a growth plate like structure as observed in human patients (Fig. 22).

Further investigations concerning the molecular mechanism perturbed by loss of HS are still required. As described previously, HS interacts with Ihh, thereby regulating proliferation and differentiation of chondrocytes in the growth plate (Koziel et al., 2004). In human osteochondromas, *Ihh* signaling is activated and is probably cell autonomous (Benoist-Lasselin et al., 2006; Hameetman et al., 2006) while PTHrP, which is downstream of *Ihh*, is absent in osteochondroma and upregulated upon malignant transformation into osteochondrosarcoma (Bovée et al., 2000; Hameetman et al., 2005). Without PTHrP signaling, chondrocyte differentiation, hypertrophy, and apoptosis occur after few cycles of proliferation (Chung et al., 2001; Kronenberg and Chung, 2001). This would acts against formation of osteochondromas but also poor diffusion of Ihh through an *Ext* deficient clone of cells might also result in lack of return signaling of PTHrP. Local loss of *Ihh* expression has been tested in *Ihh* null/wt chimeric mice, which show short and wide skeletal elements but did not develop osteochondromas (Chung et al., 2001; Kronenberg and Chung, 2001). However, this mechanism might be responsible for the phenotypic shortening of long bones in human patients affected by MO, which can also be observed in *Ext1*$^{Gt/Gt}$ and *Col2-rtTA-Cre;Ext1*$^{e2fl/e2fl}$ mice. Another possibility is that Ihh would influence directly proliferating chondrocytes with its mitogenic activity (Chung et al., 2001; Long et al., 2001; St-Jacques et al., 1999). A reduced amount of HS decorating the cell surface of *Ext1* deficient cells could lead to a stronger Ihh signaling towards cells neighbouring the mutant clones, inducing overproliferation (St-Jacques et al., 1999; Koziel et al., 2004).

However, early stage osteochondromas of *Col2-rtTA-Cre;Ext1*$^{e2fl/e2fl}$ mice do not express *Ihh* (Fig. 24) or *Ptch1* (data not shown) indicating that Ihh signaling is not active in *Ext1* mutant clones. Therefore, the results collected in this study suggest that Ihh might not play a role in the early osteochondroma but rather induce proliferation in the neighbour chondrocytes, which are surrounding the early stage osteochondromas but eventually can be included in late stage osteochondromas, as also shown by genotyping analyses (Fig. 25).

Wnt signaling and *TGF-ß* signaling have also been shown to be active in the majority of osteochondromas (Hameetman et al., 2006). In cell culture experiments HS can activate VEGF signaling pathway *in trans* (Jakobsson et al., 2006). It is likely that similar activation could work in other signaling pathways as well. For example, FGF signaling might also be affected in osteochondromas development and could be activated in the same way as VEGF. Cells from the perichondrial groove of Ranvier act as a reservoir for osteoblast and mesenchymal cell precursors, which express *FgfR3*, and is responsible for bone growth in width. My analyses on *Col2-rtTA-Cre;Ext1*$^{e2fl/e2fl}$ mice show that early stages osteochondromas are situated in proximity to the groove of Ranvier, next to the growth plate. Mutant chondrocytes and precursors from the perichondrial groove of Ranvier might interact with each other to proliferate and develop into a growth plate-like structure, the later stages osteochondromas. Analyses of loss and gain of function of *FgfR3* in *Col2-rtTA-Cre;Ext1*$^{e2fl/e2fl}$ mice will help to elucidate if and which role cells of the groove of Ranvier might play during MO development.

5.2.3 Arthritis as complication of osteochondromas

OA is the most common human joint disorder, characterized by degradation of the cartilage matrix associated with increased proteolysis of proteoglycans and collagen of the articular surface. This impairs movement of synovial joints by causing acute and chronic pain (Koopman, 1997, Resnick, 2002). A typical symptom of OA is increased expression and synthesis of degrading enzymes, like matrix Mmps and aggrecanases, in synovial tissue and cartilage, with accumulation of these in the joint fluids. It has been shown that in mouse models in which OA has been induced by injection of interleukine or lysozyme into the knee, articular cartilage shows loss of cellularity because chondrocytes become hypertrophic and undergo apoptosis. Loss of proteoglycans in the articular

cartilage is associated with increased chondrocyte death and Mmp-mediated protein degradation, as shown by immunohistochemistry. Induced OA in mice is developing fast and, within only three weeks, mice show severe loss of proteoglycans in the articular surface (Blaney Davidson et al., 2007; van Lent et al., 2005). Nevertheless, these experiments are not suitable to explain which molecular mechanisms lead to the spontaneous development of OA. Other mouse models, which are either deficient for cartilage matrix proteins or signaling molecules, develop OA spontaneously. *FgfR3* null mutants show increased *ColX* levels in the articular cartilage associated with a lacunas appearance of chondrocytes. At 9 months of age mutant mice display Mmp-mediated degradation of cartilage surface (Valverde-Franco et al., 2006). Furthermore, a mouse model for Pseudoachondroplasia also develops OA following loss of proteoglycans, but only at very late stages (Piróg-Garcia et al., 2007). Mice deficient for Mitogen-inducible gene 6 (*Mig6*-/-), a gene involved in stress response, show normal joint development at early stages but start to display the first OA symptoms with loss of articular proteoglycans at 3 months of age (Zhang et al., 2005).

In this study a new mose model for OA has been identified. In contrast to the models mentioned above, the knee joints of *Col2-rtTA-Cre;Ext1*$^{e2fl/e2fl}$ mice show early symptoms of OA already at 8 weeks of age, as shown by the presence of cells expressing high levels of *ColX* and chondrocytes with lacunae in the articular cartilage (Fig. 28). At older stages, the cellularity of the superficial and deep zone was reduced in the mutant articular cartilage and degradation of aggrecan could by shown by VDIPEN staining in the articular cartilage of *Col2-rtTA-Cre;Ext1*$^{e2fl/e2fl}$. Interestingly, the staining was also very intense at the surface of osteochondromas suggesting that activation of Mmps might be triggered by loss of HS (Fig. 29). This assumption is supported by the analysis of hypomorphic *Ext1*$^{Gt/Gt}$ mice, in which the zone of *Mmp13* expression is enlarged (Fig. 10).

Since only few mouse models develop OA spontaneously and only after several months, *Col2-rtTA-Cre;Ext1*$^{e2fl/e2fl}$ mice are an eligible model not only for the development of MO, but also to address the molecular mechanisms of early stages in osteoarthritis development. As aggrecan is one the most important articular cartilage components, induction of somatic *Ext1* deletion under the aggrecan promoter might provide new insights into the HS dependent regulation of OA, and possibly other, bone related diseases. Furthermore, as FGFR3 has a role in OA development (Valverde-Franco et al., 2006), another set of experiments

might address analysis of both loss and gain of function of *FgfR3* in *Col2-rtTA-Cre;Ext1*$^{e2fl/e2fl}$ mice.

6. Summary

Multiple osteochondromas (MO) syndrome is an autosomal dominant disease characterized by the formation of benign bone tumors (osteochondromas or exostoses) at the epiphyses of endochondral bones. Histologically, osteochondromas are peduncolate or sessile cartilage capped bony projections, usually growing until the end of puberty (Hennekam, 1991). MO has been associated to loss of function mutations in EXT genes, with a more severe phenotype associated to *EXT1* mutations rather than *EXT2* (Lüdecke et al., 1995; Porter et al., 2004; Wuyts et al., 1995). *EXT1* and *EXT2* encode for glycosyltransferases responsible for elongation of Heparan Sulfate (HS) chain. HS are polysaccharides decorating the plasma membrane of all animal cells and a major component of the extracellular matrix. They play a key role in mediating the activation of different signaling pathways, like FGF and VEGF, and regulation spatial distribution of morphogens like Ihh and BMPs. Two fundamental questions remain open about osteochondromas development.

1. Which is the cellular origin of osteochondromas? It has been proposed that the first event that leads to development of the disease could happen either in a physeal chondrocyte or in a cell of osteoblastic lineage from the adjacent perichondrium.

2. The molecular mechanism responsible for osteochondromas development is still unclear. As MO is an autosomal dominant syndrome it might be either that haploinsufficiency could be sufficient to induce misregulation of HS-dependent signaling pathways, or that loss of heterozygosity is necessary for exostoses to develop. In this study different mouse models were analyzed to find the molecular function of HS during osteochondromas development. In contrast to *Ext1*$^{-/-}$ mice which die during gastrulation *Ext1*$^{Gt/Gt}$ mice survive until midgestation. *Ext1*$^{Gt/Gt}$ produce about 20% of HS content compared to wild type. Previous data from these mice revealed a general delay in chondrocyte differentiation due to the reduced amount of HS (Koziel et al., 2004). In additional to an effect on chondrogenesis, loss of HS leads to failure in vascular development. In cell culture experiments I identified a defect in the production/release of VEGF-A protein, which regulates the correct activation of vascularization. Correlated to the perturbed vascularization, osteoclast invasion and bone formation was also

delayed in *Ext1*$^{Gt/Gt}$ mutant.

As *Ext1*$^{Gt/Gt}$ die at embryonic stage of development, rendering prohibitive to study osteochondromas development I analyzed a conditional mouse model for *Ext1* (*Col2-rtTA-Cre;Ext1*$^{e2fl/e2fl}$). In these mice, allelic recombination leads to disruption of *Ext1* function, similarly to *Ext1*$^{-/-}$ and *Ext2*$^{-/-}$ mice. *Col2-rtTA-Cre;Ext1*$^{e2fl/e2fl}$ mice developed osteochondromas at endochondral bones, both in the axial and appendicular skeleton. Femurs of *Col2-rtTA-Cre;Ext1*$^{e2fl/e2fl}$ mutant mice were analyzed at different stages (between 4 and 8 weeks old) to observe osteochondromas development at the side of the growth plate. At early stages, in 4 to 6 weeks old mice, osteochondromas are mostly chondrogenic, developing from a small chondrocyte cluster into a more complex structure, in which chondrocytes have differentiated into different cell population, resembling the organization of the growth plate. Cells from osteochondroma tissue were isolated by laser microdissection for genetic analyses and the HS amount was analyzed by immunohistochemistry.

In addition *Col2-rtTA-Cre;Ext1*$^{e2fl/e2fl}$ mice show signs of early osteoarthritis, which lead to enzymatic proteoglycan loss as shown by immunohistochemistry.

In conclusion my data support the hypothesis that MO syndrome is generated by Loss of heterozygosity in a distal chondrocyte of the growth plate, which proliferates and differentiates into a structure that resemble the growth plate organization. Moreover, HS regulate vascularization of the cartilage by modification of VEGF-A protein production or release, which influences in turn osteoblast differentiation.

7. Zusammenfassung

Multiples Osteochondrom (MO) ist eine autosomal-dominant vererbte, genetische Erkrankung, welche durch epiphysäre, gutartige Knochentumore charakterisiert ist (Hennekam, 1991). Bisherige Studien zeigten, dass Mutationen in einem der beiden Exostosin Gene *EXT1* und *EXT2* an der Entstehung von MO beteiligt sind, wobei ein stärkerer Phänotyp bei *EXT1* Mutationen beschrieben ist (Lüdecke et al., 1995; Porter et al., 2004, Wuyts et al., 1995). *EXT1* und *EXT2* kodieren für Glycosyltransferasen, welche für die Synthese von Heparansulfatketten verantwortlich sind. Heparansulfate (HS) sind Polysaccharide, die sich auf der Zelloberfläche von eukaryotischen Zellen befinden. HS spielen eine wichtige Rolle bei der Vermittlung und Aktivierung verschiedener Signalwege, z.B. FGF und VEGF, sowie bei der Bildung von Morphogengradienten von Ihh und BMP. Zwei wichtige Fragen bezüglich der Entstehung von Osteochondromen blieben bisher ungeklärt.

1. Was ist der zelluläre Ursprung von Exostosen? Vorangegangene Studien deuten daraufhin, dass die erste Mutation, die zur Entwicklung der Neoplasie führt, entweder in den Chondrozyten der Wachstumsfuge oder in den Osteoblasten des anliegenden Perichondriums stattfindet.

2. Welcher molekulare Mechanismus ist für die Osteochondromentwicklung verantwortlich? MO ist ein autosomal-dominantes Syndrom. Einerseits kann es bei Haploinsuffizienz zur Störung HS-abgängiger Signalwege kommen, andererseits kann der Verlust des noch intakten *EXT*-Allels in den Tumorzellen zur Exostosenentwicklung führen. In dieser Arbeit wurden zwei verschiedene Mausmodelle analysiert, um die Rolle von HS während der Entwicklung von Exostosen zu untersuchen. Im Gegensatz zu *Ext1*$^{-/-}$ Mäusen, die während der Gastrulation sterben, überleben *Ext1*$^{Gt/Gt}$ Mäuse bis kurz vor der Geburt. *Ext1*$^{Gt/Gt}$ produzieren ca. 20% des HS Gehalts von wildtyp Mäusen. Bisherige Studien zeigten, dass diese Mäuse aufgrund einer reduzierten HS-Menge eine generelle Verzögerung der Chondrozyten Differenzierung ausweisten (Koziel et al., 2004). In dieser Arbeit konnte ein zusätzlicher Effekt von HS auf die Blutgefäßentwicklung identifiziert werden. In Zellkulturexperimente von *Ext1*$^{Gt/Gt}$ und wildtyp Mäusen würde einen Defekt bei der Produktion oder Freisetzung von VEGF-A Protein, welches die Gefäßneubildung aktiviert, festgestellt. In Zusammenhang mit der

fehlenden Blutgefäßbildung in *Ext1*$^{Gt/Gt}$ Mutanten ist die Einwanderung der Osteoklasten und dadurch die Knochenbildung verzögert.

Da *Ext1*$^{Gt/Gt}$ Mäuse perinatal sterben und somit die Entwicklung der Osteochondrome nicht untersuchen werden können, würde eine weitere Mausmutante analysiert, in der das *Ext1* Gen in Chondrocyten konditional deletiert ist (*Col2-rtTA-Cre;Ext1*$^{e2fl/e2fl}$). In diesen Mäusen führt eine Cre-induzierte Rekombination des *Ext1* Gens zu einem kompletten Verlust der *Ext1* Funktion. *Col2-rtTA-Cre;Ext1*$^{e2fl/e2fl}$ Mäuse bilden Osteochondrome in unterschiedlichen enchondralen Knochen des axialen und appendikulären Skeletts. Femura von *Col2-rtTA-Cre;Ext1*$^{e2fl/e2fl}$ Mutanten wurden in verschiedenen Stadien (zwischen 4 und 8 Wochen) analysiert, um die Entwicklung von Osteochondromen lateral der Wachstumsfuge zu untersuchen. In jungen Stadien (4 bis 6 Wochen) sind Osteochondrome meistens chondrogen. Sie entwickeln sich aus einer kleinen Gruppe von Chondrozyten zu einer vielschichtigen Struktur. Diese Chondrozyten differenzieren in verschiedene Subpopulationen, deren Morphologie der Wachstumsfuge ähnelt. Einzellclone wurden mittels Laser Mikrodissektion aus den Osteochondrom Gewebe isoliert und deren Genome analysiert. Ebenfalls wurde ein Verlust der HS Produktion immunhistochemisch in diesem Gewebe nachgewiesen

Col2-rtTA-Cre;Ext1$^{e2fl/e2fl}$ Mäusen zeigen zusätzlich typische Symptome einer Osteoarthrose, welche mit dem enzymatischen Abbau von Proteoglycanen einhergeht.

In dieser Arbeit konnte eine Chondrozytenpopulation der Wachstumsfuge als Ursprungszellart des Osteochondroms identifiziert werden. Der Verlust der Heterozygotizität in diesen distalen Chondrozyten ist die Ursache von MO Syndrom. Diese Chondrozyten proliferieren und differenzieren in eine Struktur, die Ähnlichkeiten mit der Wachstumsfuge aufweist. Zusätzlich können die *Col2-rtTA-Cre;Ext1*$^{e2fl/e2fl}$ Mutanten als nützliches Modelsystem bei der Untersuchung der Entstehung von Osteoarthrosen dienen.

8. Literature

A

Adams, R.H., Alitalo, K. (2007). Molecular regulation of angiogenesis and lymphangiogenesis. *Nat Rev Mol Cell Biol* **8**, 464-78.

Adviezer, D., Golembo, M., Yayon, A. (2003). Fibroblast Growth Factor Receptor-3 as a Therapeutic Target for Achondroplasia- Genetic Short Limbed Dwarfism. *Current Drug Targets* **4**, 353-65.

Ahn, J., Ludecke, H. J., Lindow, S., Horton, W. A., Lee, B., Wagner, M. J., Horsthemke, B. and Wells, D. E. (1995). Cloning of the putative tumor suppressor gene for hereditary multiple exostoses (EXT1). *Nat Genet* **11**, 137-43.

Ahrens, P. B., Solursh, M., and Reiter, R. S. (1977) Stage-related capacity for limb chondrogenesis in cell culture. *Dev Biol* **60**, 69–82.

Archer, C.W., Morrison, H., Pitsillides, A.A. (1994). Cellular aspects of the development of diarthrodial joints and articular cartilage. *J Anat.* **184**, 447-56.

B

Becker, I., Becker, K. F., Rohrl, M. H. and Hofler, H. (1997). Laser-assisted preparation of single cells from stained histological slides for gene analysis. *Histochem Cell Biol* **108**, 447-51.

Benoist-Lasselin, C., de Margerie, E., Gibbs, L., Cormier, S., Silve, C., Nicolas, G., LeMerrer, M., Mallet, J. F., Munnich, A., Bonaventure, J. et al. (2006). Defective chondrocyte proliferation and differentiation in osteochondromas of MHE patients. *Bone* **39**, 17-26.

Bernfield, M., Götte, M., Park, P.W., Reizes, O., Fitzgerald, M.L., Lincecum, J., Zako, M. (1999). Functions of cell surface heparan sulfate proteoglycans. *Annu Rev Biochem* **68**, 729-77.

Bitgood, M. J. and McMahon, A. P. (1995). Hedgehog and Bmp genes are coexpressed at many diverse sites of cell- cell interaction in the mouse embryo. *Dev Biol* **172**, 126-38.

Blaney Davidson, E. N., Vitters, E. L., van Lent, P. L., van de Loo, F. A., van den Berg, W. B. and van der Kraan, P. M. (2007). Elevated extracellular matrix production and degradation upon bone morphogenetic protein-2 (BMP-2) stimulation point toward a role for BMP-2 in cartilage repair and remodeling. *Arthritis Res Ther* **9**, R102.

Blavier, L. and Delaisse, J. M. (1995). Matrix metalloproteinases are obligatory for the migration of preosteoclasts to the developing marrow cavity of primitive long bones. *J Cell Sci* **108 (Pt 12)**, 3649-59.

Blumer, M.J., Longato, S., Schwarzer, C., Fritsch, H. (2007). Bone development in the femoral epiphysis of mice: the role of cartilage canals and the fate of resting chondrocytes. *Dev Dyn* **236**, 2077-88.

Blumer, M.J., Longato, S., Fritsch, H. (2008). Structure, formation and role of cartilage canals in the developing bone. *Ann Anat* **190**, 305-15.

Bonaventure, J., Horne, W.C., Baron, R. (2007). The localization of FGFR3 mutations causing thanatophoric dysplasia type I differentially affects phosphorylation, processing and ubiquitylation of the receptor. *FEBS J.* **274**, 3078-93.

Bovée, J.V., Cleton-Jansen, A.M., Wuyts, W., Caethoven, G., Taminiau, A.H., Bakker, E., Van Hul, W., Cornelisse, C.J., Hogendoorn, P.C. (1999). EXT-mutation analysis and loss of heterozygosity in sporadic and hereditary osteochondromas and secondary chondrosarcomas. *Am J Hum Genet* **65**, 689-98.

Bovée, J. V., van den Broek, L. J., Cleton-Jansen, A. M. and Hogendoorn, P. C. (2000). Up-regulation of PTHrP and Bcl-2 expression characterizes the progression of osteochondroma towards peripheral chondrosarcoma and is a late event in central chondrosarcoma. *Lab Invest* **80**, 1925-34.

Burkus, J.K., Ganey, T.M., Ogden, J.A. (1993). Development of the cartilage canals and the secondary center of ossification in the distal chondroepiphysis of the prenatal human femur. *Yale J Biol Med* **66**, 193-202.

C

Caplan,A.I., and Pechak,D.G. (1987). *In Peck,W.A., ed. Bone and Mineral Research* **Volume 5**, (New York: Elsevier),117–184.

Cebe Suarez, S., Pieren, M., Cariolato, L., Arn, S., Hoffmann, U., Bogucki, A., Manlius, C., Wood, J. and Ballmer-Hofer, K. (2006). A VEGF-A splice variant defective for heparan sulfate and neuropilin-1 binding shows attenuated signaling through VEGFR-2. *Cell Mol Life Sci* **63**, 2067-77.

Celeste, A. J., Rosen, V., Buecker, J. L., Kriz, R., Wang, E. A. and Wozney, J. M. (1986). Isolation of the human gene for bone gla protein utilizing mouse and rat cDNA clones. *Embo J* **5**, 1885-90.

Cheung, P.K., McCormick, C., Crawford, B.E., Esko, J.D., Tufaro, F., Duncan, G. (2001). Etiological point mutations in the hereditary multiple exostoses gene EXT1: a functional analysis of heparan sulfate polymerase activity. *Am J Hum Genet* **69**, 55-66.

Chung UI, Lanske B, Lee K, Li E, Kronenberg H. (1998) The parathyroid hormone/parathyroid hormone-related peptide receptor coordinates endochondral bone development by directly controlling chondrocyte differentiation. *Proc Natl Acad Sci U S A.* **95**, 13030-5.

Chung UI, Schipani E, McMahon AP, Kronenberg HM. (2001).Indian hedgehog couples chondrogenesis to osteogenesis in endochondral bone development. *J Clin Invest.***107**, 295-304.

Clement, A., Wiweger, M., von der Hardt, S., Rusch, M. A., Selleck, S. B., Chien, C. B. and Roehl, H. H. (2008). Regulation of zebrafish skeletogenesis by ext2/dackel and papst1/pinscher. *PLoS Genet* **4**, e1000136.

Colnot, CI, Helms, J.A. (2001). A molecular analysis of matrix remodeling and angiogenesis during long bone development. *Mech Dev* **100**, 245-50.

Colnot, C., Lu, C., Hu, D., Helms, J.A. (2004). Distinguishing the contributions of the perichondrium, cartilage, and vascular endothelium to skeletal development. *Dev Biol* **269**, 55-69.

Cormack, D. (1987). Ham`s histology. *Philadelphia: Pennsylvania*.

Cormier, S., Delezoide, A.L., Benoist-Lasselin, C., Legeai-Mallet, L., Bonaventure, J., Silve, C. (2002). Parathyroid hormone receptor type 1/Indian hedgehog expression is preserved in the growth plate of human fetuses affected with fibroblast growth factor receptor type 3 activating mutations. *Am J Pathol* **161**, 1325-35.

Coumoul, X., Deng, C.X. (2003). Roles of FGF receptors in mammalian development and congenital diseases. *Birth Defects Res C Embryo Today* **69**, 286-304.

Craig, F.M., Bayliss, M.T., Bentley, G., Archer, C.W. (1990). A role for hyaluronan in joint development. *J Anat.* **171**, 17-23.

Cramer, T., Schipani, E., Johnson, R.S., Swoboda, B., Pfander, D. (2004). Expression of VEGF isoforms by epiphyseal chondrocytes during low-oxygen tension is HIF-1 alpha dependent. *Osteoarthritis Cartilage* **12**, 433-9.

D

Dai, J., Rabie, A.B. (2007). VEGF: an essential mediator of both angiogenesis and endochondral ossification. *J Dent Res* **86**, 937-50.

Dakouane Giudicelli, M., Serazin, V., Le Sciellour, C.R., Albert, M., Selva, J., Giudicelli, Y. (2008). Increased achondroplasia mutation frequency with advanced age and evidence for G1138A mosaicism in human testis biopsies. *Fertil Steril.* **89**, 1651-6.

D'Ambrosia, R. and Ferguson, A. B., Jr. (1968). The formation of osteochondroma by epiphyseal cartilage transplantation. *Clin Orthop Relat Res* **61**, 103-15.

Delgado, E., Rodríguez, J.I., Rodríguez, J.L., Miralles, C., Paniagua, R. (1987). Osteochondroma induced by reflection of the perichondrial ring in young rat radii. *Calcif Tissue Int* **40**, 85-90.

DeLisser, H. M., Christofidou-Solomidou, M., Strieter, R. M., Burdick, M. D., Robinson, C. S., Wexler, R. S., Kerr, J. S., Garlanda, C., Merwin, J. R., Madri, J. A. et al. (1997). Involvement of endothelial PECAM-1/CD31 in angiogenesis. *Am J Pathol* **151**, 671-7.

Doschak, M.R., Cooper, D.M., Huculak, C.N., Matyas, J.R., Hart, D.A., Hallgrimsson, B., Zernicke, R.F., Bray, R.C. (2003). Angiogenesis in the distal femoral chondroepiphysis of the rabbit during development of the secondary centre of ossification. *J Anat* **203**, 223-33.

Dowthwaite, G.P., Edwards, J.C., Pitsillides, A.A. (1998). An essential role for the interaction between hyaluronan and hyaluronan binding proteins during joint development. *J Histochem Cytochem.* **46**, 641-51.

E

Edwards, J.C., Wilkinson, L.S., Jones, H.M., Soothill, P., Henderson, K.J., Worrall, J.G., Pitsillides, A.A. (1994). The formation of human synovial joint cavities: a possible role for hyaluronan and CD44 in altered interzone cohesion. *J Anat.* **185**, 355-67.

Engsig, M. T., Chen, Q. J., Vu, T. H., Pedersen, A. C., Therkidsen, B., Lund, L. R., Henriksen, K., Lenhard, T., Foged, N. T., Werb, Z. et al. (2000). Matrix metalloproteinase 9 and vascular endothelial growth factor are essential for osteoclast recruitment into developing long bones. *J Cell Biol* **151**, 879-89.

Esko, J. D. and Lindahl, U. (2001). Molecular diversity of heparan sulfate. *J Clin Invest* **108**, 169-73.

Esko, J. D. and Selleck, S. B. (2002). Order out of chaos: assembly of ligand binding sites in heparan sulfate. *Annu Rev Biochem* **71**, 435-71.

F

Feinberg, R.N., Latker, C.H., Beebe, D.C. (1986). Localized vascular regression during limb morphogenesis in the chicken embryo. I. Spatial and temporal changes in the vascular pattern. *Anat Rec* **214**, 405-9.

Fenwick, S.A., Gregg, P.J., Kumar, S., Smith, J., Rooney, P. (1997). Intrinsic control of vascularization in developing cartilage rudiments. *Int J Exp Pathol.* **78**, 187-96.

Ferrara, N., Gerber, H.P., LeCouter, J. (2003). The biology of VEGF and its receptors. *Nat Med* **9**, 669-76.

Finnerty, H., Kelleher, K., Morris, G.E., Bean, K., Merberg, D.M., Kriz, R., Morris, J.C., Sookdeo, H., Turner, K.J., Wood, C.R. (1993). Molecular cloning of murine FLT and FLT4. *Oncogene* **8**, 2293-8.

Fong, G.H., Rossant, J., Gertsenstein, M., Breitman, M.L. (1995). Role of the Flt-1 receptor tyrosine kinase in regulating the assembly of vascular endothelium. *Nature* **376**, 66-70.

Fosang, A.J., Last, K., Gardiner, P., Jackson, D.C., Brown, L. (1995). Development of a cleavage-site-specific monoclonal antibody for detecting metalloproteinase-derived aggrecan fragments: detection of fragments in human synovial fluids. *Biochem J.* **310**, 337-43.

Francannet, C., Cohen-Tanugi, A., Le Merrer, M., Munnich, A., Bonaventure, J., Legeai-Mallet, L. (2001). Genotype-phenotype correlation in hereditary multiple exostoses. *J Med Genet* **38**, 430-4.

G

Ganey, T.M., Ogden, J.A., Sasse, J., Neame, P.J., Hilbelink, D.R. (1995). Basement membrane composition of cartilage canals during development and ossification of the epiphysis. *Anat Rec* **241**, 425-37.

Gerber, H.P., Vu, T.H., Ryan, A.M., Kowalski, J., Werb, Z., Ferrara, N. (1999). VEGF couples hypertrophic cartilage remodeling, ossification and angiogenesis during endochondral bone formation. *Nat Med*. **5**, 23-8.

Gigante, A., Specchia, N., Nori, S., Greco, F. (1996). Distribution of elastic fiber types in the epiphyseal region. *J Orthop Res* **14**, 810-7.

Gille, H., Kowalski, J., Li, B., LeCouter, J., Moffat, B., Zioncheck, T.F., Pelletier, N., Ferrara, N. (2001). Analysis of biological effects and signaling properties of Flt-1 (VEGFR-1) and KDR (VEGFR-2). A reassessment using novel receptor-specific vascular endothelial growth factor mutants. *J Biol Chem* **276**, 3222-30.

Goodrich, L. V., Johnson, R. L., Milenkovic, L., McMahon, J. A. and Scott, M. P. (1996). Conservation of the hedgehog/patched signaling pathway from flies to mice: induction of a mouse patched gene by Hedgehog. *Genes Dev* **10**, 301-12.

Gordon, S.L., Buchanan, J.R., Ladda, R.L. (1981). Hereditary multiple exostoses: report of a kindred. *J Med Genet* **18**, 428-30.

Grogan, S.P., Miyaki, S., Asahara, H., D'Lima, D.D., Lotz, M.K. (2009). Mesenchymal progenitor cell markers in human articular cartilage: normal distribution and changes in osteoarthritis. *Arthritis Res Ther* **11**, R85.

Grover, J. and Roughley, P. J. (2006). Generation of a transgenic mouse in which Cre recombinase is expressed under control of the type II collagen promoter and doxycycline administration. *Matrix Biol* **25**, 158-65.

H

Hadjantonakis, A. K., Gertsenstein, M., Ikawa, M., Okabe, M. and Nagy, A. (1998). Generating green fluorescent mice by germline transmission of green fluorescent ES cells. *Mech Dev* **76**, 79-90.

Haigh, J. J., Gerber, H. P., Ferrara, N. and Wagner, E. F. (2000). Conditional inactivation of VEGF-A in areas of collagen2a1 expression results in embryonic lethality in the heterozygous state. *Development* **127**, 1445-53.

Hall, B.K. (1988). The embryonic development of bone *Am. Sci.* **76**, 174-181

Hall, B.K., Miyake, T. (2000). All for one and one for all: condensations and the initiation of skeletal development. *Bioessays* **22**,138-47.

Hameetman, L., David, G., Yavas, A., White, S.J., Taminiau, A.H., Cleton-Jansen, A.M., Hogendoorn, P.C., Bovée, J.V. (2007). Decreased EXT expression and intracellular accumulation of heparan sulphate proteoglycan in osteochondromas and peripheral chondrosarcomas. *J Pathol* **211**, 399-409.

Hameetman, L., Kok, P., Eilers, P. H., Cleton-Jansen, A. M., Hogendoorn, P. C. and Bovee, J. V. (2005). The use of Bcl-2 and PTHLH immunohistochemistry in the diagnosis of peripheral chondrosarcoma in a clinicopathological setting. *Virchows Arch* **446**, 430-7.

Hameetman, L., Rozeman, L. B., Lombaerts, M., Oosting, J., Taminiau, A. H., Cleton-Jansen, A. M., Bovee, J. V. and Hogendoorn, P. C. (2006). Peripheral chondrosarcoma progression is accompanied by decreased Indian Hedgehog signalling. *J Pathol* **209**, 501-11.

Hameetman, L., Szuhai, K., Yavas, A., Knijnenburg, J., van Duin, M., van Dekken, H., Taminiau, A.H., Cleton-Jansen, A.M., Bovée, J.V., Hogendoorn, P.C. (2007). The role of *EXT1* in nonhereditary osteochondroma: identification of homozygous deletions. *J Natl Cancer Inst* **99**, 396-406.

Hartmann, C., Tabin, C.J. (2001). Wnt-14 plays a pivotal role in inducing synovial joint formation in the developing appendicular skeleton. *Cell* **104**, 341-51.

Hecht, J.T., Hall, C.R., Snuggs, M., Hayes, E., Haynes, R., Cole, W.G. (2002). Heparan sulfate abnormalities in exostosis growth plates. *Bone* **31**, 199-204.

Hennekam, R. C. (1991). Hereditary multiple exostoses. *J Med Genet* **28**, 262-6.

Henriksen, K., Karsdal, M., Delaisse, J. M. and Engsig, M. T. (2003). RANKL and vascular endothelial growth factor (VEGF) induce osteoclast chemotaxis through an ERK1/2-dependent mechanism. *J Biol Chem* **278**, 48745-53.

Hervé, M.A., Buteau-Lozano, H., Mourah, S., Calvo, F., Perrot-Applanat, M. (2005). VEGF189 stimulates endothelial cells proliferation and migration in vitro and up-regulates the expression of Flk-1/KDR mRNA. *Exp Cell Res* **309**, 24-31.

Holder, N. (1977). An experimental investigation into the early development of the chick elbow joint. *J Embryol Exp Morphol.* **39**, 115-27.

Horton, W. A. (1993). In vitro chondrogenesis in human chondrodysplasias. *Am J Med Genet* **45**, 179-82.

Houck, K.A., Ferrara, N., Winer, J., Cachianes, G., Li, B., Leung, D.W. (1991). The vascular endothelial growth factor family: identification of a fourth molecular species and characterization of alternative splicing of RNA. *Mol Endocrinol* **5**, 1806-14.

Houck, K.A., Leung, D.W., Rowland, A.M., Winer, J., Ferrara, N. (1992). Dual regulation of vascular endothelial growth factor bioavailability by genetic and proteolytic mechanisms. *J Biol Chem* **267**, 26031-7.

Huang, L.F., Fukai, N., Selby, P.B., Olsen, B.R., Mundlos, S. (1997). Mouse clavicular development: analysis of wild-type and cleidocranial dysplasia mutant mice. *Dev Dyn* **210**, 33-40.

Hunziker, E.B. (2002). Articular cartilage repair: basic science and clinical progress. A review of the current status and prospects. *Osteoarthritis Cartilage* **10**, 432-63.

Huss, W. J., Hanrahan, C. F., Barrios, R. J., Simons, J. W. and Greenberg, N. M. (2001). Angiogenesis and prostate cancer: identification of a molecular progression switch. *Cancer Res* **61**, 2736-43.

Hutchings, H., Ortega, N., Plouët, J. (2003). Extracellular matrix-bound vascular endothelial growth factor promotes endothelial cell adhesion, migration, and survival through integrin ligation. *FASEB J* **17**, 1520-2.

J

Jacenko, O., LuValle, P., Solum, K. and Olsen, B. R. (1993). A dominant negative mutation in the alpha 1 (X) collagen gene produces spondylometaphyseal defects in mice. *Prog Clin Biol Res* **383B**, 427-36.

Jakobsson, L., Kreuger, J., Holmborn, K., Lundin, L., Eriksson, I., Kjellen, L. and Claesson-Welsh, L. (2006). Heparan sulfate in trans potentiates VEGFR-mediated angiogenesis. *Dev Cell* **10**, 625-34.

Joeng, K. S. and Long, F. (2009). The Gli2 transcriptional activator is a crucial effector for *Ihh* signaling in osteoblast development and cartilage vascularization. *Development* **136**, 4177-85.

Jones, K.B., Piombo, V., Searby, C., Kurriger, G., Yang, B., Grabellus, F., Roughley, P.J., Morcuende, J.A., Buckwalter, J.A., Capecchi, M.R., Vortkamp, A., Sheffield, V.C. (2010). A mouse model of osteochondromagenesis from clonal inactivation of *Ext1* in chondrocytes. *Proc Natl Acad Sci U S A*. **107**, 2054-9.

K

Karlsson, C., **Thornemo, M**., **Henriksson, H.B**., **Lindahl, A.** (2009). Identification of a stem cell niche in the zone of Ranvier within the knee joint. *J Anat* **215**, 355-63.

Karp, S. J., Schipani, E., St-Jacques, B., Hunzelman, J., Kronenberg, H., McMahon, A. P. (2000). Indian hedgehog coordinates endochondral bone growth and morphogenesis via parathyroid hormone related-protein-dependent and –independent pathways. *Development* **127**, 543-8.

Karsenty, G., Wagner, E.F. (2002). Reaching a genetic and molecular understanding of skeletal development. *Dev Cell* **2**, 389-406.

Khan, I.M., Redman, S.N., Williams, R., Dowthwaite, G.P., Oldfield, S.F., Archer, C.W. (2007). The development of synovial joints. *Curr Top Dev Biol.* **79**, 1-36.

Kinto, N., Iwamoto, M., Enomoto-Iwamoto, M., Noji, S., Ohuchi, H., Yoshioka, H., Kataoka, H., Wada, Y., Yuhao, G., Takahashi, H. E. et al. (1997). Fibroblasts expressing Sonic hedgehog induce osteoblast differentiation and ectopic bone formation. *FEBS Lett* **404**, 319-23.

Kitagawa, H., Shimakawa, H. and Sugahara, K. (1999). The tumor suppressor EXT-like gene EXTL2 encodes an alpha1, 4-N-acetylhexosaminyltransferase that transfers N-acetylgalactosamine and N-acetylglucosamine to the common glycosaminoglycan-protein linkage region. The key enzyme for the chain initiation of heparan sulfate. *J Biol Chem* **274**, 13933-7.

Kitsukawa, T., Shimizu, M., Sanbo, M., Hirata, T., Taniguchi, M., Bekku, Y., Yagi, T., Fujisawa, H. (1997). Neuropilin-semaphorin III/D-mediated chemorepulsive signals play a crucial role in peripheral nerve projection in mice. *Neuron* **19**, 995-1005.

Klagsbrun, M., Takashima, S., Mamluk, R. (2002). The role of neuropilin in vascular and tumor biology. *Adv Exp Med Biol* **515**, 33-48.

Koga, C., Adati, N., Nakata, K., Mikoshiba, K., Furuhata, Y., Sato, S., Tei, H., Sakaki, Y., Kurokawa, T., Shiokawa, K., Yokoyama, K.K. (1999). Characterization of a novel member of the FGF family, XFGF-20, in Xenopus laevis. *Biochem Biophys Res Commun*. 261, 756-65.

Kohno, K., Martin, G. R. and Yamada, Y. (1984). Isolation and characterization of a cDNA clone for the amino-terminal portion of the pro-alpha 1(II) chain of cartilage collagen. *J Biol Chem* **259**, 13668-73.

***Koopman,* W**. (*1997*) *Editor*, *Arthritis and Allied Conditions*: A Textbook of Rheumatology. *13th ed*, *Williams & Wilkins*, *Baltimore*, 1985–2011

Koziel, L., Kunath, M., Kelly, O. G. and Vortkamp, A. (2004). *Ext1*-dependent heparan sulfate regulates the range of *Ihh* signaling during endochondral ossification. *Dev Cell* **6**, 801-13.

Kronenberg HM, Chung U. (2001) The parathyroid hormone-related protein and Indian hedgehog feedback loop in the growth plate. *Novartis Found Symp.* **232**, 144-52.

L

Lander, A. D. and Selleck, S. B. (2000). The elusive functions of proteoglycans: in vivo veritas. *J Cell Biol* **148**, 227-32.

Lanske, B., Karaplis, A. C., Lee, K., Luz, A., Vortkamp, A., Pirro, A., Karperien, M., Defize, L. H. K., Ho, C., Mulligan, R. C. et al. (1996). PTH/PTHrP receptor in early development and Indian hedgehog-regulated bone growth. *Science* **273**, 663-6.

Lark, M.W., Bayne, E.K., Flanagan, J., Harper, C.F., Hoerrner, L.A., Hutchinson, N.I., Singer, I.I., Donatelli, S.A., Weidner, J.R., Williams, H.R., Mumford, R.A., Lohmander, L.S. (1997). Aggrecan degradation in human cartilage. Evidence for both matrix metalloproteinase and aggrecanase activity in normal, osteoarthritic, and rheumatoid joints. *J Clin Invest.* **100**, 93-106.

Lee, K. S., Kim, H. J., Li, Q. L., Chi, X. Z., Ueta, C., Komori, T., Wozney, J. M., Kim, E. G., Choi, J. Y., Ryoo, H. M. et al. (2000). Runx2 is a common target of transforming growth factor beta1 and bone morphogenetic protein 2, and cooperation between Runx2 and Smad5 induces osteoblast-specific gene expression in the pluripotent mesenchymal precursor cell line C2C12. *Mol Cell Biol* **20**, 8783-92.

Legeai-Mallet, L., Munnich, A., Maroteaux, P., Le Merrer, M. (1997). Incomplete penetrance and expressivity skewing in hereditary multiple exostoses. *Clin Genet* **52**, 12-6.

Leighton, P. A., Mitchell, K. J., Goodrich, L. V., Lu, X., Pinson, K., Scherz, P., Skarnes, W. C. and Tessier-Lavigne, M. (2001). Defining brain wiring patterns and mechanisms through gene trapping in mice. *Nature* **410**, 174-9.

Lievens, P.M., Liboi, E. (2003). "The thanatophoric dysplasia type II mutation hampers complete maturation of fibroblast growth factor receptor 3 (FGFR3), which activates signal transducer and activator of transcription 1 (STAT1) from the endoplasmic reticulum". *J Biol Chem* **278**, 17344–9.

Lin, X., Wei, G., Shi, Z., Dryer, L., Esko, J. D., Wells, D. E. and Matzuk, M. M. (2000). Disruption of gastrulation and heparan sulfate biosynthesis in *EXT1*-deficient mice. *Dev Biol* **224**, 299-311.

Lind, T., Tufaro, F., McCormick, C., Lindahl, U. and Lidholt, K. (1998). The putative tumor suppressors *EXT1* and *EXT2* are glycosyltransferases required for the biosynthesis of heparan sulfate. *J Biol Chem* **273**, 26265-8.

Lindahl, U., Kusche-Gullberg, M. and Kjellen, L. (1998). Regulated diversity of heparan sulfate. *J Biol Chem* **273**, 24979-82.

Linsenmayer, T.F., Chen, Q.A., Gibney, E., Gordon, M.K., Marchant, J.K., Mayne, R., Schmid, T.M. (1991). Collagen types IX and X in the developing chick tibiotarsus: analyses of mRNAs and proteins. *Development* **111**, 191-6.

Logan, M., Martin, J. F., Nagy, A., Lobe, C., Olson, E. N. and Tabin, C. J. (2002). Expression of Cre Recombinase in the developing mouse limb bud driven by a Prxl enhancer. *Genesis* **33**, 77-80.

Long, F., Chung, U. I., Ohba, S., McMahon, J., Kronenberg, H. M., McMahon, A.P. (2004). Ihh signaling is directly required for the osteoblast lineage in the endochondral skeleton. *Development* **131**, 1309-18. Epub 2004 Feb 18.

Long, F., Zhang, X. M., Karp, S., Yang, Y. and McMahon, A. P. (2001). Genetic manipulation of hedgehog signaling in the endochondral skeleton reveals a direct role in the regulation of chondrocyte proliferation. *Development* **128**, 5099-5108.

Lüdecke, H.J., Ahn, J., Lin, X., Hill, A., Wagner, M.J., Schomburg, L., Horsthemke, B., Wells, D.E. (1997). Genomic organization and promoter structure of the human *EXT1* gene. *Genomics* **40**, 351-4.

M

Maes, C., Carmeliet, P., Moermans, K., Stockmans, I., Smets, N., Collen, D., Bouillon, R., Carmeliet, G. (2002). Impaired angiogenesis and endochondral bone formation in mice lacking the vascular endothelial growth factor isoforms VEGF164 and VEGF188. *Mech Dev* **111**, 61-73.

Maes C., Kobayashi T., Kronenberg H.M. (2007) A novel transgenic mouse model to study the osteoblast lineage in vivo. *Ann N Y Acad Sci* **1116**:149–164.

Maes, C., Stockmans, I., Moermans, K., Van Looveren, R., Smets, N., Carmeliet, P., Bouillon, R., Carmeliet, G. (2004). Soluble VEGF isoforms are essential for establishing epiphyseal vascularization and regulating chondrocyte development and survival. *J Clin Invest* **113,** 188-99.

Mariani, F.V., Martin, G.R. (2003). Deciphering skeletal patterning: clues from the limb. *Nature* **423**, 319-25.

Mäkinen, T., Veikkola, T., Mustjoki, S., Karpanen, T., Catimel, B., Nice, E.C., Wise, L., Mercer, A., Kowalski, H., Kerjaschki, D., Stacker, S.A., Achen, M.G., Alitalo, K. (2001). Isolated lymphatic endothelial cells transduce growth, survival and migratory signals via the VEGF-C/D receptor VEGFR-3. *EMBO J* **20**, 4762-73.

McCormick, C., Duncan, G., Goutsos, K. T. and Tufaro, F. (2000). The putative tumor suppressors EXT1 and EXT2 form a stable complex that accumulates in the Golgi apparatus and catalyzes the synthesis of heparan sulfate. *Proc Natl Acad Sci U S A* **97**, 668-73.

McCormick, C., Leduc, Y., Martindale, D., Mattison, K., Esford, L. E., Dyer, A. P.

and Tufaro, F. (1998). The putative tumour suppressor *EXT1* alters the expression of cell-surface heparan sulfate. *Nat Genet* **19**, 158-61.

Mercuri, F,A., Doege, K.J., Arner, E.C., Pratta, M.A., Last, K., Fosang, A.J. (1999). Recombinant human aggrecan G1-G2 exhibits native binding properties and substrate specificity for matrix metalloproteinases and aggrecanase. *J Biol Chem.* **274**, 32387-95.

Minina, E., Kreschel, C., Naski, M. C., Ornitz, D. M. and Vortkamp, A. (2002). Interaction of FGF, Ihh/Pthlh, and BMP signaling integrates chondrocyte proliferation and hypertrophic differentiation. *Dev Cell* **3**, 439-49.

Minina, E., Wenzel, H. M., Kreschel, C., Karp, S., Gaffield, W., McMahon, A. P., Vortkamp, A. (2001). BMP and Ihh/PTHrP signaling interact to coordinate chondrocyte proliferation and differentiation. *Development* **128**, 4523-34.

Mitchell, K. J., Pinson, K. I., Kelly, O. G., Brennan, J., Zupicich, J., Scherz, P., Leighton, P. A., Goodrich, L. V., Lu, X., Avery, B. J. et al. (2001). Functional analysis of secreted and transmembrane proteins critical to mouse development. *Nat Genet* **28**, 241-9.

Mullis, K., Faloona, F., Scharf, S., Saiki, R., Horn, G. and Erlich, H. (1986). Specific enzymatic amplification of DNA in vitro: the polymerase chain reaction. *Cold Spring Harb Symp Quant Biol* **51 Pt 1**, 263-73.

N

Nakagawa, M., Kaneda, T., Arakawa, T., Morita, S., Sato, T., Yomada, T., Hanada, K., Kumegawa, M. and Hakeda, Y. (2000). Vascular endothelial growth factor (VEGF) directly enhances osteoclastic bone resorption and survival of mature osteoclasts. *FEBS Lett* **473**, 161-4.

Nakashima, K., Zhou, X., Kunkel, G., Zhang, Z., Deng, J. M., Behringer, R. R. and de Crombrugghe, B. (2002). The novel zinc finger-containing transcription factor osterix is required for osteoblast differentiation and bone formation. *Cell* **108**, 17-29.

Naski, M. C., Colvin, J. S., Coffin, J. D. and Ornitz, D. M. (1998). Repression of hedgehog signaling and BMP4 expression in growth plate cartilage by fibroblast growth factor receptor 3. *Development* **125**, 4977-88.

Naski, M.C., Wang, Q., Xu, J., Ornitz, D.M. (1996). Graded activation of fibroblast growth factor receptor 3 by mutations causing achondroplasia and thanatophoric dysplasia. *Nat Genet* **3**, 233-7.

Neufeld, G., Cohen, T., Gengrinovitch, S., Poltorak, Z. (1999). Vascular endothelial growth factor (VEGF) and its receptors. *FASEB J* **13**, 9-22.

Niida, S., Kaku, M., Amano, H., Yoshida, H., Kataoka, H., Nishikawa, S., Tanne, K., Maeda, N. and Kodama, H. (1999). Vascular endothelial growth factor can substitute for macrophage colony-stimulating factor in the support of osteoclastic bone resorption. *J Exp Med* **190**, 293-8.

O

Ohno, T., Stribley, J. A., Wu, G., Hinrichs, S. H., Weisenburger, D. D. and Chan, W. C. (1997). Clonality in nodular lymphocyte-predominant Hodgkin's disease. *N Engl J Med* **337**, 459-65.

Olsen, S.K., Garbi, M., Zampieri, N., Eliseenkova, A.V., Ornitz, D.M., Goldfarb, M., Mohammadi, M. (2003). Fibroblast growth factor (FGF) homologous factors share structural but not functional homology with FGFs. *J Biol Chem* **278**, 34226-36.

Ornitz, D.M., Itoh, N. (2001). Fibroblast growth factors. *Genome Biol* **2**, REVIEWS3005.

Ortega, N., Behonick, D. J. and Werb, Z. (2004). Matrix remodeling during endochondral ossification. *Trends Cell Biol* **14**, 86-93.

P

Park, K.J., Shin, K.H., Ku, J.L., Cho, T.J., Lee, S.H., Choi, I.H., Phillipe, C., Monaco, A.P., Porter, D.E., Park, J.G. (1999). Germline mutations in the *EXT1* and *EXT2* genes in Korean patients with hereditary multiple exostoses. *J Hum Genet* **44**, 230-4.

Peterson, H.A. (1989). Multiple hereditary osteochondromata. *Clin Orthop Relat Res* **239**, 222-30.

Pfander, D., Cramer, T., Schipani, E., Johnson, R.S. (2003). HIF-1alpha controls extracellular matrix synthesis by epiphyseal chondrocytes. *J Cell Sci* **116**, 1819-26.

Piróg-Garcia, K.A., Meadows, R.S., Knowles, L., Heinegård, D., Thornton, D.J., Kadler, K.E., Boot-Handford, R.P., Briggs, M.D. (2007). Reduced cell proliferation and increased apoptosis are significant pathological mechanisms in a murine model of mild pseudoachondroplasia resulting from a mutation in the C-terminal domain of COMP. *Hum Mol Genet* **16**, 2072-88.

Pitsillides, A.A., Archer, C.W., Prehm, P., Bayliss, M.T., Edwards, J.C. (1995). Alterations in hyaluronan synthesis during developing joint cavitation. *J Histochem Cytochem* **43**, 263-73.

Poltorak, Z., Cohen, T., Sivan, R., Kandelis, Y., Spira, G., Vlodavsky, I., Keshet, E., Neufeld, G. (1997). VEGF145, a secreted vascular endothelial growth factor isoform that binds to extracellular matrix. *J Biol Chem* **272**, 7151-8.

Poole, A.R. (*1991). The growth plate:* Cellular physiology, cartilage assembly and mineralization. *In Cartilage: Molecular Aspects*, ed. BK Hall, SA Newman, pp.179-211. Boca Raton, FL: CRC

Porter, D.E., Lonie, L., Fraser, M., Dobson-Stone, C., Porter, J.R., Monaco, A.P., Simpson, A.H. (2004). Severity of disease and risk of malignant change in hereditary multiple exostoses. A genotype-phenotype study. *J Bone Joint Surg Br* **86**, 1041-6.

Q

Quinn, T.P., Peters, K.G., De Vries, C., Ferrara, N., Williams, L.T. (1993). Fetal liver kinase 1 is a receptor for vascular endothelial growth factor and is selectively expressed in vascular endothelium. *Proc Natl Acad Sci U S A.* **90**, 7533-7.

R

Raskind, W.H., Conrad, E.U. 3rd, Matsushita, M., Wijsman, E.M., Wells, D.E., Chapman, N., Sandell, L.J., Wagner, M., Houck, J. (1998). Evaluation of locus heterogeneity and *EXT1* mutations in 34 families with hereditary multiple exostoses. *Hum Mutat* **11**, 231-9.

Resnick, D. (1975). Patterns of migration of the femoral head in osteoarthritis of the hip. Roentgenographic-pathologic correlation and comparison with rheumatoid arthritis. *AJR Am J Roentgenol* **124**, 62–74.

Richette, P., Bardin, T., Stheneur, C. (2008). Achondroplasia: from genotype to phenotype. *Joint Bone Spine* **75**, 125-30.

Rivas, R., Shapiro, F. (2002). Structural stages in the development of the long bones and epiphyses: a study in the New Zealand white rabbit. *J Bone Joint Surg Am* **84-A**, 85-100.

Roberts, D.M., Kearney, J.B., Johnson, J.H., Rosenberg, M.P., Kumar, R., Bautch, V.L. (2004). The vascular endothelial growth factor (VEGF) receptor Flt-1 (VEGFR-1) modulates Flk-1 (VEGFR-2) signaling during blood vessel formation. *Am J Pathol* **164**, 1531-5.

Robinson, D., Hasharoni, A., Cohen, N., Yayon, A., Moskowitz, R.M., Nevo, Z. (1999). Fibroblast growth factor receptor-3 as a marker for precartilaginous stem cells. *Clin Orthop Relat Res*. **367 Suppl**, 163-75.

Robinson, D., Hasharoni, A., Oganesian, A., Sandell, L.J., Yayon, A., Nevo, Z. (2001). Role of FGF9 and FGF receptor 3 in osteochondroma formation. *Orthopedics* **24**, 783-7.

S

Saiki, R. K., Scharf, S., Faloona, F., Mullis, K. B., Horn, G. T., Erlich, H. A. and Arnheim, N. (1985). Enzymatic amplification of beta-globin genomic sequences and restriction site analysis for diagnosis of sickle cell anemia. *Science* **230**, 1350-4.

Sansone, P., Storci, G., Tavolari, S., Guarnieri, T., Giovannini, C., Taffurelli, M., Ceccarelli, C., Santini, D., Paterini, P., Marcu, K. B. et al. (2007). IL-6 triggers malignant features in mammospheres from human ductal breast carcinoma and normal mammary gland. *J Clin Invest* **117**, 3988-4002.

Schmale, G.A., Conrad, E.U. 3rd, Raskind, W,H. (1994). The natural history of hereditary multiple exostoses. *J Bone Joint Surg Am* **76**, 986-92.

Seibel, M. J. and Woitge, H. W. (1999). Basic principles and clinical applications of biochemical markers of bone metabolism: biochemical and technical aspects. *J Clin Densitom* **2**, 299-321.

Seki, H., Kubota, T., Ikegawa, S., Haga, N., Fujioka, F., Ohzeki, S., Wakui, K., Yoshikawa, H., Takaoka, K., Fukushima, Y. (2001). Mutation frequencies of *EXT1* and *EXT2* in 43 Japanese families with hereditary multiple exostoses. *Am J Med Genet* **99**, 59-62.

Shalaby, F., Rossant, J., Yamaguchi, T.P., Gertsenstein, M., Wu, X.F., Breitman, M.L., Schuh, A.C. (1995). Failure of blood-island formation and vasculogenesis in Flk-1-deficient mice. *Nature* **376**, 62-6.

Shapiro, F., Holtrop, M.E., Glimcher, M.J. (1977). Organization and cellular biology of the perichondrial ossification groove of ranvier: a morphological study in rabbits. *J Bone Joint Surg Am* **59**, 703-23.

Shraga-Heled, N., Kessler, O., Prahst, C., Kroll, J., Augustin, H., Neufeld, G. (2007). Neuropilin-1 and neuropilin-2 enhance VEGF121 stimulated signal transduction by the VEGFR-2 receptor. *FASEB J* **21**, 915-26.

Solchaga, L.A., Goldberg, V.M., Caplan, A.I. (2001). Cartilage regeneration using principles of tissue engineering. *Clin Orthop Relat Res* **391 Suppl**, 161-70.

Solursh, M., Ahrens, P., and Reiter, R. (1978) A tissue culture analysis of the steps in limb chondrogenesis. *In Vitro* **14**, 41–61.

Soker, S., Takashima, S., Miao, H.Q., Neufeld, G., Klagsbrun, M. (1998). Neuropilin-1 is expressed by endothelial and tumor cells as an isoform-specific receptor for vascular endothelial growth factor. *Cell* **92**, 735-45.

St-Jacques, B., Hammerschmidt, M. and McMahon, A. P. (1999). Indian hedgehog signaling regulates proliferation and differentiation of chondrocytes and is essential for bone formation [published erratum appears in Genes Dev 1999 Oct 1;13(19):2617]. *Genes Dev* **13**, 2072-86.

Stickens, D., Brown, D. and Evans, G. A. (2000). EXT genes are differentially expressed in bone and cartilage during mouse embryogenesis. *Dev Dyn* **218**, 452-64.

Stickens, D., Clines, G., Burbee, D., Ramos, P., Thomas, S., Hogue, D., Hecht, J. T., Lovett, M. and Evans, G. A. (1996). The EXT2 multiple exostoses gene defines a family of putative tumour suppressor genes. *Nat Genet* **14**, 25-32.

Stickens, D., Zak, B.M., Rougier, N., Esko, J.D., Werb, Z. (2005). Mice deficient in Ext2 lack heparan sulfate and develop exostoses. *Development* **132**, 5055-68.

Storm, E.E., Kingsley, D.M. (1999). GDF5 coordinates bone and joint formation during digit development. *Dev Biol.* **209**, 11-27.

Stricker, S., Fundele, R., Vortkamp, A. and Mundlos, S. (2002). Role of Runx genes in chondrocyte differentiation. *Dev Biol* **245**, 95-108.

T

Tagariello, A., Luther, J., Streiter, M., Didt-Koziel, L., Wuelling, M., Surmann-Schmitt, C., Stock, M., Adam, N., Vortkamp, A., Winterpacht, A. (2008). Ucma--A novel secreted factor represents a highly specific marker for distal chondrocytes. *Matrix Biol* **27**, 3-11.

Tischer, E., Mitchell, R., Hartman, T., Silva, M., Gospodarowicz, D., Fiddes, J.C., Abraham, J.A. (1991). The human gene for vascular endothelial growth factor. Multiple protein forms are encoded through alternative exon splicing. *J Biol Chem* **266**, 11947-54.

Toole, B.P. (1991). Glycosaminoglycans in morphogenesis. In: Hay ED, editor. Cell biology of the extracellular matrix. *New York. Plenum Press.* 259-294.

Trebicz-Geffen, M., Robinson, D., Evron, Z., Glaser, T., Fridkin, M., Kollander, Y., Vlodavsky, I., Ilan, N., Law, K. F., Cheah, K. S. et al. (2008). The molecular and cellular basis of exostosis formation in hereditary multiple exostoses. *Int J Exp Pathol* **89**, 321-31.

Tyyni, A., Karlsson, J. (2000) Biological treatment of joint cartilage damage. *Scand J Med Sci Sports* **10**, 249-65.

V

Vajo, Z., Francomano, C.A., Wilkin, D.J. (2000). "The molecular and genetic basis of fibroblast growth factor receptor 3 disorders: the achondroplasia family of skeletal dysplasias, Muenke craniosynostosis, and Crouzon syndrome with acanthosis nigricans". *Endocr Rev* **21**, 23–39.

Valverde-Franco, G., Binette, J.S., Li, W., Wang, H., Chai, S., Laflamme, F., Tran-Khanh, N., Quenneville, E., Meijers, T., Poole, A.R., Mort, J.S., Buschmann, M.D., Henderson, J.E. (2006). Defects in articular cartilage metabolism and early arthritis in fibroblast growth factor receptor 3 deficient mice. *Hum Mol Genet* **15**, 1783-92.

Vanhoenacker, F.M., Van Hul, W., Wuyts, W., Willems, P.J., De Schepper, A.M. (2001). Hereditary multiple exostoses: from genetics to clinical. *Eur J Radiol* **40**, 208-17.

van Lent, P.L., Nabbe, K.C., Blom, A.B., Sloetjes, A., Holthuysen, A.E., Kolls, J., Van De Loo, F.A., Holland, S.M., Van Den Berg, W.B. (2005). NADPH-oxidase-driven oxygen radical production determines chondrocyte death and partly regulates metalloproteinase-mediated cartilage matrix degradation during interferon-gamma-stimulated immune complex arthritis. *Arthritis Res Ther* **7**, 885-95.

Vanzulli, S., Gazzaniga, S., Braidot, M. F., Vecchi, A., Mantovani, A. and Wainstok de Calmanovici, R. (1997). Detection of endothelial cells by MEC 13.3 monoclonal antibody in mice mammary tumors. *Biocell* **21**, 39-46.

Vecchi, A., Garlanda, C., Lampugnani, M. G., Resnati, M., Matteucci, C., Stoppacciaro, A., Schnurch, H., Risau, W., Ruco, L., Mantovani, A. et al. (1994). Monoclonal antibodies specific for endothelial cells of mouse blood vessels. Their application in the identification of adult and embryonic endothelium. *Eur J Cell Biol* **63**, 247-54.

Vortkamp, A., Lee, K., Lanske, B., Segre, G. V., Kronenberg, H. M. and Tabin, C. J. (1996). Regulation of rate of cartilage differentiation by Indian hedgehog and PTH-related protein [see comments]. *Science* **273**, 613-22.

Vu, T.H., Shipley, J.M., Bergers, G., Berger, J.E., Helms, J.A., Hanahan, D., Shapiro, S.D., Senior, R.M., Werb, Z. (1998). MMP-9/gelatinase B is a key regulator of growth plate angiogenesis and apoptosis of hypertrophic chondrocytes. *Cell* **93**, 411-22.

W

Westling, J., Fosang, A.J., Last, K., Thompson, V.P., Tomkinson, K.N., Hebert, T., McDonagh, T., Collins-Racie, L.A., LaVallie, E.R., Morris, E.A., Sandy, J.D. (2002). ADAMTS4 cleaves at the aggrecanase site (Glu373-Ala374) and secondarily at the matrix metalloproteinase site (Asn341-Phe342) in the aggrecan interglobular domain. *J Biol Chem* **277**, 16059-66.

Wicklund, C.L., Pauli, R.M., Johnston, D., Hecht, J.T. (1995). Natural history study of hereditary multiple exostoses. *Am J Med Genet* **55**, 43-6.

Wise, G.E., Yao, S. (2003). Expression of vascular endothelial growth factor in the dental follicle. *Crit Rev Eukaryot Gene Expr* **13**, 173-80.

Wuyts, W., Van Hul, W. (2000). Molecular basis of multiple exostoses: mutations in the *EXT1* and *EXT2* genes. *Hum Mutat* **15**, 220-7.

Wuyts, W., Van Hul, W., De Boulle, K., Hendrickx, J., Bakker, E., Vanhoenacker, F., Mollica, F., Lüdecke, H.J., Sayli, B.S., Pazzaglia, U.E., Mortier, G., Hamel, B., Conrad, E.U., Matsushita, M., Raskind, W.H., Willems, P.J. (1998). Mutations in the *EXT1* and *EXT2* genes in hereditary multiple exostoses. *Am J Hum Genet* **62**, 346-54.

Wuyts, W., Van Hul, W., Hendrickx, J., Speleman, F., Wauters, J., De Boulle, K., Van Roy, N., Van Agtmael, T., Bossuyt, P. and Willems, P. J. (1997). Identification and characterization of a novel member of the EXT gene family, EXTL2. *Eur J Hum Genet* **5**, 382-9.

Wuyts, W., Van Hul, W., Wauters, J., Nemtsova, M., Reyniers, E., Van Hul, E.V., De Boulle, K., de Vries, B.B., Hendrickx, J., Herrygers, I., Bossuyt, P., Balemans, W., Fransen, E., Vits, L., Coucke, P., Nowak, N.J., Shows, T.B., Mallet, L., van den Ouweland, A.M., McGaughran, J., Halley, D.J., Willems, P.J. (1996). Positional cloning of a gene involved in hereditary multiple exostoses. *Hum Mol Genet* **5**, 1547-57.

X

Xu, L., Deng, H., Xia, J., Li, H., Zhou, J., Wang, D., Pan, Q., Long, Z. (1999). Identification of mutation in a candidate gene for hereditary multiple exostoses type II. *Chin Med J (Engl)* **112**, 72-5.

Y

Yamada, S., Busse, M., Ueno, M., Kelly, O. G., Skarnes, W. C., Sugahara, K. and Kusche-Gullberg, M. (2004). Embryonic fibroblasts with a gene trap mutation in *Ext1* produce short heparan sulfate chains. *J Biol Chem* **279**, 32134-41.

Yamagiwa, H., Tokunaga, K., Hayami, T., Hatano, H., Uchida, M., Endo, N. and Takahashi, H. E. (1999). Expression of metalloproteinase-13 (Collagenase-3) is induced during fracture healing in mice. *Bone* **25**, 197-203.

Yin, M., Pacifici, M. (2001). Vascular regression is required for mesenchymal condensation and chondrogenesis in the developing limb. *Dev Dyn* **22**, 522-33.

Youn, I., Choi, J.B., Cao, L., Setton, L.A., Guilak, F. (2006). Zonal variations in the three-dimensional morphology of the chondron measured in situ using confocal microscopy. *Osteoarthritis Cartilage* **14,** 889-97.

Yuan, L., Moyon, D., Pardanaud, L., Bréant, C., Karkkainen, M.J., Alitalo, K., Eichmann, A. (2002). Abnormal lymphatic vessel development in neuropilin 2 mutant mice. *Development* **129**, 4797-806.

Z

Zelzer, E., Glotzer, D.J., Hartmann, C., Thomas, D., Fukai, N., Soker, S., Olsen, B.R. (2001). Tissue specific regulation of VEGF expression during bone development requires Cbfa1/Runx2. *Mech Dev* **106**, 97-106.

Zelzer, E., Mamluk, R., Ferrara, N., Johnson, R.S., Schipani, E., Olsen, B.R. (2004). VEGFA is necessary for chondrocyte survival during bone development. *Development* **131**, 2161-71.

Zelzer, E., McLean, W., Ng, Y.S., Fukai, N., Reginato, A.M., Lovejoy, S., D'Amore, P.A., Olsen, B.R. (2002). Skeletal defects in VEGF(120/120) mice reveal multiple roles for VEGF in skeletogenesis. *Development* **129**, 1893-904.

Zeng, H., Dvorak, H.F., Mukhopadhyay, D. (2001). Vascular permeability factor (VPF)/vascular endothelial growth factor (VEGF) peceptor-1 down-modulates VPF/VEGF receptor-2-mediated endothelial cell proliferation, but not migration, through phosphatidylinositol 3-kinase-dependent pathways. *J Biol Chem* **276**, 26969-79.

Zhang, L. and Esko, J. D. (1994). Amino acid determinants that drive heparan sulfate assembly in a proteoglycan. *J Biol Chem* **269**, 19295-9.

Zhang, Y. W., Su, Y., Lanning, N., Swiatek, P. J., Bronson, R. T., Sigler, R., Martin, R. W. and Vande Woude, G. F. (2005). Targeted disruption of Mig-6 in the mouse genome leads to early onset degenerative joint disease. *Proc Natl Acad Sci U S A* **102**, 11740-5.

Zoeller, J. J., Whitelock, J. M. and Iozzo, R. V. (2009). Perlecan regulates developmental angiogenesis by modulating the VEGF-VEGFR2 axis. *Matrix Biol* **28**, 284-91.

Zoltan, V., Francoman, C., Wilkin, D. (2000). The Molecular and Genetic Basis of Fibroblast Growth Factor Receptor 3 Disorders: The Achondroplasia Family of Skeletal Dysplasias, Muenke Craniosynostosis, and Crouzon Syndrome with Acanthosis Nigricans. *J. Endocrine Reviews* **21**, 23–39.

9. Abbreviations

ACH	Achondroplasia
Agc1	Aggrecan1
AgNO3	Silver nitrate
ß2M	Beta-2-microglobulin
β-gal	β-Galactosidase
Bglap	Bone Gla protein
BMPs	Bone morphogenetic proteins
bp	Basepair(s)
BSA	Bovine serum albumin
C	Celsius
CaCl2	Calcium cloride
cm	Centimeter
CO2	Carbon dioxide
Col	Collagen
Cre	Cre recombinase
CS	Chondroitin sulfates
CT-value	Fluorescence threshold value
DAB	Diaminobenzidine substrate
DEPC	Diethylpyrocarbonat
DMSO	Dimethylsulfoxid
DNA	Deoxyribonucleic acid

dNTPs	Desoxyribonukleotidtriphosphat (dATP, dTTP, dCTP, dGTP)
DPX	Di-n-butylPhthalate
DZ	Deep Zone
E	Embryonic day
ECM	Extracellular matrix
EDTA	Ethylendiamintetraacetate
EtOH	Ethanol
Ext	Exostosin
FCS	fetal calf serum
FGF	fibroblast growth factor
FGFR	FGF receptor
Flt1	Fms-like tyrosine kinase receptor1
KDR	kinase insert domain-containing receptor
Flk1	Fetal liver kinase 1
fw	Forward
GAG	Glycosaminoglycan
Gal	Galactose
Gbw	gram body weight
GDF	Growth/differentiation factor
GFP	Green fluorescent protein
GlcA	D-glucuronic acid
GlcNAc	N-acetyl-D-glucosamine
Gly	Glycerol
H2O2	Hydrogen Peroxyde

H&E	Hematoxylin/Eosin
HA	Hyaluronan
HSPG	Heparan sulfate proteoglycan
HS	Heparan sulfate
HRP	Horseradish peroxidase
Hspg2	Perlecan
IdoA	Iduronic acid
Ig	Immunoglobulin
Ihh	Indian hedgehog
Kb	Kilobasepairs
KDa	Kilodalton
KOH	Potassium hydroxyde
LB	Luria Bertani
LCM	Laser capture microdissection
LiCl	Litium cloride
LOH	Loss of heterozygosity
M	Molar
mg	Milligram
MgCl2	Magnesium cloride
ml	Milliliter
Mmp	Matrix metalloprotease
MO	Multiple osteochondromas
MZ	Middle zone
n	Nano

n	Number
NaCl	Sodium cloride
NaOH	Sodium hydroxide
NEO	Neomycin
Nrp	Neuropilin
OA	Osteoarthritis
OD	Optical density
O/N	Over night
Osc	Bglap, Bone Gla protein 1
P	Postnatal day
p	Chromosome short arm
PBS	Phosphat Buffered Saline
PECAM1	Platelet endothelial cell adhesion molecule 1
Pen/Strep	Penicillin/Streptomycin
PFA	Paraformaldehyde
pH	Negative logarithm base 10 of the molar concentration of dissolved hydronium ions
pg	Picogram
PTHrP	Parathyroid hormone (PTH) related protein
PTCH1	Patched-1
PPR	PTH/PTHrP receptor
q	Chromosome long arm
qRT-PCR	Quantitative reverse transcription polymerase chain reaction
RA	Rheumatoid arthritis

RNA	ribonucleic acid
Rpm	Revolution per minute
RT	Room temperature
rtTA	Tetracycline reverse transcriptional activator
RTK	Receptor tyrosin kinase
Rv	Reverse
SSC	Standard saline citrate
SZ	Superficial zone
Taq	Termus aquaticus
TD	Thanatophoric dysplasia
TRAP	Tartrate resistant acid phosphatase
U	Unit
UCMA	Unique cartilage matrix-associated protein
UV	Ultra violet
X	Times
Xyl	Xylose
V	Volume
VEGF	Vascular endothelial growth factor
VEGF-A	Vascular endothelial growth factor (Mouse protein)
Vegf-A	Vascular endothelial growth factor (Mouse gene)
VEGFR	VEGF receptor
Wt	Wild type
µ	Micro-
µCi	Microcurie

10. Index of figures

11. Index of tables

12. Acknowledgments

I would like to express my gratitude to my supervisor Prof. Andrea Vortkamp for having given me the possibility to work in her lab to do the job that I love and for helping me to grow as a scientist.

As promised I thank my good friends and colleagues Jessica Morgner and Andrea Thiesen for all the fun in and out the lab, and for helping my learning of the German language.

I thank all the colleagues of the Vortkamp´s lab for the nice time during my PhD. Special thanks goes to Dr. Tabea Dierker for the critical reading of this work.

I thank all the staff of ZTL-Uniklinikum Essen for their help and care, especially my good friend Anna Giesen, without whom I would be lost.

My last thank goes to my friend, colleague and mentor Dr. Manuela Wülling, who has always been kind, patient and taught me so much during all these years. Thanks are also due for the critical reading of this work.

I dedicate this work to my family

To my mother Anna, who always pushed me to not give up, even in the darkest times, and always hope one day I win a Nobel Price.

To my father Bruno, hoping he would be proud of me.

To my sister Viviana and my brother Davide for having loved me all along and taught me all that I know.

Dedico questo lavoro alla mia famiglia

A mia madre Anna, che mi ha sempre spinto a non arrendermi persino nei moment piú bui, e spera sempre che un giorno io vinca un Premio Nobel.

A mio padre Bruno, spero sarebbe fiero di me.

A mia sorella Viviana e mio fratello Davide per avermi amato sempre e avermi insegnato tutto quello che so.

13. Curriculum Vitae

Der Lebenslauf ist in der Online-Version aus Gründen des Datenschutzes nicht enthalten

Der Lebenslauf ist in der Online-Version aus Gründen des Datenschutzes nicht enthalten

14. Eidesstattliche Erklärungen

Erklärung:
Hiermit erkläre ich, gem. § 6 Abs. 2, Nr. 6 der Promotionsordnung der Math.-Nat.-Fachbereiche zur Erlangung des Dr. rer. nat., dass ich die vorliegende Dissertation selbständig verfasst und mich keiner anderen als der angegebenen Hilfsmittel bedient habe.

Essen, den _____ _____

(Virginia Piombo)

Erklärung:
Hiermit erkläre ich, gem. § 6 Abs. 2, Nr. 8 der Promotionsordnung der Math.-Nat.-Fachbereiche zur Erlangung des Dr. rer. nat., dass ich keine anderen Promotionen bzw. Promotionsversuche in der Vergangenheit durchgeführt habe und dass diese Arbeit von keiner anderen Fakultät abgelehnt worden ist.

Essen, den _____ _____

(Virginia Piombo)

Erklärung:

Hiermit erkläre ich, gem. § 6 Abs. 2, Nr. 7 der Promotionsordnung der Math.-Nat.-Fachbereiche zur Erlangung des Dr. rer. nat., dass ich das Arbeitsgebiet, dem das Thema „Analysis of Heparan Sulfate role in bone development and Multiple Osteochondromas syndrome.“ zuzuordnen ist, in Forschung und Lehre vertrete und den Antrag von Virginia Piombo befürworte.

Essen, den _____ _____

(Prof. Dr. Andrea Vortkamp)